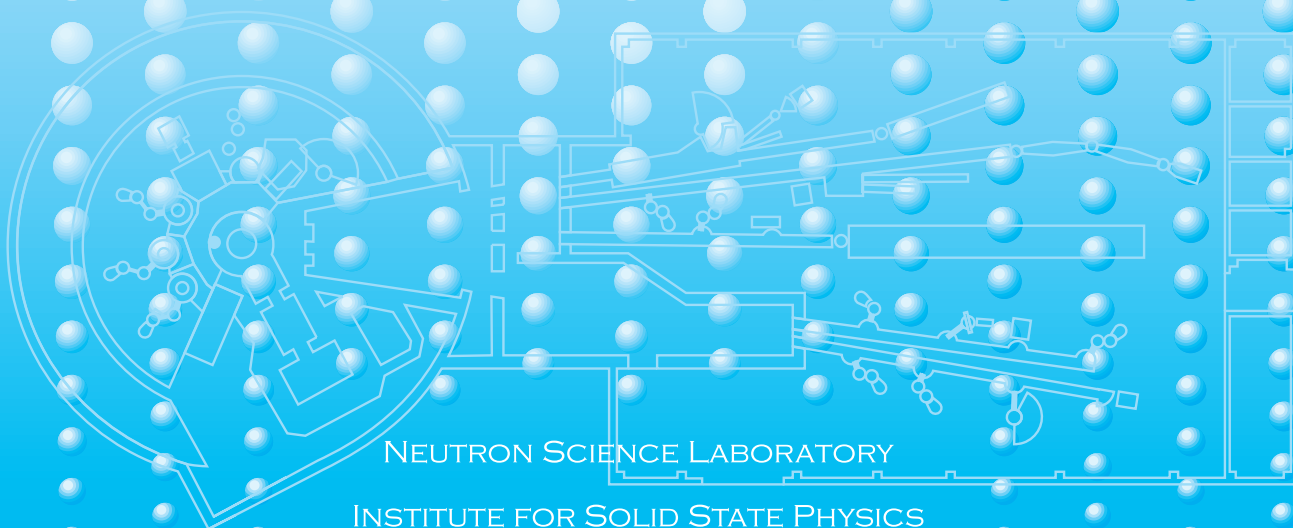




ACTIVITY REPORT
ON
NEUTRON SCATTERING RESEARCH:
EXPERIMENTAL REPORTS

VOL.24

2018



NEUTRON SCIENCE LABORATORY
INSTITUTE FOR SOLID STATE PHYSICS

THE UNIVERSITY OF TOKYO

PREFACE

This is the 24th issue of the “Activity Report on Neutron Scattering Research” which describes the experiments performed under the General-User Program of Neutron Science Laboratory, Institute for Solid State Physics, The University of Tokyo. The General-User Program is conducted with 14 university-owned spectrometers installed at the research reactor JRR-3 of Japan Atomic Energy Agency (JAEA) in Tokai. The Activity Report was first issued in 1994 (vol. 1) as a booklet form, and lasted until 2008 (vol. 15). Since 2007 (vol. 14), the activity report has been issued as a digital form, i.e., a compact disk or web file.

However, due to the Great East Japan Earthquake, JRR-3 has not been operated and is waiting for the permission for resumption. Tentatively, the General-User Program runs a program that supports neutron scattering users to conduct their experiments at facilities overseas. 47 scientists have conducted their experiments during the fiscal year of 2018, FY2018. The current issue is a collection of experimental reports in JFY2018 and a list of publication of those researches during the period from April 2010 through March 2019.

The General-User Program is supported by Nuclear Professional School, The University of Tokyo which is a university representative to interface with JAEA. We thank both Nuclear Professional School Center and JAEA for their strong support. The present volume cannot be issued without the devoted contribution from users, contact persons and editors.

A handwritten signature in black ink, appearing to read 'M. Shibayama'.

Mitsuhiro Shibayama
Director,
Neutron Science Laboratory
Institute for Solid State Physics
The University of Tokyo

CONTENTS

PREFACE

CONTENTS

EXPERIMENTAL REPORTS (2018)	• • • • •	1
STRUCTURES AND EXCITATIONS	• • • • •	6
MAGNETISM	• • • • •	15
STRONGLY CORRELATED ELECTRON SYSTEMS	• • • • •	33
BIOLOGY	• • • • •	37
SOFT MATTERS	• • • • •	39
USER-PROGRAM SUPPORT FOR OVERSEAS EXPERIMENTS (2012 - 2018)	• •	52
PUBLICATIONS AND DISSERTATIONS (2010 - 2019)	• • • • •	70
PUBLICATIONS	• • • • •	71
DISSERTATIONS	• • • • •	112

EXPERIMENTAL REPORTS

(2018)

Activity Report on Neutron Scattering Research: Experimental Reports Vol. 24 (2018)

Published by:
Neutron Science Laboratory,
Institute for Solid State Physics,
University of Tokyo
106-1, Shirakata, Tokai,
Ibaraki 319-1106,
JAPAN

This volume contains experimental reports submitted in the following period of time: 2018/8/1 to 2019/7/31.
Visit our [on-line database](#) for updated information.

Structures and Excitations

- Phonon dynamics on thermoelectric material of Mg₃Sb₂
C. H. Lee, H. Kunioka, H. Mori, T. Hasegawa
Activity Report on Neutron Scattering Research: Experimental Reports **24** (2018) Report Number: 1903
- Structure and catalytic activity of PdRu alloy nanoparticles
O. Yamamuro, H. Akiba, K. Kusada, M. Haneda, H. Kitagawa, D. Keen
Activity Report on Neutron Scattering Research: Experimental Reports **24** (2018) Report Number: 1915
- Crystal structure analysis of high temperature neutron diffraction data of novel oxide-ion conductor HoGaTi₂O₇
Kotaro Fujii, Yuta Yasui, Masatomo Yashima
Activity Report on Neutron Scattering Research: Experimental Reports **24** (2018) Report Number: 1916

Magnetism

- Magnetic structure of Spin S=1/2 linear trimer system Na₂Cu₃Ge₄O₁₂
Yukio Yasui, Rusei Toma, Lukas Keller, and Jonathan White
Activity Report on Neutron Scattering Research: Experimental Reports **24** (2018) Report Number: 1897
- Low Energy Excitations of Magnetic Skyrmions in MnSi
M. Soda and H. Furukawa
Activity Report on Neutron Scattering Research: Experimental Reports **24** (2018) Report Number: 1905
- Uniaxial-stress-control of domain growth kinetics in isosceles-triangular lattice Ising magnet CoNb₂O₆
Setsuo Mitsuda, Yutaro Shimoda
Activity Report on Neutron Scattering Research: Experimental Reports **24** (2018) Report Number: 1913

- Determination of the Magnetic Structure under Magnetic Field of the Noncentrosymmetric Heavy-Electron Metamagnet CePtSi₃
Daichi Ueta, Yoichi Ikeda, Takatsugu Masuda, and H. Yoshizawa
Activity Report on Neutron Scattering Research: Experimental Reports **24** (2018) Report Number: 1919
- Spin excitations in the magnetic skyrmion-lattice phase
Seno Aji, Shinichiro Yano, and Taku J Sato
Activity Report on Neutron Scattering Research: Experimental Reports **24** (2018) Report Number: 1922
- Neutron diffraction study on the Pd-Ga-Tb 2/1 quasicrystal approximant
Taku J. Sato, Maxim Avdeev, Kyohei Takagi, and Yeong-Ge So
Activity Report on Neutron Scattering Research: Experimental Reports **24** (2018) Report Number: 1923
- Neutron diffraction study on the Yb₃Ru₄Al₁₂ itinerant kagome antiferromagnet
Taku J Sato, Noriyuki Kabeya, Maxim Avdeev, Shintaro Nakamura, and Akira Ochiai
Activity Report on Neutron Scattering Research: Experimental Reports **24** (2018) Report Number: 1924
- Dynamics of the magnetic skyrmion under an alternative current in MnSi
D. Okuyama, M. Bleuel, Q. Ye, A. Kikkawa, Y. Taguchi, Y. Tokura D. Higashi, J. D. Reim, Y. Nambu, and T. J. Sato
Activity Report on Neutron Scattering Research: Experimental Reports **24** (2018) Report Number: 1925
- Determination of the spin system in Ni₂V₂O₇ using neutron diffraction in magnetic fields
Masashi Hase Matsuo, James R. Hester, and Kirrily C. Rule
Activity Report on Neutron Scattering Research: Experimental Reports **24** (2018) Report Number: 1931
- Full control of magnetic moment in multiferroics Ba₂CoGe₂O₇
Shunsuke Hasegawa and Takatsugu Masuda
Activity Report on Neutron Scattering Research: Experimental Reports **24** (2018) Report Number: 1933
- Quantum spin liquid state of Tb_{2+x}Ti_{2-x}O_{7+y}
H. Kadowaki, B. F{aa}k, J. Ollivier, T. J. Sato
Activity Report on Neutron Scattering Research: Experimental Reports **24** (2018) Report Number: 1935

Strongly Correlated Electron Systems

- Investigation of vortex lattices on non-centrosymmetric superconductor LaNiC₂
M. Soda, V. Ryukhtin, P. Strunz, and H. Furukawa
Activity Report on Neutron Scattering Research: Experimental Reports **24** (2018) Report Number: 1901
- Investigation of magnetic ordering in high pressure phase of DyMnO₃
Noriki Terada, Navid Qureshi, Mechthild Enderle, Fabio Orlandi, Dmitry Khalyavin, Pascal

- Nesting features and the superconducting mechanism in Ce(Co,Rh)In₅

Kanae Shinohara

Activity Report on Neutron Scattering Research: Experimental Reports **24** (2018) Report Number: 1914

Biology

- Elucidation of tri-ubiquitin dynamics concerning about status of interaction interfaces

Masaaki Sugiyama, Rintaro Inoue, Ken Morishima, Maho Yagi-Utsumi, Methanee Hiranyakorn, Michihiro Nagao, Hiroshi Nakagawa

Activity Report on Neutron Scattering Research: Experimental Reports **24** (2018) Report Number: 1926

Soft Matters

- Solvent dependence in Platonic structures of resorcinarene-based capsule

Shota Fujii, Kazuo Sakurai

Activity Report on Neutron Scattering Research: Experimental Reports **24** (2018) Report Number: 1900

- Elucidating hydration state of poly (propylene oxide) in the glyco polymer vesicle membranes by SANS measurement.

Tomoki Nishimura

Activity Report on Neutron Scattering Research: Experimental Reports **24** (2018) Report Number: 1904

- Distribution of Additives in Ordered-Bicontinuos-Double-Network Structure Formed in Block Copolymer Systems Revealed by Small Angle Neutron Scattering

Katsuhiro Yamamoto, Tsukasa Miyazaki, Isamu Akiba

Activity Report on Neutron Scattering Research: Experimental Reports **24** (2018) Report Number: 1908

- Investigation of Microscopic Structural Changes in Poly(oligo-ethylene glycol methyl ether methacrylate)-Based Hydrogels

Takuma Kureha, Xiang Li

Activity Report on Neutron Scattering Research: Experimental Reports **24** (2018) Report Number: 1911

- Structural Characterization of DNA-module gel by Small-Angle Neutron Scattering

Masashi Ohira, Xiang Li, and Mitsuhiro Shibayama

Activity Report on Neutron Scattering Research: Experimental Reports **24** (2018) Report Number: 1920

- Length dependent effect of added alkane on fluidity and inter-leaflet coupling of lipid membranes

Hatsuho Usuda, Mafumi Hishida, Elizabeth Kelley, Michihiro Nagao

Activity Report on Neutron Scattering Research: Experimental Reports **24** (2018) Report Number: 1928

- Investigation of Microscopic Structural Changes in Poly(oligo-ethylene glycol methyl ether methacrylate)-Based Hydrogels
Takuma Kureha, Xiang Li
Activity Report on Neutron Scattering Research: Experimental Reports **24** (2018) Report Number: 1932

STRUCTURES AND EXCITATIONS

Phonon dynamics on thermoelectric material of Mg₃Sb₂

C. H. Lee¹, H. Kunioka¹, H. Mori², T. Hasegawa³

¹AIIST, Japan, ²Osaka Univ., Japan, ³Hiroshima Univ., Japan

Thermoelectric power generation is expected to contribute to energy conservation through the generation of electricity from waste heat. To realize this technique, intense efforts have been devoted to improving the performance. The difficulty in improving material performance comes from the conflicting requirements to exhibit high electrical conductivity while keeping the thermal conductivity low.

Mg₃Sb₂ is one of promising candidate exhibiting high thermoelectric performance. It shows high value of the dimensionless figure of merit $ZT \sim 1.65$ with quite low lattice thermal conductivity of $\kappa_L \sim 0.7$ W/mK at $T = 725$ K [1,2]. Great attention has been attracted in this compound for the origin of its low κ_L . One assumption is based on the existence of lone pairs around Sb atoms. It has been argued that interatomic potential could be anharmonic due to lone pairs, thus, heat carrying phonons can be heavily scattered. But there is no clear evidence about the claim. Therefore, phonon must be studied using inelastic neutron scattering.

In this experiment, we aim to clarify the origin of low κ_L of Mg₃Sb₂ by examining phonons at FRM2 using PUMA. The weight of Mg₃Sb₂ single crystal was 1.21 g. Measurements were done on scattering planes of (hk0) and (hhl) to cover wide range of Brillouin zone. Phonon calculations were performed using the ABINIT program.

Mg₃Sb₂ has CaAl₂Si₂-type crystal structure with the P-3m1 space group. Mg atoms occupy both Ca and Al sites. Thus, it is basically a 122 Zintl phase compound. Charge density calculations on SrZn₂Sb₂ that has the same crystal structure as Mg₃Sb₂ reveal the existence of lone pairs around Sb atoms [3].

Figure 1 shows phonon dispersion at $T = 298$ K. Solid lines are results of calculations.

Overall, observed peaks agree well with the calculations, ensuring the correctness of the mode assignment. Observed modes are demonstrating by colored lines. Gray lines are remaining modes that we must measure next time. To find anharmonic phonons that can be the origin of low lattice thermal conductivity in Mg₃Sb₂, we will measure temperature dependences in the near future. Further experiments are required to obtain overall picture of phonon dynamics and to clarify the role of lone pairs that are believed to be responsible for the anharmonicity.

[1] H. Tamaki et al., *Adv. Mater.* 28, 10182 (2016). [2] J. Zhang et al., *Nature Commun.* 8, 13901 (2017). [3] E. S. Toberer et al., *Dalton Trans.* 39, 1046 (2010)

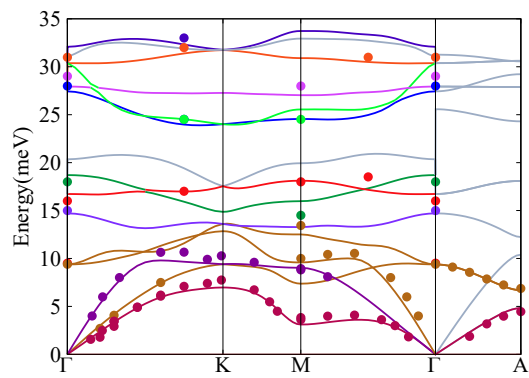


Fig. 1. Phonon dispersions of Mg₃Sb₂ at T = 298K. Solid lines are results of calculations. Color and gray lines depict observed and unobserved modes, respectively.

Structure and catalytic activity of PdRu alloy nanoparticles

O. Yamamuro^A, H. Akiba^A, K. Kusada^B, M. Haneda^C, H. Kitagawa^B, D. Keen^D
^AISSP-NSL, Univ. of Tokyo, ^BKyoto Univ., ^CNagoya Institute of Technology, ^DISIS, RAL

Recently, metal nanoparticles attract much attention as catalytic systems for chemical reactions of gasses. We focus our attention on PdRu-based alloys since they are expected to be high-performance and low-cost catalysts to remove CO and NO_x in exhaust gas of cars. Pd and Ru form bulk solid solutions only at much higher temperatures than room temperature. This is mainly because Pd has an fcc structure while Ru has an hcp one. We have found that Pd_xRu_{1-x} with a diameter of 5-7 nm are miscible in the whole composition range around room temperature [1]. However, there is still microscopic phase separation between the fcc and hcp phases in a single nanoparticle and transpiration of Ru atoms occurs at higher temperatures. It is the present largest problem why the endurance of catalytic ability strongly depends on the composition of the flow gases which are similar to actual exhaust gases of cars:

Stoichi: NO:0.15%, O₂:0.3%, CO:0.35%, C₃H₆:0.033%, H₂:0.1%

Rich: NO:0.15%, O₂:0.15%, CO:0.35%, C₃H₆:0.033%, H₂:0.1%

Lean: NO:0.15%, O₂:0.45%, CO:0.35%, C₃H₆:0.033%, H₂:0.1%

Rich and lean correspond to amounts of CO gas compared with the stoichiometric compositions for the CO and C₃H₆ oxidation and NO reduction; we change the ratio of O₂ gas in the actual experiments as shown above. In this study, we have performed the neutron powder diffraction (NPD) experiments on PdRu nanoparticles supported on CZ (CeO₂-ZrO₂) to elucidate the structural change of nanoparticles caused by the catalytic reactions with the three gases given above. The NPD measurements were performed using the high-intensity neutron powder diffractometer (GEM) installed at RAL, ISIS. NPD is pow-

erful to distinguish between neighboring atoms in the periodic table such as Pd and Ru.

Figure 1 shows the NPD patterns of Pd_{0.5}Ru_{0.5} nanoparticles supported on CZ before and after the Rich and Lean gas treatments at 673 K. The black, blue and red bars represent the peak positions calculated for the fcc structure of CZ, and the fcc and hcp structures of PdRu nanoparticles, respectively. The Lean sample (blue curve) has larger fcc intensity than the Rich sample (red curve). This result indicates that Ru atoms inside the nanoparticles move to the surface and the Pd-rich fcc phase increases in the interior region. This is consistent with our previous IR study and will be more definite by an on-going pdf (pair-distribution function) analyses. It should be noted that this is the first in-situ NPD data showing the structural change of nanoparticles due to catalytic reactions.

[1] K. Kusada et al., J. Am. Chem. Soc. 136, 1864 (2014).

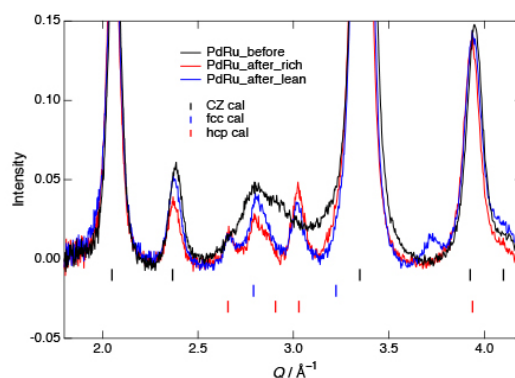


Fig. 1. Neutron diffraction patterns of Pd_{0.5}Ru_{0.5} nanoparticles supported on CZ before (black) and after (red and blue) the catalytic reactions with Rich and Lean gases.

Crystal structure analysis of high temperature neutron diffraction data of novel oxide-ion conductor HoGaTi₂O₇

Kotaro Fujii, Yuta Yasui, Masatomo Yashima
Tokyo Institute of Technology

Oxide-ion conductors, which include pure ionic conductors and mixed oxide-ion and electronic conductors, attract significant interest because of their varied uses in oxygen separation membranes and cathodes for solid-oxide fuel cells (SOFCs). The oxide-ion conductivity is strongly dependent on the crystal structure. At present, several structures, such as fluorites, perovskites, K₂NiF₄, mellilites, and apatites, are known to show high oxide-ion conductivities. For further development of oxide-ion conductors is investigating materials with new types of structures. According to such background, we are exploring new structure family of oxide-ion conductors. For example, we have discovered a new structural family of oxide-ion conductor BaNdInO₄ which has a monoclinic *P*2₁/*c* perovskite-related phase with a layered structure, in 2014. More recently, we found novel material, SrYbInO₄ with CaFe₂O₄-type structure, showed higher oxide-ion conductivity compared to the other CaFe₂O₄-type materials. In order to understand the mechanism of oxide-ion conduction, it is necessary to precisely determine the crystal structure (particularly position, occupancy factor, and anisotropic displacement parameters of oxygens) at high-temperature because oxide-ion conductors are generally used at high-temperature. In the present study, we investigated the crystal structure of HoGaTi₂O₇ at high temperature using high resolution neutron powder diffractometer Echidna installed at the research reactor OPAL, ACNS, ANSTO. The material was prepared by the solid-state reaction. Sintered pellets of the reaction products were introduced into a vanadium can and used for the neutron diffraction experiment. The measurements were car-

ried out from room temperature to high temperature (1000 °C). Each measurement took about 6 hours. The structural analyses for these data are carried out by Rietveld method using the program RIETAN-FP. The Rietveld structure refinements of the diffraction data of HoGaTi₂O₇ taken at the room temperature 23 °C, and 1000 °C using the orthorhombic *Pbcn* GdGaTi₂O₇-type structure gave good quality of the fit and the reliability factors ($R_{wp} = 2.31\%$, $R_B = 1.48\%$ for 23 °C data, and $R_{wp} = 2.07\%$, $R_B = 2.44\%$ for 1000 °C data). The unit-cell parameters and unit-cell volume *V* of HoGaTi₂O₇ at 1000 °C ($a = 9.8658(3)$ Å, $b = 7.4117(2)$ Å, $c = 13.6497(4)$ Å, $V = 998.09(5)$ Å³) are larger than those at RT ($a = 9.77095(16)$ Å, $b = 7.35349(13)$ Å, $c = 13.5334(2)$ Å, $V = 972.38(3)$ Å³), due to the thermal expansion. The bond lengths and equivalent isotropic atomic displacement parameters of HoGaTi₂O₇ at 1000 °C are higher than those at RT, which indicates the larger thermal vibration at 1000 °C. The higher equivalent atomic displacement of oxygen atoms at 1000 °C suggests higher oxide-ion conductivity at 1000 °C compared to RT.

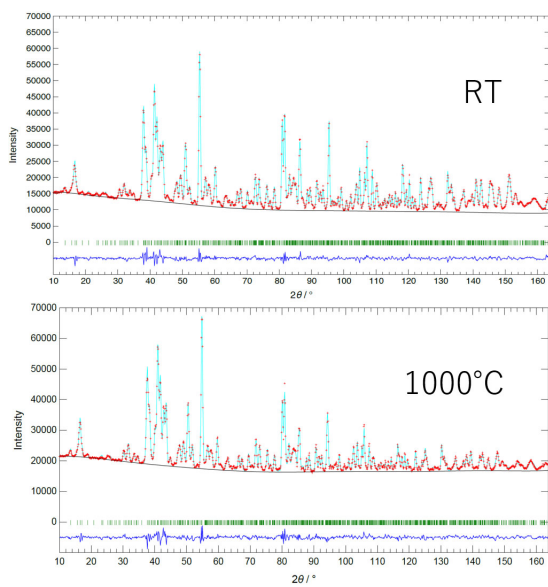


Fig. 1. Results of Rietveld refinement

MAGNETISM

Magnetic structure of Spin $S=1/2$ linear trimer system $\text{Na}_2\text{Cu}_3\text{Ge}_4\text{O}_{12}$

Yukio Yasui (A), Rusei Toma (A), Lukas Keller (B), and Jonathan White (B)

(A) Meiji University, (B) Paul Scherrer Institut

Low dimensional quantum spin systems attract much attention. In particular, the frustrated quantum spin systems due to geometrical arrangement or competing interactions are expected to exhibit various interesting properties. $\text{Na}_2\text{Cu}_3\text{Ge}_4\text{O}_{12}$ has a Cu_3O_8 trimer formed of edge-sharing three CuO_4 square planes [1]. For Cu^{2+} spins ($S=1/2$) within the Cu_3O_8 trimer, the second-neighbor exchange interaction J_2 is antiferromagnetic ($J_2 > 0$), and the nearest-neighbor exchange interaction J_1 is weak ferromagnetic or antiferromagnetic (AF). Such competing interactions between J_1 and J_2 can lead to novel quantum magnetic phenomena.

The T-dependence of magnetic susceptibility χ of $\text{Na}_2\text{Cu}_3\text{Ge}_4\text{O}_{12}$ in the T-region $70 \text{ K} < T < 650 \text{ K}$ can be explained by the isolated $S = 1/2$ Heisenberg trimer model, and it is obtained $J_2/k_B = 340 \pm 20 \text{ K}$ (AF), and $J_1/k_B = 30 \pm 20 \text{ K}$. [2] On the other hand, T-dependence of χ of $\text{Na}_2\text{Cu}_3\text{Ge}_4\text{O}_{12}$ in the T-region $4 \text{ K} < T < 70 \text{ K}$ can be explained by the $S = 1/2$ uniform Heisenberg chain model called as Bonner-Fisher model [3], and it is obtained $J_3/k_B = 18 \pm 1 \text{ K}$ where J_3 is an inter-trimer exchange interaction. [2] The ground state of the isolated $S = 1/2$ trimer is found that two spins of the edge in the Cu_3O_8 trimers form a nonmagnetic singlet state by strong AF interaction J_2 . The center spin of the Cu_3O_8 trimer only survives in low T-region $T < 70 \text{ K}$. The behavior of the specific heat in the T-region $4 \text{ K} < T < 70 \text{ K}$ can also be explained by the $S = 1/2$ uniform Heisenberg chain model. As results of measurements of magnetic susceptibility, specific heat, and dielectric constant, the center spin of the Cu_3O_8 trimer of $\text{Na}_2\text{Cu}_3\text{Ge}_4\text{O}_{12}$ exhibits an antiferromagnetic transition at $T_N = 2 \text{ K}$ accompanied with a ferroelectricity (called multiferroic phenomenon). From the detailed magneti-

zation measurements, we found the existence of dM/dH anomaly at $H_c = 0.37 \text{ T}$ at $T = 1.9 \text{ K}$ ($< T_N$). It is indicating that the magnetic structure changes at H_c . The determination of the magnetic structure at $H = 0$ and $H = 1 \text{ T}$ ($> H_c$) give us important information to understand the magnetic behavior of the $S = 1/2$ linear trimer system.

We investigated the magnetic structure of $\text{Na}_2\text{Cu}_3\text{Ge}_4\text{O}_{12}$ below T_N through powder neutron diffraction experiments using cold neutron powder diffractometer DMC at PSI. We used amount of 15 g of powder for $\text{Na}_2\text{Cu}_3\text{Ge}_4\text{O}_{12}$. The superconducting magnet and the dilution refrigerator were used to reach down to 0.1 K and up to 1 T.

We obtained powder neutron diffraction patterns at $T = 0.1 \text{ K}$, 3K, and 12 K, respectively, in $H = 0$ as well as that of $T = 0.1 \text{ K}$ applied the magnetic field $H = 1 \text{ T}$. The figure (a) show the diffraction patterns at $T=0.1 \text{ K}$ and 12 K, respectively. We can clearly observe the super-lattice magnetic Bragg peaks below T_N assigned by the arrows. The figure (b) show the intensity profile of difference between at $T = 0.1 \text{ K}$ and 12 K, $I(0.1\text{K}) - I(12\text{K})$. We also found the possible magnetic Bragg peaks assigned by the short arrows. By applied the magnetic field $H = 1 \text{ T}$, no difference found the magnetic Bragg intensities at $T = 0.1 \text{ K}$ in the error bar. Then, changing the magnetic structure at H_c seems to be small. Recently, the aligned powder of $\text{Na}_2\text{Cu}_3\text{Ge}_4\text{O}_{12}$ can be obtained in the magnetic field $H = 9 \text{ T}$. For determination of the magnetic structure of $\text{Na}_2\text{Cu}_3\text{Ge}_4\text{O}_{12}$, the results of the various measurements of the aligned powder give us important information. We are analyzing the neutron diffraction data and various measurements data.

[1] X. Mo et al.: Inorg. Chem. 45 3478 (2006).

[2] Y. Yasui et al.: J. Appl. Phys. 115 17E125

(2014).

[3] J. C. Bonner et al.: Phys. Rev. 135 A640

(1964).

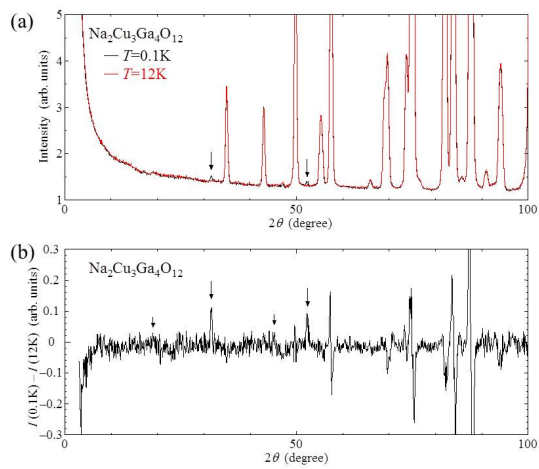


Fig. 1. (a). Neutron powder diffraction patterns measured at 0.1 K and 12 K. The arrows indicate the magnetic Bragg peaks. (b). Intensity profile of difference between at $T = 0.1\text{ K}$ and 12 K.

Low Energy Excitations of Magnetic Skyrmions in MnSi

M. Soda and H. Furukawa
RIKEN, Ochanomizu University,

Topological spin textures have been extensively investigated both experimentally and theoretically. Among them, a vortex-like spinswirling texture of so-called magnetic skyrmions has attracted much attention. A helimagnet MnSi possesses a magnetic skyrmion phase in a small magnetic field and temperature region.[1] Since the magnetic skyrmions in MnSi have a long periodicity (~ 18 nm), the structure has been examined by using small angle neutron scattering (SANS) and Lorentz Transmission Electron Microscope (LTEM) techniques. On the other hand, the dynamics of magnetic skyrmions has not been clear because inelastic neutron scattering measurements with an energy scale of $1\sim 5$ micro-eV in a small q region is not easy. Then magnetic excitations only in the helical phase has been reported.

Recently, a theoretical study on the magnetic skyrmions has been carried out by our theoretical group[2]. The string of skyrmions appears to be parallel to the magnetic field. Not only the difference between the magnetic dispersions for the helical and skyrmion structures but also the different q dependence of magnetic excitations along $+q_z$ and $-q_z$ have been predicted.

We have carried out the neutron spin-echo experiment with IN15 installed in ILL in MnSi to clarify the low energy excitation of skyrmion. Figure 1 shows the experimental setting in IN15. The profiles obtained by spin-echo experiment had the large phase shift which corresponds to the energy transfer. This behavior becomes opposite with changing the magnetic field direction. The obtained results mean that the skyrmion has the asymmetric dispersion.

reference

- [1] S. Muhlbauer et al., Science 323 (2009) 915.
- [2] W. Koshibae et al. private commun.

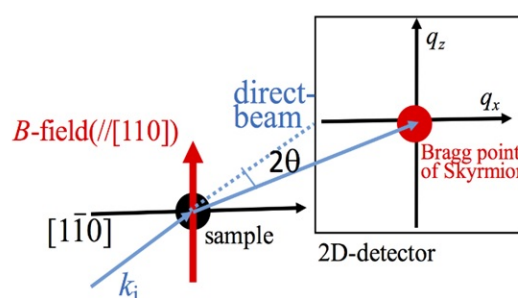


Fig. 1. Experimental setting in neutron spin-echo measurement

Uniaxial-stress-control of domain growth kinetics in isosceles-triangular lattice Ising magnet CoNb₂O₆

Setsuo Mitsuda, Yutaro Shimoda

Department of Physics, Faculty of Science, Tokyo University of Science

The isosceles triangular lattice (ITL) Ising antiferromagnet is characterized by the ratio of exchange interactions defined as $\gamma = J_1$ (along the base direction) / J_2 (along the equilateral direction), and its magnetic property dramatically changes, depending on whether γ is larger than 1.0 or not. As one of the model materials, we have studied an Ising magnet CoNb₂O₆, where the quasi-1D ferromagnetic zigzag chains along the c axis form a frustrated antiferromagnetic ITL with $\gamma \simeq 1.33$ in the a - b plane. If the exchange ratio γ can be controlled in CoNb₂O₆ via anisotropic deformation of ITL by uniaxial pressure, variety of interesting magnetic features intrinsic to γ would be observed.

Actually along this context, we succeeded in crossing the Wannier point ($\gamma = 1$) and providing access to the region of $\gamma < 1$ by applying uniaxial pressure p up to 1.1GPa along the c axis, where entirely different $H_{\parallel c}$ - T magnetic phase diagram with ground-state AF-I magnetic ordering appears, as is in the experimental reports of No.1802 and No.1841. Note that in those experiments we used a good single crystal of CoNb₂O₆ prepared by the floating zone(FZ) technique, instead of the sample prepared by flux method, which is accompanied by extrinsic magnetic ordering due to crystal imperfection.

As a continuation of the proposal, we performed the neutron-diffraction measurements at the two-axis diffractometer E4 installed at the Berlin Neutron Scattering Center in the Helmholtz Centre Berlin for Materials and Energy, using transverse- as well as longitudinal- uniaxial pressure device so that we can provide access to the ($HK0$) scattering zone under applied vertical magnetic field to the c axis.

As is in the experimental reports of No.

1683, the uniaxial pressure dependence of the ratio γ along both the a - and b -axes were already measured but using the flux-sample with crystal imperfection. Therefore, in present experiment, changing the original plan of “uniaxial-stress control of magnetic domain-growth kinetics characteristic to ITL”, we re-measured these up to 0.6 GPa using FZ-sample. Results shown in Fig.1 are qualitatively agree with these of flux-sample, but are quantitatively different, which are crucial to estimate the uniaxial pressure dependence of coupling constants J_1 and J_2 in combination with magnetic phase transition fields obtained by dc- and ac-susceptibility.

As shown in Fig.2(a1-a3), we also investigated temperature variation in the magnetic correlations at $\gamma \sim 1.3$ ($p_{\parallel c} = 0$ MPa), $\gamma \sim 1$. ($p_{\parallel c} = 0.8$ GPa) and $\gamma \sim 0.9$ ($p_{\parallel c} = 1.1$ GPa) in detail. Because of unavoidable inhomogeneity of uniaxial pressure, at $p_{\parallel c} \sim 0.8$ GPa ($\gamma \sim 1$), AF-I and AF-II magnetic LRO coexist so that unfortunately we were not able to investigate magnetic correlations specific to Wannier point ($\gamma = 1$) at the lowest temperature. As shown in Fig.2(b), however, the temperature dependence of propagation wavenumber q of sinusoidally-amplitude-modulated incommensurate (IC) state at specific γ is qualitatively consistent with Stephenson's exact calculation for 2D isosceles triangular lattice Ising antiferromagnet.

In contrast to that both AF-I and AF-II magnetic orderings coexist at $p_{\parallel c} \sim 0.8$ GPa ($\gamma \sim 1$) as is seen in Fig.3(a), almost flat diffraction profile can be seen at $p_{\parallel b} \sim 0.6$ GPa ($\gamma \sim 1$) as shown in Fig.3(b), suggesting good “spot” to investigate field-induced magnetic states specific to Wannier point ($\gamma = 1$). Further beam experiments are desired.

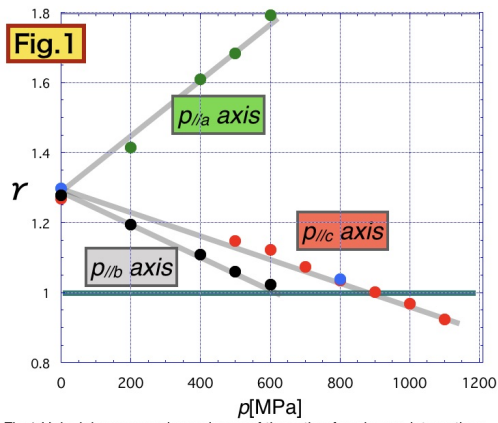


Fig.1 Uniaxial-pressure dependence of the ratio of exchange interactions γ along the a-, b- and c- axes.

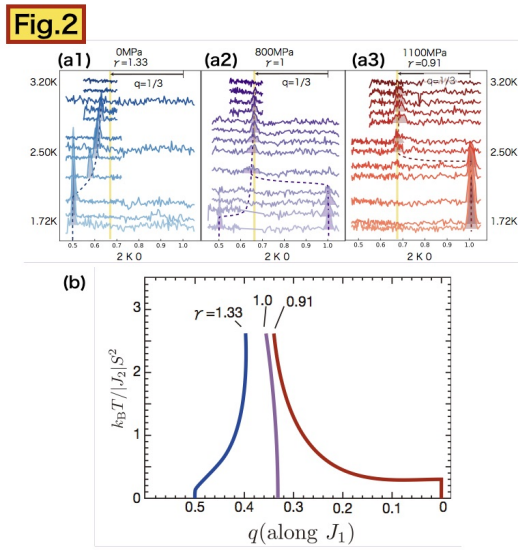


Fig.2 Temperature dependence of (2 k 0) scan profiles in zero magnetic field at (a1) $\gamma \sim 1.33$ ($p_{//c} = 0$ GPa), (a2) $\gamma \sim 1.0$ ($p_{//c} = 0.8$ GPa) and (a3) $\gamma \sim 0.9$ ($p_{//c} = 1.1$ GPa), respectively. (b) Temperature variation of propagation wavenumber q of short range magnetic correlation at specific γ , which is obtained from Stephenson's exact calculation for 2D isosceles triangular lattice using antiferromagnet.

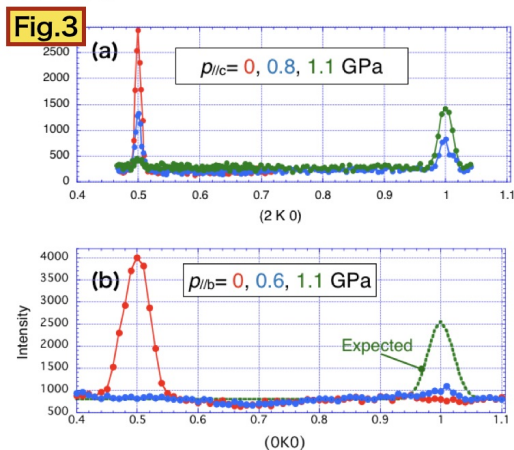


Fig.3 (a) (2 k 0) scan profiles in zero magnetic field at $T=1.7$ K and $p_{//c} = 0, 0.8$ and 1.1 GPa, (b) (0 k 0) scan profiles in zero magnetic field at $T=1.7$ K and $p_{//b} = 0, 0.6$ and 1.1 GPa.

Fig. 1.

Determination of the Magnetic Structure under Magnetic Field of the Noncentrosymmetric Heavy-Electron Metamagnet CePtSi₃

Daichi Ueta, Yoichi Ikeda^B, Takatsugu Masuda, and H. Yoshizawa
ISSP-NSL, the University of Tokyo, IMR, Tohoku University^B

Non-centrosymmetric *f*-electron materials have attracted much attention because the lack of inversion symmetry leads to significant and interesting physical properties. Recently, we observed that the non-centrosymmetric BaNiSn₃-type compound, CePtSi₃, exhibits successive magnetic transitions, multiple metamagnetic transitions, yielding an unusually complex *H* – *T* phase diagram. We defined three phases (III, II and I) at elevated temperature. From elastic neutron diffraction experiments at zero field performed last summer, we found that the magnetic peaks observed at the commensurate position in phase III and at the incommensurate position in phase I. In addition, the *h*- and *k*-domains coexist in CePtSi₃ at zero field.

In order to determine magnetic structures in CePtSi₃ under fields in the next step, we performed elastic neutron scattering experiments at BL-09 (CORELLI), SNS in Oak Ridge National Laboratory. A single crystalline sample of CePtSi₃ was grown using a flux method at the Institute for Solid State Physics. The sample was mounted on a Cu pin such that both the *a*- and *c*-axes set into the equatorial plane and installed in SlimSam. Temperature was set to 1.8 K, and a magnetic-field was applied from 0 to 50 kOe along the *h*-direction (the *a*-axis).

We succeeded in observing clear and interesting field-dependence of magnetic peaks (Figure 1). It was suggested that the field region from 5 to 20 kOe can be classified into two phases. The *k*-domain in the magnetic field region of 5 to 14 kOe is still in the commensurate phase, but the *h*-domain changes to the incommensurate phase, and its magnetic propagation vector, q_{2h} , changes from 0.283 to 0.31 and the scattering intensity decrease sharply. In the

magnetic field region from 14 to 20 kOe, the *h*-domain saturates at $q_{2h} = 0.31$, and the scattering intensity of magnetic peaks further decreases and disappears at 20 kOe. On the other hand, in the *k*-domain at 14 to 20 kOe, an incommensurate phase of $q_{1k} = 0.283$ appears, which is a crossover region between the incommensurate and commensurate phase. Finally, all magnetic superlattice peaks disappear above 45 kOe because of forced ferromagnetism. We are in the process of determining the mechanism of such magnetic structures in field. Travel expenses were supported by General User Program for Neutron Scattering Experiments, Institute for Solid State Physics, The University of Tokyo (proposal no. 18508), at JRR-3, Japan Atomic Energy Agency, Tokai, Japan.

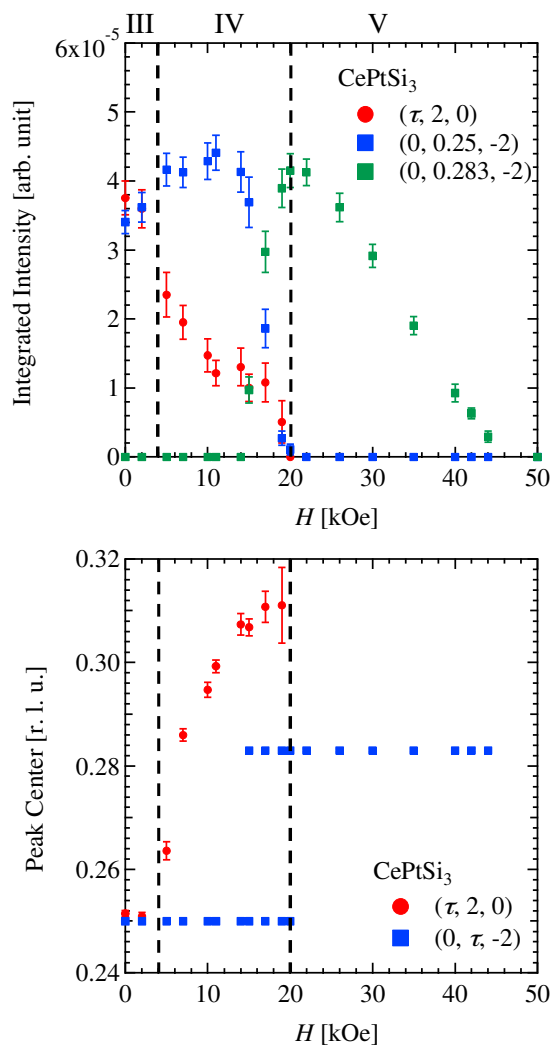


Fig. 1. Magnetic field dependence of the integrated intensity and peak position related to propagation vectors in h - and k -domains.

Spin excitations in the magnetic skyrmion-lattice phase

Seno Aji, Shinichiro Yano(A), and Taku J Sato
IMRAM, Tohoku University, (A) NSRRC

MnSi attracts renewed interest because of the recent discovery of the magnetic skyrmion-lattice structure under finite magnetic field [1]. The magnetic skyrmion is a topological spin texture made of swirling magnetic moments. The magnetic skyrmion carries integer topological number, called skyrmion number. In the real magnets, such as MnSi, the skyrmion forms a triangular lattice. The elementary excitation of ordered magnet is "magnon", which is a propagating quantized wave of spin fluctuations. The magnon would exist in the skyrmion-lattice phase, forming magnon bands with the Brillouin zone set by the periodicity of the triangular lattice. In addition, the topological nature of the scatterers (i.e. skyrmions) will give rise to non-trivial characters to the magnon bands, forming the topological magnon band [2]. Such a topological magnon is of current interest and are under active scrutiny, recently.

In search for the topological magnons, it was necessary to use Ge-doped MnSi, as Ge-doping increases the magnetic modulation vector k , relaxing Q -resolution requirement for the experiment. A single crystal sample $\text{MnSi}_{0.98}\text{Ge}_{0.02}$ of 15.5 grams was grown using Bridgman method. We performed elastic and inelastic neutron scattering using the cold-neutron triple-axis spectrometer SIKA, ANSTO. The collimations were Open-20'-20'-60' with vertically focusing monochromator. The final neutron energy was fixed to 2.75 meV. Pyrolytic graphite 002 reflections were used for monochromator and analyzer. The sample was mounted on the aluminum plate, aligned with 110 and 001 in the scattering plane. The vertical superconducting magnet was used in the experiment, applying external magnetic field along the $\bar{1}10$ direction.

From elastic neutron measurement, we obtained the modulation vector and the helical ordering temperature as $k = 0.0462 \text{ \AA}^{-1}$ and $T_c = 32 \text{ K}$, respectively. The obtained modulation vector and the helical ordering temperature are larger compared to MnSi ($k = 0.036 \text{ \AA}^{-1}$ and $T_c = 29.5 \text{ K}$). In the inelastic neutron measurement, the magnetic excitation in the skyrmion-lattice phase was measured at Γ , M , and their midpoint at $T = 30.5 \text{ K}$ and $H = 0.2 \text{ T}$. Shown in the figure is the representative magnetic excitation spectrum observed at the midpoint. Broad inelastic peak can be seen around $\hbar\omega \sim 0.13 \text{ meV}$. We confirmed that this excitation is intrinsic in the skyrmion-lattice phase, by comparing it to the excitation spectra both in the fully-polarized and helical phases. Detailed analysis, including theoretical estimation of the magnon scattering intensity in the skyrmion-lattice phase, is in progress.

[1] S. Mühlbauer *et al.* Science 323, 915-919 (2009); [2] K. A. van Hoogdalem *et al.*, Phys. Rev. B 87, 024402 (2013).

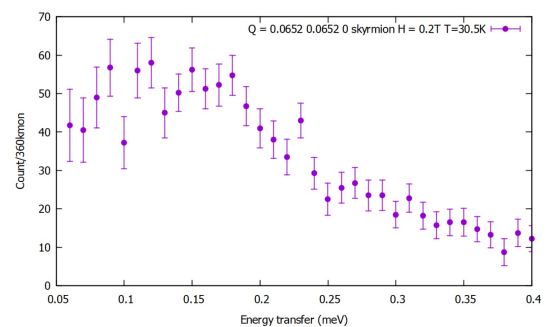


Fig. 1. Neutron inelastic spectrum at the mid point of the Γ and M points observed in the magnetic skyrmion-lattice phase

Neutron diffraction study on the Pd-Ga-Tb 2/1 quasicrystal approximant

Taku J. Sato, Maxim Avdeev(A), Kyohei Takagi(B), and Yeong-Ge So(B)
IMRAM, Tohoku University, (A)ANSTO, (B)Akita University

Quasicrystal is a substance with long-range quasiperiodic atomic arrangement, nonetheless, with the rotational symmetry that is prohibited in the periodic crystals, such as the five-fold symmetry. The quasicrystal is, therefore, different from periodic crystals and random glasses, and now is regarded as the third form of solids. There is a class of crystals, called “approximants”, in which the high-symmetry (such as icosahedral) atomic clusters, identical to those in the quasicrystals, form periodic array, and thus being approximation of the quasicrystalline structure. The degree of approximation is expressed by the fractional numbers, such as 1/1 and 2/1. The 1/1 approximant is the lowest order approximation, in which the atomic clusters form a bcc cubic lattice. The 2/1 approximant has a larger unit cell, becoming a better approximation to the quasicrystal. As the fractional number becomes the irrational golden ratio $\tau \sim 1.618\dots$, the unit cell becomes infinitely large, i.e. quasicrystal.

Recently, for the first time we have determined magnetic structure of the antiferromagnetic 1/1 Au-Al-Tb approximant using ECHIDNA [1], which turns out to be a very intriguing non-collinear and non-coplanar whirling order. Quite recently, one of the proposers further found a magnetic 2/1 approximant in the Ga-Pd-Tb system, which orders antiferromagnetically at 5.8 K [2]. This is definitely the first 2/1 approximant that shows antiferromagnetic long-range order, which excites us enough to perform this neutron powder diffraction study.

A polycrystalline alloy of the Pd-Ga-Tb 2/1 approximant was prepared by arc melting with high purity (> 99.9 wt%) Pd, Ga and Tb elements. The neutron powder diffraction experiment has been performed using the high-resolution powder

diffractometer ECHIDNA installed at the OPAL reactor, Australian Nuclear Science and Technology Organisation [3]. For most of the magnetic diffraction measurement, neutrons with $\lambda = 2.4395$ Å was selected using the Ge 311 reflections, whereas for the structure analysis, to obtain reflections in a wide Q -range, we select $\lambda = 1.622$ Å using the Ge 335 reflections. The sample was set in the $\phi 6$ mm vanadium sample can, and then set to the cold head of the closed cycle ^4He refrigerator with the base temperature 3.5 K.

Figure shows the overall diffractograms at various temperatures ranging from the base ($\simeq 3.5$ K) to the paramagnetic temperature 7 K. One can clearly see the development of sharp magnetic reflections below 5 K. They are the clear indication of magnetic long-range order in this 2/1 approximant. We further note that the magnetic reflection appearing at $2\theta \simeq 21.9$ degrees is relatively weak, compared to that observed in the Au-Al-Tb 1/1 approximant [1]. On the other hand, quite a few magnetic reflections can be seen in the Pd-Ga-Tb 2/1 approximant, number of which is much larger than that in the Au-Al-Tb 1/1 approximant. These results suggest that the magnetic structure would be much more complicated in the Pd-Ga-Tb 2/1 approximant, and is of significant interest in view of larger unit cell of the 2/1 approximant. The magnetic structure analysis using the representation analysis is in progress.

[1] T. J. Sato *et al.* (submitted); [2] Y. -G. So *et al.* (in preparation); [3] M. Avdeev and J. R. Hester, *J. Appl. Crystallogr.* 51, 1597 (2018).

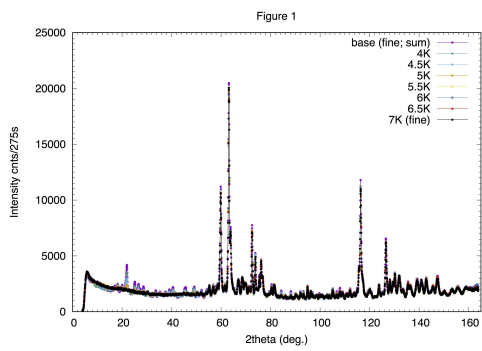


Fig. 1. Neutron diffraction patterns obtained in the temperature range $4 < T < 7$ K at ECHIDNA.

Neutron diffraction study on the $\text{Yb}_3\text{Ru}_4\text{Al}_{12}$ itinerant kagome antiferromagnet

Taku J Sato, Noriyuki Kabeya(A), Maxim Avdeev(B), Shintaro Nakamura(C),
and Akira Ochiai(A)

*IMRAM Tohoku University, (A)Dept. Phys. Tohoku University, (B)ANSTO,
and (C)IMR Tohoku University*

Geometrically frustrated spin systems have been studied extensively for decades because of many intriguing phenomena, exemplified by the non-magnetic quantum disordered states. Despite a large number of both experimental and theoretical studies, the ground states and excitations in geometrical frustrated quantum magnets are still largely unrevealed. This is the case for kagome compounds where even theoretically the ground state is controversial with gapped (such as Z2 spin liquid) or gapless (U(1) Dirac spin liquid) states. Experimentally, on the other hand, due to the small number of model compounds, the work is further less conclusive, and much efforts have been devoted to find out new model materials possessing the geometrically frustrated lattices. Recently, a new direction has been taken to discover new frustrated systems in Yb^{3+} rare-earth ions; several reports indicate quantum nature of the Yb^{3+} rare-earth magnetism, such as spinon continuum in quasi-one-dimensional Yb_4As_3 [1] and $\text{Yb}_2\text{Pt}_2\text{Pb}$ [2]. The key ingredient of such quantum spin formation is doubly degenerated ground states (pseudo spin 1/2) made of strongly coupled L and S . Hence, there now appears a chance to study geometrically frustrated quantum magnetism using Yb-based compounds. The present proposer group found a Yb^{3+} based compound $\text{Yb}_3\text{Ru}_4\text{Al}_{12}$ [3], which has an archetypal frustrated lattice, called breathing kagome lattice. This compound shows intriguing low-dimensional frustrated behavior [3], and hence, we have investigated microscopic magnetism using powder neutron diffraction.

A polycrystalline alloy of $\text{Yb}_3\text{Ru}_4\text{Al}_{12}$ was prepared by crushing the single crystals. The neutron powder diffraction

experiment has been performed using the high-resolution powder diffractometer ECHIDNA installed at the OPAL reactor, Australian Nuclear Science and Technology Organisation [4]. For most of the magnetic diffraction measurement, neutrons with $\lambda = 2.4395 \text{ \AA}$ was selected using the Ge 311 reflections, whereas for the structure analysis, to obtain reflections in a wide Q -range, we select $\lambda = 1.622 \text{ \AA}$ using the Ge 335 reflections. The sample was set in the $\phi 4$ mm Cu sample can, and then set to the cold head of the ^3He one-shot-type refrigerator with the base temperature 0.37 K. For the high- T (6.5 K), base- T and intermediate- T ($T_{\text{set}} = 1.6$ K) scans, the total data acquisition time was 15 hours.

Figure shows the comparison of the diffraction patterns in the 2θ -range of $10 < 2\theta < 60$ degrees observed at the three temperatures. Clearly, magnetic signal develops at $2\theta \simeq 15^\circ$ and 18.5° at low temperatures. We note that $2\theta \simeq 15^\circ$ corresponds to the (0,0,1) (forbidden) nuclear reflection position, indicating that the magnetic structure is antiferromagnetic along the c -axis. The 18.5° peak corresponding to the (1,0,0) position. While magnetic signal was clearly observed in the low temperature phase, the nature of the intermediate phase is still unclear, but some hints may be obtained by carefully analyzing the present dataset. Magnetic structure analysis of the base-temperature phase is in progress, while we look for a way to elucidate nature of the intermediate phase, too. [1] M. Kohgi, K. Iwasa, J.-M. Mignot, A. Ochiai, and T. Suzuki, Phys. Rev. B 56, R11388 (1997); [2] L. S. Wu, W. J. Gannon, I. A. Zaliznyak, A. M. Tselvik, M. Brockmann, J.-S. Caux, M. S. Kim, Y. Qiu, J. R. D. Copley, G. Ehlers, A. Podlesnyak, and

M. C. Aronson, Science 352, 1206 (2016); [3] S. Nakamura, S. Toyoshima, N. Kabeya, K. Katoh, T. Nojima and A. Ochiai, Phys. Rev. B 91, 214426 (2015); [4] M. Avdeev and J. R. Hester, J. Appl. Crystallogr. 51, 1597 (2018).

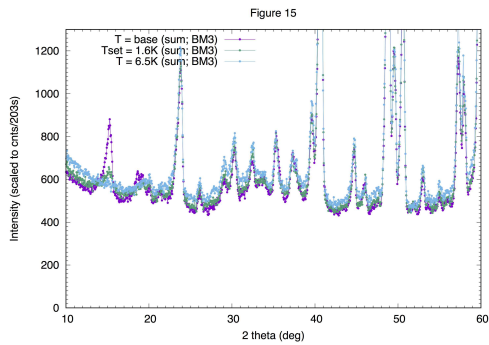


Fig. 1. Neutron diffraction patterns at the base temperature, 1.6 K and 6.5 K obtained at ECHIDNA. The temperatures are the “set” temperatures, and actual temperatures were slightly lower.

Dynamics of the magnetic skyrmion under an alternative current in MnSi

D. Okuyama(A), M. Bleuel(B), Q. Ye(B), A. Kikkawa(C), Y. Taguchi(C), Y. Tokura(C,D)
D. Higashi(A), J. D. Reim(A), Y. Nambu(E), and T. J. Sato(A)

(A)IMRAM, Tohoku Univ., (B)NCNR, NIST, (C)RIKEN-CEMS, (D)Univ. of Tokyo, (E)IMR,
Tohoku Univ.

A magnetic skyrmion is swirling spin texture characterized by a discrete topological number, called the skyrmion number. In experiment, magnetic skyrmions quite often condensate in the triangular-lattice form, giving rise to six-fold magnetic Bragg reflections in small angle neutron scattering (SANS) patterns, as first discovered by Muhlbauer et al. in the prototypical chiral magnet MnSi [1]. To date, the skyrmion lattice structures are widely confirmed in various magnets ranging from metallic to insulating compounds. There are several prominent characteristics in magnetic skyrmions that make them quite intriguing. One of such characteristics is its topological protection; once created, the skyrmion can hardly be annihilated. In metallic skyrmion compounds, there is another important characteristic, i.e., its surprisingly large coupling with the electric current flow. The electric current density required to realize the skyrmion lattice motion is considerably small as $j \sim 1$ MA/m² [2]. Hence, the magnetic skyrmion attracts growing attention recently, and is under intense scrutiny for elucidating its dynamical behavior under electric current.

To investigate the dynamics of the magnetic skyrmion lattice under the electric current flow, we performed SANS experiment with suppressing the thermal gradient as much as experimentally achievable. SANS experiments were carried out at NG7 (National Institute of Standards and Technology). The incident neutron wave-length was selected using the velocity selector as $\lambda_i = 6$ Å. An direct or alternative electric current with square wave was applied along the [0 0 1] direction. The sample mount was attached to the sample stick, and was installed in the horizontal

field magnet with the magnetic field applied along [1 -1 0] parallel to the incident neutron beam.

We observed the six-fold magnetic skyrmion reflections at 28.6 K, respectively, under $B = 0.2$ T and $j = 0$ MA/m². By comparing to SANS data at $j = 0$, one can clearly see considerable broadening of the skyrmion-lattice peaks in the azimuthal direction. The peak broadening is apparently temperature dependent; the width is considerably larger at $T = 28.3$ K compared to that at $T = 28.6$ K. This result clearly indicates significant deformation of the skyrmion lattice under large electric current. To investigate the origin of the broadening of the skyrmion reflections, we performed SANS measurements on the left-edge (+) or right-edge (-) of the sample. The size of the neutron illumination area is approximately 0.2 mm (width) \times 1.0 mm (height). The observed patterns are identical for the two edges. In marked contrast to the zero-current condition, under $j = 2.7$ MA/m² the reflection patterns taken from the left- and right-edge parts exhibit counterclockwise and clockwise rotations, respectively. The effect of inverting the current and magnetic-field directions was also investigated. The rotation direction does not change by inverting the magnetic field direction. On the other hand, the inversion of the current direction (from $j = +2.7$ to -2.7 MA/m²) results in a sign change of the rotation angle. This indicates that the skyrmion-lattice rotation observed in the thermally homogeneous condition depends not on the magnetization direction, but only on the current direction [3]. To observe the time dependence of the magnetic skyrmion rotation, we also performed the SANS experiment with applying the alter-

native electric current. The observed relaxation time of the skyrmion rotation is several seconds order, which is the very slow dynamics as a magnetic material.

In summary, we have used SANS to study skyrmion-lattice motion in bulk MnSi under electric current flow. The azimuthal width of the skyrmion-lattice peaks shows significant broadening above a threshold current density $jt \sim 1 \text{ MA/m}^2$. We show this peak broadening originates from a spatially inhomogeneous rotation of the skyrmion lattice, that shows opposite senses of rotation at the sample edges.

Reference:

[1] S. Muhlbauer, B. Binz, F. Jonietz, C. Pfleiderer, A. Rosch, A. Neubauer, R. Georgii, and P. Boni, *Science* 323, 915 (2009).

[2] F. Jonietz, S. Muhlbauer, C. Pfleiderer, A. Neubauer, W. Munzer, A. Bauer, T. Adams, R. Georgii, P. Boni, R. A. Duine, K. Everschor, M. Garst, and A. Rosch, *Science* 330, 1648 (2010).

[3] D. Okuyama, M. Bleuel, J.S. White, Q. Ye, J. Krzywon, G. Nagy, Z.Q. Im, I. Zivkovic, M. Bartkowiak, H.M. Ronnow, S. Hoshino, J. Iwasaki, N. Nagaosa, A. Kikkawa, Y. Taguchi, Y. Tokura, D. Higashi, J.D. Reim, Y. Nambu, and T.J. Sato, accepted in *Commun. Phys.*; arXiv:1807.07388.

Determination of the spin system in $\text{Ni}_2\text{V}_2\text{O}_7$ using neutron diffraction in magnetic fields

Masashi Hase Matsuo¹, James R. Hester², and Kirrily C. Rule²

¹National Institute for Materials Science (NIMS), ²Australian Nuclear Science and Technology Organisation (ANSTO)

Neutron diffraction has made great contribution to studies of magnetism because magnetic structures can be determined. We can also study magnetism in paramagnetic states by combining neutron diffraction and magnetic fields. Magnetic moments are induced by magnetic fields and generate magnetic reflections. In a magnet with plural crystallographical magnetic-ion sites, we can evaluate a field-induced magnetic moment (magnetization) on each site from analyses of the magnetic reflections.

Our objective in this study is to show that neutron diffraction in magnetic fields is a powerful tool to determine spin systems. We investigated $\text{Ni}_2\text{V}_2\text{O}_7$ as an example. We briefly summarize the magnetism of $\text{Ni}_2\text{V}_2\text{O}_7$ [1]. Magnetic phase transitions occur at $T_{\text{N1}} = 6.7$ and $T_{\text{N2}} = 5.7$ K. The magnetic structures have not been determined. A 1/2 quantum magnetization plateau was observed between 8 and 30 T at 2 K. There are two crystallographical Ni^{2+} -ion sites having spin-1. There are three types of short Ni-Ni pairs having antiferromagnetic exchange interactions. A few sets of the values were reported and were inconsistent with one another [1,2].

In order to determine the spin system (the values of the exchange interactions) in $\text{Ni}_2\text{V}_2\text{O}_7$, we performed neutron diffraction experiments on $\text{Ni}_2\text{V}_2\text{O}_7$ pellets using the WOMBAT diffractometer and the AVM-1 magnet. We can see several magnetic reflections in a difference pattern made by subtracting a neutron powder diffraction pattern at 10 K in 0 T from that at 1.8 K in 0 T. We infer an incommensurate magnetic structure from the positions of the magnetic reflections.

Figure 1 shows a difference pattern made

by subtracting a neutron powder diffraction pattern at 20 K in 10 T from that at 1.8 K in 10 T. As described, the 1/2 quantum magnetization plateau appears above 8 T at low temperature. Therefore, the state at 1.8 K in 10 T is a kind of paramagnetic state (without magnetic long-range order). We can see several magnetic reflections generated by field-induced magnetic moments. The red circles indicate intensities of magnetic reflections calculated in the case that $M2/M1 = 5$. Here, M1 and M2 are the magnitude of field-induced magnetic moments on Ni1 and Ni2 sites, respectively. The calculated intensities seem consistent with the experimental ones. Several reflections indicated by triangles, however, cannot be explained by the field-induced magnetic moments. The magnetic reflections at 1.8 K in 0 T seem to remain, suggesting the coexistence of the two phases.

We measured difference patterns at 1.8 K in several magnetic fields. As the magnetic field increases, the intensities of the magnetic reflections at 1.8 K in 0 T and those generated by field-induced magnetic moments decrease and increase, respectively. We can see magnetic reflections that are different from those in 0 and 10 T at 1.8 K. Probably, the indices of the magnetic reflections are integers. The intensity of the magnetic reflections increases with increasing magnetic field and is strongest around 6 to 8 T, suggesting another magnetic long-range order in finite magnetic fields below the magnetization-plateau fields. The magnetic reflections disappear in 10 T.

We will determine the magnetic structures in zero and finite magnetic fields and evaluate M1 and M2 at 1.8 K in 10 T. We will be able to determine the spin system

(the values of the exchange interactions).

[1] Z. W. Ouyang et al., Phys. Rev. B. 97, 144406 (2018).

[2] Y. C. Sun et al., Eur. Phys. J. Plus 131, 343 (2016).

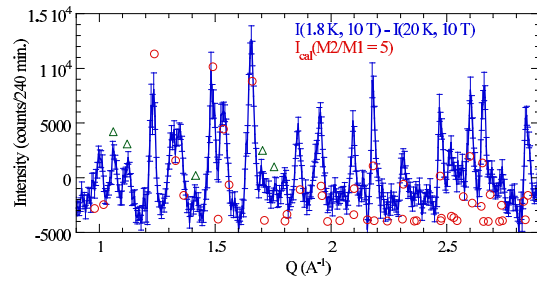


Fig. 1. A difference pattern made by subtracting a neutron powder diffraction pattern at 20 K in 10 T from that at 1.8 K in 10 T.

Full control of magnetic moment in multiferroics Ba₂CoGe₂O₇

Shunsuke Hasegawa and Takatsugu Masuda

ISSP, the University of Tokyo

Electric control of magnetic moment is an intriguing topic in condensed matter physics since it can be applied to a novel device. Coexistence of magnetic order and electric polarization, multiferroicity, has a possibility to realize such a control. So far spin helicity was controlled in TbMnO₃ [1] and magnetic domain was controlled in Hexaferrite [2], but controlling local magnetic moment by applying electric field has not been demonstrated yet. Ba₂MGe₂O₇ ($M = \text{Co, Mn}$) are multiferroic compounds with spin-dependent $p - d$ hybridization mechanism [3]. The crystal structure is a tetragonal and the space group is P-421m. Below $T_N = 6.7$ K, the spin antiferromagnetically lies along the crystallographic a axis, and the electric polarization antiferroelectrically lies along the c axis. It is expected that the applying electric field along the c axis changes the antiferroelectric state to ferroelectric state with the magnetic moment rotating from [100] to [110]. Soda et al. demonstrated the rotation of the magnetic moment in the ab plane [4], but the moment did not make complete rotation by 45 degrees due to a large in-plane magnetic anisotropy. It was only 6 degrees at $T = 1.5$ K and $E = 1.5$ MV/m at best. Then we performed a similar experiment on Ba₂MnGe₂O₇ [5] having smaller anisotropy energy at PSI. The rotation of the magnetic moment was observed at 1.5 K, and the angle as large as 20 degrees was achieved by increasing the temperature. The perfect rotation of 45 degrees was, however, not achieved because of the short of the electric field. It should be noted that a non-linear behavior was observed in the field dependence of the rotation angle, and a non-trivial plateau was found at $2 \text{ MV/m} < E < 5 \text{ MV/m}$, even though a simple linear behavior was expected [4]. Even though the anisotropy energy of Ba₂MnGe₂O₇ is

smaller than that of Ba₂CoGe₂O₇, the electric polarization is also smaller, resulting in the smaller rotation angle at the same electric field at the base temperature: 1.5 degree for Ba₂MnGe₂O₇ and 6 degrees for Ba₂CoGe₂O₇ at $E = 1.5$ MV/m. Use of Ba₂CoGe₂O₇ is better choice. We have done the Polarized Neutron Diffraction to achieve the perfect rotation by applying stronger electric field on thinner Ba₂CoGe₂O₇ sample and by reducing the anisotropy energy at high temperature. Then we tried to detect non-trivial field dependence of the rotation angle of the magnetic moment to understand. A single crystal sample was grown by the floating-zone method. The single crystal was aligned so that the crystallographic ab plane was in the horizontal plane. For the single crystal with a thickness of 2.65 mm, aluminum electrodes were deposited onto the faces of (001) to apply the electric field. The sample was set in the Al sample can, and then sample space was vacuumed. Maximum voltage in the used equipment was 7.0 kV. Heusler alloy was used to obtain the polarized neutrons with the energy of 13.5 meV. Magnetic Bragg peaks are observed below T_N . From the analysis of the peaks, it is found that the easy-plane type antiferromagnetic structure having a magnetic propagation vector $\mathbf{k}_{mag} = (0, 0, 0)$ is realized, which is consistent with the previous report [6]. Since the sample has crystallographic domains, we performed the $\theta - 2\theta$ scan at maximum point of omega scan in order to estimated integrated intensity. $(h, k, l) = (2, 1, 0)$ and its equivalent reflections were measured to investigate the electric field and temperature dependence. We assume that the magnetic moments continuously rotate from [100] (or [010]) to [110] directions when the antiferroelectric state becomes the ferroelectric state retaining an-

tiferromagnetic structure by applying the electric field along the c axis as same as the previous report [4]. Under this assumption the intensity variation at $(2, 1, 0)$ and its equivalent position is represented by the sinusoidal curve as follows:

$$I \propto 1 + \sin 2\theta \sin 2\omega \quad (1)$$

where I is the intensity of each magnetic reflections, and the ω is a rotation angle of the magnetic moment from $[100]$ or $[010]$ to $[110]$. The θ is the angle between the scattering vector and a axis. The rotation angle of the magnetic moment is evaluated from the amplitude of the sinusoidal curve. Figure 1 shows electric field dependences of the normalized magnetic intensities as a function of θ at 1.5 K. Normalized magnetic intensities were got from intensities divided by the average of intensities which were evaluated from magnetic intensities divided nuclear intensities at same Q position. The data show a sinusoidal curve at each electric field like equation (1). The amplitude increases with increase of the electric field, which means that the rotation angle of magnetic moment increases with. From fitting the data by equation (1), we obtained the rotation angle of magnetic moment against the electric field at 1.5 K, 6.0 K and 6.3 K. At 1.5 K data, the rotation angle is almost consistent with previous report. The rotation angle at 6.0 K and 6.3 K was reproduced by the theoretical calculation at 1.5 K in previous study [4], even though we apply higher electric field. This means that the controllability of magnetic moment is independence of temperature. Furthermore, non-trivial field dependence of the rotation angle of the magnetic moment was not observed.

[1] Y. Yamasaki et al., Phys. Rev. Lett. 98, 147204 (2007). [2] S. Ishiwata et al., Science 319, 1643 (2008). [3] H. Murakawa et al., Phys. Rev. B 85, 174196 (2012). [4] M. Soda et al., Phys. Rev. B 94, 094418 (2016). [5] T. Masuda et al., Phys. Rev. B 81, 100402 (2010). [6] A. Zheludev *et al.*, Phys. Rev. B 68, 024428 (2003).

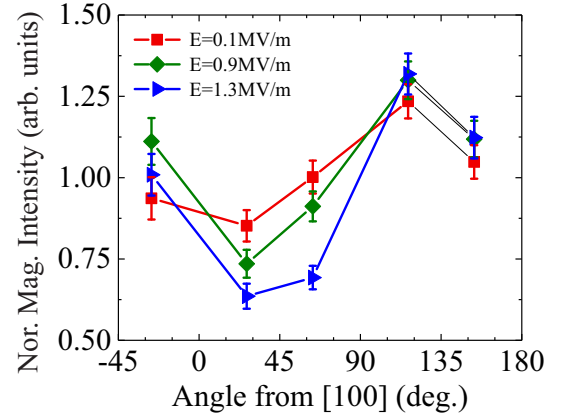


Fig. 1. Electric field dependences of normalized magnetic intensity at 1.5K.

Quantum spin liquid state of $\text{Tb}_{2+x}\text{Ti}_{2-x}\text{O}_{7+y}$

H. Kadowaki^A, B. Fåk^B, J. Ollivier^B, T. J. Sato^C

^A*Department of Physics, Tokyo Metropolitan University, Hachioji, Tokyo 192-0397*

^B*Institute Laue Langevin, BP156, F-38042 Grenoble, France*

^C*IMRAM, Tohoku University, Sendai*

Geometrically frustrated magnets have been actively studied in recent years [1]. These include classical and quantum spin systems on two-dimensional triangular [2] and kagome [3] lattices, and three-dimensional pyrochlore-lattice systems [4]. For classical systems, prototypes of which are the triangular-lattice antiferromagnet [2] and the spin ice [5], many investigations have been performed for a few decades using a number of theoretical and experimental techniques [1]. Possibilities of quantum spin liquid (QSL) states in frustrated magnets, which date back to the theoretical proposal of the RVB state [6], are recently under hot debate. Highly-entangled many-body wave functions without magnetic long-range order (LRO), anticipated in QSL states, provide theoretically challenging problems [7]. Experimentally, finding out real QSL substances, e.g. [8], and investigating QSL states using available techniques, e.g. [9], have been attracting much interest. However, to date, nobody has found clear evidence of a QSL state, despite many trial experiments performed in the past decade [7,9].

A non-Kramers pyrochlore system $\text{Tb}_2\text{Ti}_2\text{O}_7$ (TTO) has attracted much attention since an interesting report of absence of magnetic LRO down to 0.1 K [10], which could be interpreted that TTO is a QSL candidate or quantum spin ice (QSI) [11]. On the other hand, a phase transition at $T_c \sim 0.5$ K detected by a specific heat peak suggesting a hidden LRO [12], seemed to contradict with the QSL interpretation. We resolved this contradiction by showing that ground states of TTO are highly sensitive to off-stoichiometry, i.e., x (and/or y) of $\text{Tb}_{2+x}\text{Ti}_{2-x}\text{O}_{7+y}$ [13], and that there are two ground states: an electric quadrupole

ordered (QO) state ($x > x_c \sim -0.0025$) and the putative QSL state ($x < x_c$) [14] (Fig. 1 inset).

We now think that the QO state proposed in Ref. [14] or its variant likely account for the hidden LRO of TTO. On the other hand, the long-standing question of “what is the putative QSL state of TTO?” or even a simpler question of “is it really a QSL state?” are still difficult problems for present-day experimental techniques, which are not well optimized for studying QSL states. For example, in Fig. 1 we show inelastic neutron scattering (INS) spectra of TTO samples carried out at 0.1 K on IN5 and AMATERAS, which are normally known as good-energy-resolution spectrometers [16]. The energy spectrum of the QSL powder sample with $x = -0.005$ shown in Fig. 1 looks as though there are both elastic and inelastic scattering contributions. However, if this sample is in a QSL state at 0.1 K, this elastic scattering should be (at least partly) inelastic scattering with a very small energy scale [17,18].

Recently we proposed to perform INS experiments on $x = -0.005$ (QSL) and 0.005 (QO) powder samples using the extremely good energy-resolution ($\Delta E \sim 1 \mu\text{eV}$) spectrometers IN16B and HFBS, which have not commonly been used for studies of QSL states. Thereby, we have a good chance to observe that the seemingly elastic scattering shown in Fig. 1 is (partly) inelastic scattering, which consequently proves that the putative QSL TTO sample is definitely in a QSL state at $T = 0$. In addition, by simply comparing quasi-elastic spectra of the QSL and QO samples, distinct difference due to the two ground states can be observed. We performed an ILL-DDT

experiment (2018 May) of the QSL sample using IN16B, which shows interesting experimental data. However an NCNR-QAP experiment (2018 Aug.) of the QO sample using HFBS was not successful owing to large instrumental background. Now we are waiting for another experiment of the QO sample using DNA (J-PARC) to answer the questions.

- [1] C. Lacroix et al. Introduction to Frustrated Magnetism (Springer, Berlin, Heidelberg, 2011).
- [2] G. H. Wannier, Phys. Rev. 79, 357 (1950).
- [3] I. Syôzi, Prog. Theor. Phys. 6, 306 (1951).
- [4] J. S. Gardner et al. Rev. Mod. Phys. 82, 53 (2010).
- [5] S. T. Bramwell and M. J. P. Gingras, Science 294, 1495 (2001).
- [6] P. W. Anderson, Mater. Res. Bull. 8, 153 (1973).
- [7] L. Savary and L. Balents, Rep. Prog. Phys. 80, 016502 (2017).
- [8] K. Hirakawa, H. Kadowaki, K. Ubukoshi, J. Phys. Soc. Jpn. 54, 3526 (1985).
- [9] B. Fåk et al. Phys. Rev. B 95, 060402 (2017); Y. Shen et al. Nature 540, 559 (2016); Z. Zhu et al. Phys. Rev. Lett. 119, 157201 (2017).
- [10] J. S. Gardner et al. Phys. Rev. Lett. 82, 1012 (1999).
- [11] H. R. Molavian et al. Phys. Rev. Lett. 98, 157204 (2007).
- [12] N. Hamaguchi et al. Phys. Rev. B 69, 132413 (2004).
- [13] T. Taniguchi, H. Kadowaki, B. Fåk, J. Ollivier et al. Phys. Rev. B 87, 060408(R) (2013).
- [14] H. Takatsu, S. Kittaka, A. Kasahara, Y. Kono, T. Sakakibara, Y. Kato, S. Onoda, B. Fåk, J. Ollivier, J.W. Lynn, T. Taniguchi, M. Wakita, H. Kadowaki, Phys. Rev. Lett. 116, 217201 (2016).
- [15] M. Wakita, T. Taniguchi, H. Edamoto, H. Takatsu, H. Kadowaki, J. Phys. CS 683, 012023 (2016).
- [16] H. Kadowaki, M. Wakita, B. Fåk, J. Ollivier, S. Ohira-Kawamura, K. Nakajima, H. Takatsu, M. Tamai, J. Phys. Soc. Jpn. 87, 064704 (2018); H. Kadowaki, M. Wakita, B. Fåk, J. Ollivier, S. Ohira-Kawamura, K. Nakajima, J. W. Lynn, Phys. Rev. B 99, 014406 (2019).
- [17] M. Hermele et al., Phys. Rev. B 69, 064404 (2004).
- [18] C-J. Huang et al. Phys. Rev. Lett. 120, 167202 (2018); Y. Kato and S. Onoda, Phys. Rev. Lett. 115, 077202 (2015).

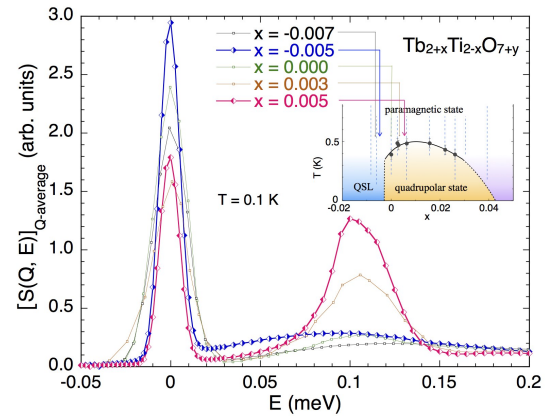


Fig.1 Energy spectra $S(Q,E)$ averaged in a wide Q -range taken using crystal samples ($x = -0.007, 0.000, 0.003$) and powder samples ($x = -0.005, 0.005$) [16]. Inset shows the x - T phase diagram of Ref. [15].

Fig. 1.

STRONGLY CORRELATED ELECTRON SYSTEM

Investigation of vortex lattices on non-centrosymmetric superconductor LaNiC₂

M. Soda, V. Ryukhtin, P. Strunz, and H. Furukawa
RIKEN, Nuclear Physics Institute, Ochanomizu University,

Non-centrosymmetric superconductor LaNiC₂ attracts high interest in last decade due to rather unusual nature of superconductivity. It was supposed that lanthanum atoms participate to Cooper pair creation, because C is non magnetic and Ni magnetic contribution is practically zero [1]. Although, conventional superconductors can only have one spin states (either singlet or triplet) due to Pauli's principle and law of parity conservation, superconductors without inversion symmetry, however, can have a mixed spin states [2]. It was concluded from resistivity measurements at low T that the non-centrosymmetric compound LaNiC₂ as a nonmagnetic and weakly-correlated superconductor with two-gap Bardeen-Cooper-Schrieffer.

We have used SANS-1 instrument installed at PSI for vortex lattice (VL) structure of mixed state in LaNiC₂ measurements. Magnetic field H was applied along main crystal axes during the measurements. Angular scans were performed at 20 m from sample to detector. Wavelength was set to 12 Å or 8 Å depending on magnetic field value.

Structures of VL measured at H = 0.1 T is shown in Fig. 1. The data were collected with scanning over vertical axis by 0.2 degree, summed up, and corrected by background data collected using same scan.

The observed measurements show that vortex structure changes from triangle at H parallel to a-axis (Fig. 1(a)) to square lattice at H//c or H//b (Figs. 1(b) and 1(c)). One can see that VL structure is correlated with positioning of La atoms in orthorhombic cell for corresponded projection. The plane with lanthanum atoms (green spheres in Figs. 1 (d-f)) in triangu-

lar symmetry form triangular VL (Fig. 1 (a, d)) as it was measured by H//a. In case of orientations H//b, H//c lanthanum atoms arranged rectangular in plane perpendicular to H (Fig. 1(e), (f)) and resulted VL structures contain four spots.

Temperature dependencies of vortex spot intensities were measured for several magnetic fields in order to study important characteristic of superconductivity: coherence length, penetration depth, full gap/nodal state and superconducting symmetry. At this moment, we try to analyze the data.

[1] P. Kotsanidis, J. Yakinthos, and E. Gamari-Seale: *J. Less-Common Met.* 152 (1989) 287.

[2] V.M. Edel'stein: *Sov. Phys. JETP*68 (1989) 1244.

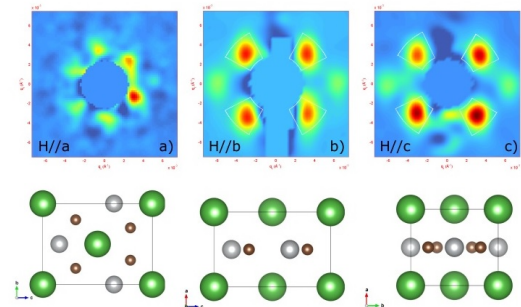


Fig. 1. VL as measured at 1000 Oe with magnetic field applied along main axis of LaNiC₂ (a-c) and corresponding projection of crystal (d-f).

Investigation of magnetic ordering in high pressure phase of DyMnO₃

Noriki Terada(A), Navid Qureshi(B), Mechthild Enderle(B), Fabio Orlandi(C), Dmitry Khalyavin(C), Pascal Manuel(C) and Dharmalingam Prabhakaran(D)

(A)National Institute for Materials Science, (B)ILL, (C)ISIS and (D)University of Oxford

Abstract: In the experiments, we have succeeded in measuring the pressure dependence of the magnetic k -vector and polarization matrices of multiferroic DyMnO₃ under high pressure condition, by using the WISH TOF diffractometer and the CryoPAD apparatus on IN20 beamline in combination with our developed Hybrid-Anvil-Cell (HAC). This experiment determined the pressure dependence of some of neutron polarization matrices as well as magnetic propagation vector up to 5 GPa.

Unpolarized and polarimetry neutron experiments were carried out using WISH at ISIS and IN20 at ILL. Single crystal samples of DyMnO₃ for both the experiments, grown by the floating zone technique, were cut into rectangular shapes with dimension of $0.5 \times 0.5 \times 0.2$ mm³ for experiments up to 5 GPa. The crystal qualities were kept even under pressure up to 5.0 GPa, by using glycerin as the pressure transmission medium. The cut samples were mounted in the HAC with the a -axis vertical, in order to provide access to the monoclinic $(0, K, L)$ reflections. For the polarimetry experiment on IN20, the incident neutrons are polarized and monochromatized at the Heusler monochromator. The incident wavelength 1.53 Å was employed. A sapphire anvil with a 2.4 mm diameter culet, supported by MP35N was used.

In the experiment on WISH and IN20 in July and September 2018, we succeeded in measuring the pressure dependence of k -vector and neutron polarization matrix up to 5 GPa. We could observe tendency that one of matrix elements, P_{yy} , significantly changes above 4 GPa, which indicates that Dy spin ordering gradually changes from spiral to collinear structure. However, in the previous experiments on IN20, due to limitation of machinetime, I have not mea-

sured the complete set of pressure dependence beyond 5 GPa.

In conclusion, we have determined the pressure dependence of the d -vector and polarization matrix elements. However, it is necessary to perform additional experiments to make this complete and clarify the magnetic ordering for higher pressure phase with the giant electric polarization in DyMnO₃.

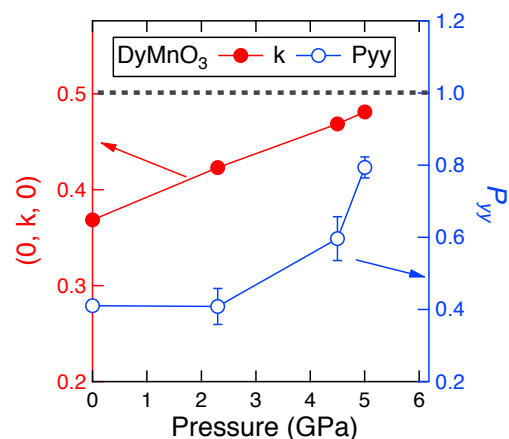


Fig. 1. Pressure dependence of propagation wave number k and polarization matrix element P_{yy} . The data were measured in the previous measurements on IN20.

Nesting features and the superconducting mechanism in Ce(Co,Rh)In5

Kanae Shinohara
Ochanomizu University

Heavy-fermion superconductor CeMIn5 (M=Co, Rh, Ir, tetragonal structure, space group P4/mmm) has been studied to understand relationship between the magnetism and the unconventional superconductivity. Neutron experiments revealed that CeCoIn5 ($T_c \sim 2.3$ K) shows a resonance peak at $(1/2, 1/2, 1/2)$ [1], and CeRhIn5 ($T_N \sim 4$ K) has an incommensurate magnetic order with a propagation vector of $q = (1/2, 1/2, 0.297)$ [2]. Mixed crystal CeRh $_{1-x}$ Co $_x$ In5 in the middle x region possesses a commensurate magnetic order with the $q = (1/2, 1/2, 1/2)$, and this requests that the superconductivity realized in the middle x region uses a different fermi surface if they use and that the resonance peak should move to some other q position.

To check the q position of the resonance peak in CeRh $_{1-x}$ Co $_x$ In5 with the middle x region, we carried out an inelastic neutron scattering experiment. For this experiment, we prepared a co-aligned mosaic of the single crystals of CeRh $_{0.6}$ Co $_{0.4}$ In5 with the total volume ~ 3 g with $(h h l)$ -scattering plane because we expected that resonance peak would appear in $q = (1/2, 1/2, l)$. Neutrons with $E_i = 3.8$ meV and Fermi chopper speed 240 Hz were used. We measured scattering data at 0.3 K, 2 K, 5 K, 50 K which correspond to the SC + AFM phase, the AFM phase, normal phase, normal phase at high temperature using for background, respectively. We are now analyzing data carefully.

This travel was done with a financial support by ISSP, University of Tokyo. We appreciate it pretty much since it could not be done without it.

References

- [1] C. Stock et al., Phys. Rev. Lett. 100, 087001 (2008).
- [2] W. Bao et al., Phys. Rev. B 62 (2000) R14621; Phys. Rev. B 67 (2003) 099903(E).

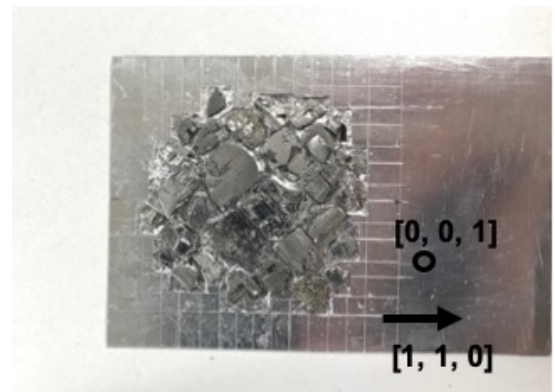


Fig. 1. Fig1. Co-aligned single crystals of CeRh $_{0.6}$ Co $_{0.4}$ In5

BIOLOGY

Elucidation of tri-ubiquitin dynamics concerning about status of interaction interfaces

Masaaki Sugiyama (A), Rintaro Inoue (A), Ken Morishima (A), Maho Yagi-Utsumi (B, C), Methanee Hiranyakorn (B, C), Michihiro Nagao (D), Hiroshi Nakagawa (E)
(A) *Kyoto University*, (B) *National Institutes of Natural Sciences*, (C) *SOKENDAI*, (D) *NIST*, (E) *Japan Atomic Energy Agency*

Ubiquitin is a small protein with 76 residues and regulates many functions in a cell: proteolysis, DNA-repair, post-translational modification, signal transduction and so on. The ubiquitin has a hydrophobic interface, and through the interface, the ubiquitin makes connection with a protein having ubiquitin-interaction motif. The functions depend upon which Lys-residue are used for the connection. When Lys48 is used for the connection, this poly-ubiquitin (K48 poly-ubiquitin) works as a degrading index of protein in a proteasome-ubiquitin system.

We investigated the structure and dynamics of K48 di-ubiquitin (K48-di-Ub) with NMR [1]. K48-di-Ubs are in an equilibrium and/or has transit dynamics between open and closed forms in solution. In the closed form, the activity of K48-di-Ub becomes low due to store of the interaction interface and, therefore, this conformational change regulates the ubiquitin functions. The aim of the NSE experiment is to reveal an inner domain motions between Ub domains in K48-tri-Ub in the closed and open forms. The equilibrium between the two conformations is dependent on temperature; the closed and open ones are dominant in the higher (42 degrees) and lower (10 degrees) temperature.

We measured NSE of K48-tri-Ub at the two temperature of 10 and 42 degrees at about 10 mg/ml. An incident neutron wavelength of 6 and 8 angstroms was used to cover fourier times up to 20 ns in a q-range from 0.06 to 0.22 inverse angstroms. Intermediate scattering functions for both states were successfully obtained. The effective diffusion constants (D_{eff}) were obtained by exponential fittings at each q. D_{eff} should

include translational and rotational diffusion as well as internal domain motions. The experimentally obtained D_{eff} are consistent with the MD simulation derived ones at 10 degrees (see Fig.). Based on these results, the contribution of the internal motions can be estimated. The analysis on the temperature dependence of the internal dynamics is on progress. We are trying to analyze the NSE data combined with computational analysis to observe the functional domain motions of K48-tri-Ub.

Reference:

[1] T. Hirano, M. Yagi-Utsumi, K. Kato, et al., *J. Biol. Chem.*, 286, 37496 (2011).

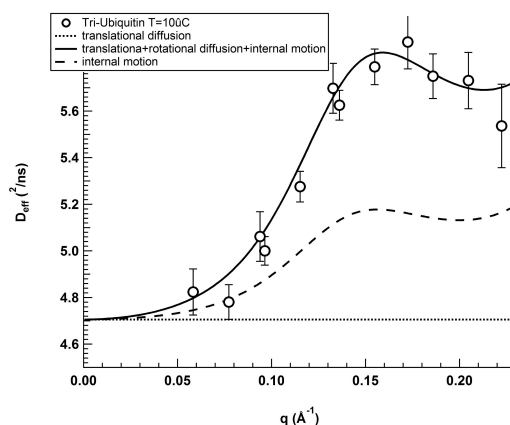


Fig. 1. Q-dependence of effective diffusion constants (D_{eff}) from NSE experiment and MD simulation (translational diffusion, translational diffusion + rotational diffusion + internal motion, and internal motion).

SOFT MATTERS

Solvent dependence in Platonic structures of resorcinarene-based capsule

Shota Fujii, Kazuo Sakurai

Department of Chemistry and Biochemistry, University of Kitakyushu

Resorcinarene-based amphiphiles including C-Methylresorcinarene and C-undecylresorcinarene (Figure 1a) self-assemble into spherical hexameric structures in apolar solvents such as chloroform and benzene.[1] The pioneer work for the characterization of the hexameric structure based on single-crystal X-ray diffraction was demonstrated by MacGillivray and Atwood in 1997.[1] The X-ray analysis was conducted for the single-crystal prepared from nitrobenzene, which elucidated the formation of a capsule-like structure consisting of 6 resorcinarene units and 8 water molecules with incorporating 60 hydrogen bonding. This resorcinarene-based hexameric capsule possesses high applied potential for catalysis carriers and still gets attention as interesting supramolecular aggregates.[2] The structural configuration of C-undecylresorcinarene capsule is associated with core-shell structures where undecyl-tails are placed on the surface on the core composed of hydrogen bonding network and solvent molecules, which might be categorized into reverse micelle structures.

As mentioned above, the structure of resorcinarene-based hexameric capsule has been clarified by single-crystal X-ray structural analysis. Though the way is extremely useful in elucidating the real structure in molecular level, the greatest problem is that the effects of environmental conditions such as various temperature and solvent composition on the aggregate structure are ignored when preparing single crystals. As an alternative method for visualizing the aggregate structure in solutions as it is, small angle neutron scattering (SANS) is very useful and can be conducted at the required experimental conditions (e.g. various temperature levels and solvent compositions). Atwood,

Kumari, and coworkers have revealed that C-alkylpyrogallolarene, whose structure is almost identical with that of C-alkylresorcinarene, forms hexameric capsules with a core-shell geometry in chloroform by using SANS measurements.[3] The SANS study also has illuminated the structure of metal-organic pyrogallolarene-based capsules whose morphologies can be controlled by metal ion species. In this experiment, we investigate the solvent effect on the Platonic structure of C-undecylresorcinarene capsules using SANS measurements.

Figure 1b shows SANS profiles of C-undecylresorcinarene capsules in deuterated apolar solvent including toluene-d₈ and chloroform-d. The scattering intensity approached to $q=0$ at low- q region in the both systems, indicating the formation of spherical scatterers. The oscillation behaviors of the both profiles are similar to each other, but the q value at minimum position in toluene-d₈ is larger than that in chloroform-d, indicating a difference in their structures. Since the inside of the C-undecylresorcinarene capsule contains the apolar solvent, and the large difference in the values of SLD between the deuterated solvents and the C-undecylresorcinarene molecule, we employed spherical hollow model as the fitting model where solvent molecules are located in the core. The fitting model could reproduce the experimental data, indicating the presence of solvent molecule in the capsule core. The size of the solvent pool in the capsule core in chloroform-d is almost consistent with reported value. However, it is relatively large compared to that in toluene-d₈, which indicates the difference in the network structure through the hydrogen bonding among the hydroxyl groups in resorcinarene moiety and water molecules in each apolar

solvent. In toluene-*d*8, the full-stretched length of resorcinarene molecule (~1.6 nm) almost agree with that of shell thickness while the shell thickness in chloroform-*d* is smaller than the actual molecular size. This presumably suggests that the alkyl chains are flexibly mobile in the hexameric structure and efficiently cover the capsule core to minimize the interfacial free energy between the capsule core and the outer solvent.

[1] Leonard R. MacGillivray et al. *Nature*, 1997, 389, 469-472

[2] Qi Zhang et al. *Acc. Chem. Res.* 2018, 51, 2107 – 2114

[3] Harshita Kumari et al. *J. Am. Chem. Soc.*, 2011, 133, 18102-18105

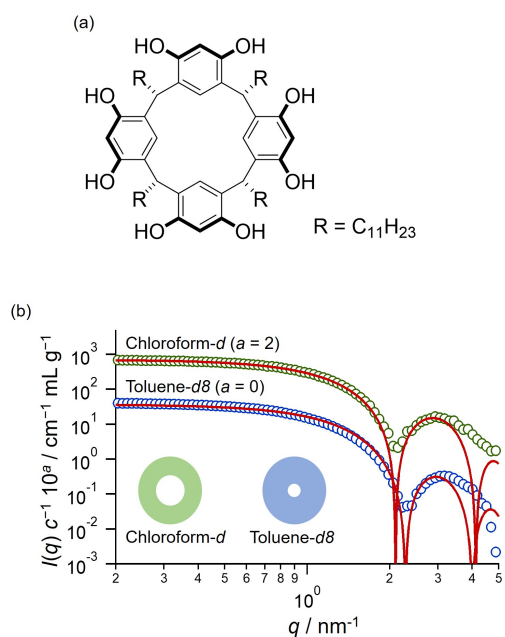


Fig. 1. Figure 1. (a) Chemical structure of C-undecylresorcinarene. (b) SANS profiles of C-undecylresorcinarene capsule. The red curves were calculated using spherical hollow model whose cross-sectional images are inserted.

Elucidating hydration state of poly (propylene oxide) in the glyco polymer vesicle membranes by SANS measurement.

Tomoki Nishimura

Kyoto University, Graduate school of engineering, Department of polymer chemistry

We have recently developed intrinsically permeable polymer vesicles based on maltopentaose-b-poly(propylene oxide) block-co-polymers (Figure 1a).[1] In aqueous solution, the polymer self-assembles into unilamellar vesicles. In contrast to other vesicles, the vesicles show molecular-weight-dependent molecular permeability. Low-molecular-weight compounds ($< 5 \times 10^3$ g/mol) diffuse into the vesicles. We also proved that the permeability is due to the partition of solute molecules into the polymer membrane. Accordingly, we hypothesized that this permeation should be ascribed to the weakly hydrophilic nature of the PPO block. Specifically, the degree of hydration of the PPO layer in the membrane should contribute to facilitating the partition and, therefore, enhance molecular permeation.

To determine the degree of hydration of the PPO layer in the membrane, we previously used SAXS measurements in a preliminary study to obtain the corresponding electron-density profile using a theoretical fitting equation from a bilayer membrane model. The model fit of the SAXS data was consistent with an electron density of the hydrophobic layer (330 e/nm^3) that is almost identical to that of solvent (H_2O ; 334 e/nm^3). Given that the electron density of PPO is comparable to that of H_2O , the degree of hydration in the PPO layer cannot be quantified using SAXS measurements.

We therefore proposed to subject carbohydrate-b-PPO vesicles to SANS measurements in order to quantify the degree of hydration of the PPO layer in the polymer-bilayer membranes of such polymer vesicles. Figure 1b shows SANS profile from maltopentaose-b-poly(propylene oxide) block polymer vesicles in D_2O . The scattering curve showed a slope of -2 at

low q region, suggesting the presence of thin plate structure. To gain further structural information, the scattering curve was fitted with the bilayer membrane model, which provide information on a bilayer cross-sectional structure. The model fits the SAXS data almost overall q -range and is consistent with a hydrophobic layer thickness of 9.3 nm, hydrophilic layer thickness of 2.0 nm, SLD of a hydrophobic layer (PPO layer) of $1.0 \times 10^{10} \text{ cm}^{-2}$ and SLD of a hydrophilic layer (maltopentaose layer) of $6.4 \times 10^{10} \text{ cm}^{-2}$ (Figure 1c). The size of hydrophobic and hydrophilic segment was identical to the data obtained from the previous SAXS analysis. It should be noted that SLD of the PPO layer was much higher than theoretical SLD value of PPO ($3.43 \times 10^9 \text{ cm}^{-2}$). This difference can be attributed to the hydration of PPO with D_2O . To obtain volume fraction of D_2O in PPO layers, we assumed that all the entire polymers are included in the bilayer region of the vesicles. We also imposed the hydrophobic layer is composed of all the PPO group and of a small amount of D_2O . Based on these assumptions, we are able to calculate the volume fraction of D_2O in the PPO layer by using following equation.

$\rho_{\text{core}} = y_{\text{core}} \rho_{\text{ppo}} + (1 - y_{\text{core}}) \rho_{\text{D}_2\text{O}}$, where ρ_{core} , ρ_{ppo} , $\rho_{\text{D}_2\text{O}}$, y_{core} is experimental SLD value of PPO layer, theoretical SLD value of PPO, theoretical SLD value of D_2O , and volume fraction of PPO in the hydrophobic layer, respectively. The volume fraction of D_2O in PPO layer was calculated to be ca. 11% by above equation. More interestingly, in the presence of kosmotropic salt such as Na_2SO_4 , the SLD of hydrophobic layer was decreased to $5.5 \times 10^{10} \text{ cm}^{-2}$, indicating that the degree of hydration in the hydrophobic layer reduced. Since the degree of hydra-

tion would affect on the molecular permeability as mentioned above, the rate of molecular permeation would be controlled by changing external environment.

In summary, we conducted SANS measurements of maltopentaose-block-poly(propylene oxide) in D₂O. We successfully obtained a clear evidence for the hydration of the hydrophobic PPO layer in the polymer bilayer membrane and were able to quantify the volume fraction of D₂O in PPO layer. To the best of our knowledge, this is the first observation showing the hydration of hydrophobic layer in polymer bilayer membranes.

[1] T. Nishimura, Y. Sasaki, K. Akiyoshi, *Adv. Mater.*, 2017, 29, 1702406

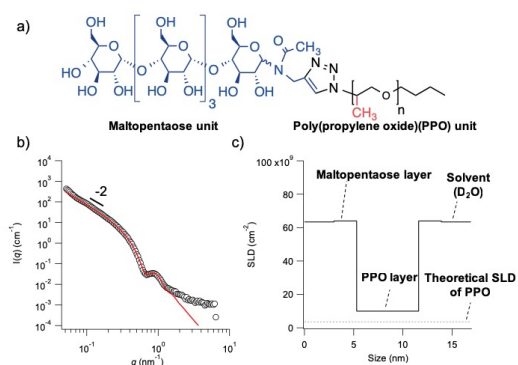


Figure 1 a) Chemical structure of maltopentaose-b-PPO, b) SANS profile of maltopentaose-b-PPO vesicles and a theoretical curve from the bilayer membrane model, c) SLD profile of maltopentaose-b-PPO vesicles

Fig. 1. a) Chemical structure of maltopentaose-b-PPO, b) SANS profile of maltopentaose-b-PPO vesicles and a theoretical curve from the bilayer membrane model, c) SLD profile of maltopentaose-b-PPO vesicles

Distribution of Additives in Ordered-Bicontinuous-Double-Network Structure Formed in Block Copolymer Systems Revealed by Small Angle Neutron Scattering

Katsuhiro Yamamoto(A), Tsukasa Miyazaki(B), Isamu Akiba(C)

(A)Nagoya Institute of Technology, (B)CROSS, (C)The University of Kitakyushu

Introduction. It is well known that block copolymer forms several periodic network structures due to phase-separation with nanoscale features. Well-defined network nanostructures have been expected to be utilized as hybrid porous filtration membranes, photonic crystals, and optical metamaterials, etc. There are two types of defined bicontinuous network structure in a block copolymer: gyroid (Gyr) and Fddd. Gyr is constructed from 3-fold nodes connected with Ia3d symmetry, whereas Fddd also has 3-fold nodes but has an orthorhombic unit cell. Recently, an ordered-bicontinuous- double-diamond (OBDD) structure which is constructed by 4-fold nodes connected with Pn3m symmetry was discovered in syndiotactic polypropylene(sPP)-polystyrene(PS) block copolymer [1,2]. The reason why the OBDD in this copolymer was thermodynamically stabilized was that the higher packing frustration of block copolymer chains in nodes was relaxed due to the existence of the population of helical segments of sPP. We also discovered OBDD structure in PS-b-polyisoprene(PI) (PS-b-PI) blended with PI. OBDD structures in Block copolymer (BCP)/HP systems was theoretically predicted [3,4] and experimentally observed [5]. Pure BCP melt never forms OBDD except for those with a favored helical conformation of sPP as mentioned above. However, in a BCP/HP system, the addition of the HP may reduce the frustration due to localization of the HP in the nodes, which is likely to occur when HP is longer than the identical chain in a BCP. The localization of the HP at the specific site is the key to understand the stabilization of OBDD. We aim to elucidate this point experimentally. SAXS experiment for such a system gives only morphological information, i.e., emer-

gence of the OBDD. On the other hand, SANS expectedly gives not only morphology but also information of the distribution of the HP added when deuterated HP is used. We expect that the SANS profile will be very different from SAXS one if the added deuterated HP is located in specific sites.

Experimental. PS-b-PI ($M_{n,PS} = 32800$, $M_{n,PI} = 18500$, $M_w/M_n = 1.03$, volume fraction of PS = 38.6 vol%, NMR) synthesized by anionic polymerization. Fully deuterated PI (dPI) ($M_n = 20,000$) was purchased from Polymer Source Incorporation. Block copolymer PS-b-PI and homopolymer dPI were mixed in toluene and blended film samples were made from slow casting at 25 degree C for a week. Dried film samples were further dried at 140 degree C in a vacuum oven for 72 h. The films were cut into diameter of 1.5 cm and thickness of 0.5 mm. Blend ratios of dPI relative to PS-b-PI was 15, 20, and 25 wt%. Chain length ratio of BCP to dPI and the blend ratio was chosen to be form ordered double diamond network structure, which was predicted in literature [3,4] and our previous work [5]. SAXS and SANS measurements were conducted at BL10C (wave length of X-ray 0.1nm, camera length 3 m) in Photon Factory KEK (Tsukuba) and at BILBY (time-of-flight) in ANSTO (Australia), respectively.

Result and Discussion. Figure 1 shows SAXS and SANS profiles of PS-b-PI/dPI with a blend ratio of 25wt%. SAXS profile of the original PS-b-PI was also indicated in Figure 1. Original PS-b-PI indicates a hexagonally packed cylindrical morphology. As dPI was blended in PS-b-PI, the morphology changed to others depending

on the blend ratio of dPI. When the blend ratios of 15 and 20 wt%, the microphase separated structure was Gyr. At higher the blend ratio, the morphology was the cylinders with a larger lattice constant. (the periodicity became large). SANS profiles also indicated the identical structures observed in SAXS. In the case of blend ratio of 15 and 20 wt%, the difference in scattering profile between SAXS and SANS was small, indicating dPI was distributed uniformly PI domain. On the other hand, the significant difference was clearly observed at blend ratio of 25 wt%, e.g., the intensity of the first order peak in SANS was relatively smaller than that in the SAXS. This difference can be interpreted by taking into account for homopolymer distribution in the PI domain. Chain length of dPI was larger than that in BCP, meaning the “dry-brush” system. The dPI can be distributed preferentially in the core-region of the PI domain. SAXS and SANS profile were fitted with calculation (paracrystal distortion theory) of cylindrical model as shown in Figure 1 for the PS-b-PI/dPI (25wt%) sample. As for pure BCP, the estimated volume fraction of cylindrical domain was 33.3 vol% that is slightly deviated from the value estimated from NMR because of a larger error in NMR. In the blend system, the radius of the cylinder obtained in SANS fitting was found to be smaller than that in SAXS. Based on the volume fraction (40 vol%) of cylinder obtained from SAXS after blending, added dPI was mostly dissolved in PI domains. In the SANS measurement, the scattering contrast between deuterated region and hydrogenated materials is enhanced. Thus dPI distributed region was shown up. Thinner cylinder indicates the dPI should distribute in the core of the PI cylinder. From the value of the volume fraction of thin cylinder, most of the dPI was located in the core-region. Unfortunately, we did not get morphology of OBDD. This may be caused by inappropriate chain length ratio of dPI to BCP for forming the OBDD.

References

- [1]C.-Y. Chu, et al., *Macromolecules* 45, (2012) 2471.
- [2]C.-Y. Chu, et al. *Soft matter* 11, (2015) 1871.
- [3]M.W.Matsen, *Macromolecules* 28 (1995) 5765.
- [4]M.-V.Francisco J. et al. *Macromolecules* 42 (2009) 9058.
- [5]H.Takagi, et al. *EPL* 110 (2015), 48003.

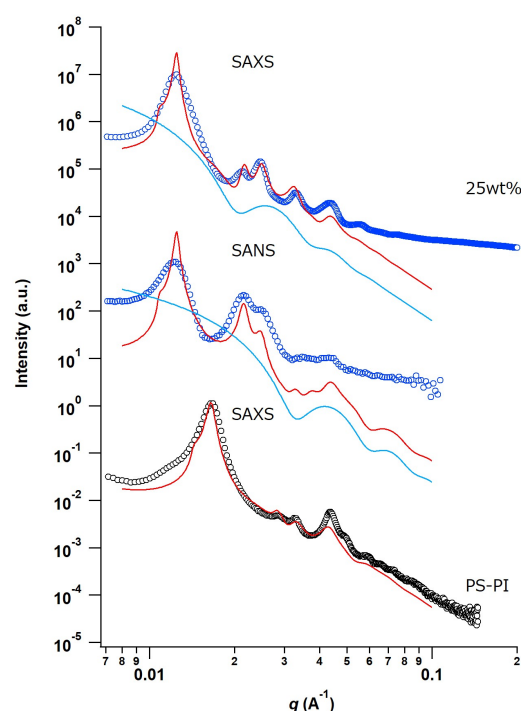


Fig. 1. SAXS (symbols) and SANS (lines) profiles of PS-b-PI/dPI with dPI blend ratio of 25wt% and PS-b-PI. The solid lines were obtained from the calculation. Blue lines indicate the form factor of the cylinder.

Investigation of Microscopic Structural Changes in Poly(oligo-ethylene glycol methyl ether methacrylate)-Based Hydrogels

Takuma Kureha, Xiang Li
The Institute for Solid State Physics

Polymer hydrogels are soft and water-swollen materials. Physicochemical properties, such as polarity and softness of gels, can be changed greatly by the stimuli-responsiveness of hydrogels, which make hydrogels promising materials for the advanced applications, including controlled uptake/release and actuators. More recently, poly(oligo-ethylene glycol methyl ether methacrylate) (POEGMA)-based polymers have been developed as a new type of thermo-responsive polymer (Lutz et al., *Macromolecules* 2006, 39, 893-896.). They offer a potential alternative to the use of thermo-responsive polymers and PEG for a design of hydrogels for biomedical applications.

However, to the best of our knowledge, very few studies have been reported on the physical properties of POEGMA-based gels, especially for the volume transition during changes in temperature. So far, we have investigated the dynamics of POEGMA-based gels by dynamic light scattering (DLS) (Kureha et al., *Macromolecules* 2018, 51, 8932-8939). Here, the formation mechanism of hydrophobic domains in the gels was investigated from the slow mode in the correlation functions. The hydrophobic domains composed of polymer aggregation grew in the gels by rising temperature and they were copolymerization ratio dependent. The domain formation was suppressed as the copolymerization ratio of the longer side chain was increased.

In this study, in order to investigate the domain formation mechanism in the molecular level, we carried out a systematic study of network structural changes in POEGMA gels by small-angle neutron scattering (SANS) as a function of temperature.

SANS results of POEGMA gels show the peak (Fig. 1), which correspond to the characteristic distance between the hydrophobic domains. Moreover, with increasing temperature, the scattering contribution of the peak was gradually decreased, suggesting that the correlation of the distance between domains disappeared because the heterogeneity of the polymer network was increased due to the growth of domain.

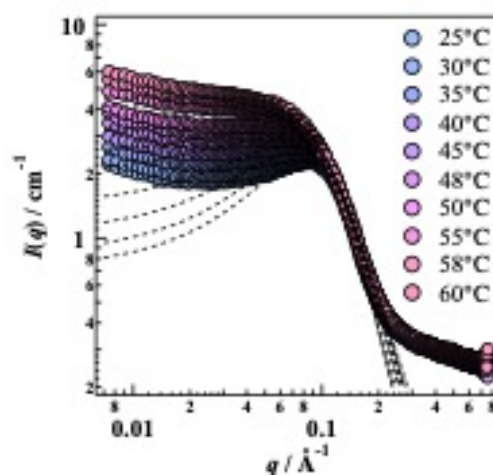


Fig. 1. Temperature dependence of SANS profiles of POEGMA-based gels.

Structural Characterization of DNA-module gel by Small-Angle Neutron Scattering

Masashi Ohira, Xiang Li, and Mitsuhiro Shibayama
The Institute for Solid State Physics, The University of Tokyo

Physical gels such as gelatin gel or agarose gel, which exist generally like natural materials, are used in various fields, such as food, industrial and medical applications. They are composed of polymer networks crosslinked with physical bonding such as hydrogen bonding, Coulomb's interaction or hydrophobic interactions. In conventional chemical or physical gels, it is restricted to control the polymer network of physical gels due to the randomness of crosslinking (branching) and the network structure became very heterogeneous. However, by a simple strategy, just mixing two mutual four-arm polyethylene glycols carrying reactive end-groups together, the network will be homogenized because the branching point in each tetra-PEG macromer is uniformly distributed in the network (Figure 1). Our previous SANS study has proved the excellent homogeneity of networks of tetra-PEG gels.

Recently, we have applied the strategy of tetra-PEG gel into physical gels by modifying the chemically reactive end-group on each arm of tetra-PEG to a physically reactive end-group: sense and anti-sense single-stranded DNA (Figure 1). Because of the high specificity of hydrogen binding between two complementary DNA, the reproducible sol-gel transition was observed by rheological measurement. We carried out small angle neutron scattering with Quokka at ANSTO to investigate its thermo-dependency of the structure. In the previous study, the data is a bit complicated because it contains both PEG and DNA information. In this proposed experiment, in order to focus PEG polymer and DNA crosslinkers exclusively and obtain more accurate information about PEG and DNA structural change such as association and dissociation of double-helix along with the sol-gel transition. Thus, we inves-

tigated this gel with SANS measurement with a contrast matching technique.

The SANS measurement result is shown in Figure 2. With elevating temperature, scattering intensity becomes bigger but SANS profiles do not change clearly at the sol-gel transition point ($T_{gel} \sim 60^\circ\text{C}$) and the melting point of double-stranded DNA. Therefore, this gel has a homogenous structure. Additionally, the SANS profile does not have hysteresis.

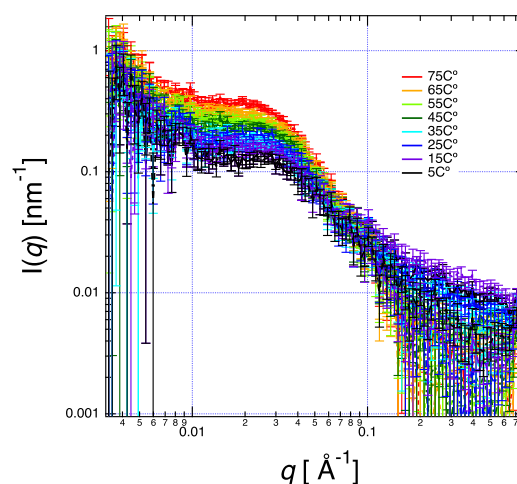


Fig. 1. The SANS profiles of DNA-module gel at various temperature

Length dependent effect of added alkane on fluidity and inter-leaflet coupling of lipid membranes

Hatsuho Usuda¹, Mafumi Hishida¹, Elizabeth Kelley², Michihiro Nagao³

¹Dept. Chem. Univ. Tsukuba, ²NIST Center for Neutron Research, ³Dept. Phys. Indiana Univ.

[Background] In biomembranes, various kinds of small organic molecules, such as sterols and fatty acids, regulate the physical properties of lipid bilayers to maintain cell functions. One of the typical effects of these organic molecules is on membrane fluidity, which has long been an important topic in biomembranes. Studies in biologically relevant systems have suggested that membrane fluidity affects various cell functions, such as enzyme activity, transport process, hormone action, and immune response. [1] Not only the bilayer's fluidity itself but also the dynamic coupling/decoupling of the outer and inner leaflets of bilayers is possibly controlled by such small organic molecules. However, the effects of small organic molecules on the bilayer fluidity and the inter-leaflet coupling have not been fully understood.

The inter-leaflet coupling is known to connect the elastic bending modulus, κ , and the area compressibility modulus, K_A , in a thin elastic sheet theory. [2] As explained more in detail in the following section, recent neutron spin echo (NSE) studies start to measure both κ and K_A independently by measuring both bending and thickness fluctuations in a lipid bilayer. [3,4]

In this experiment, we investigated the effect of small organic molecules on the membrane fluidity utilizing NSE. We used synthetic lipid bilayers with *n*-alkanes. The effects of *n*-alkanes on the phase behavior, the bilayer structure, and its elasticity, have been extensively studied by us. [5,6] Change in the phase behavior of the lipid bilayers strongly depends on the alkane length.[5] We speculated that the membrane fluidity also relates to the intermolecular force in the membrane. For the systematic understanding of the effects of var-

ious organic molecules on the membrane properties, the alkane length dependence of the membrane fluidity will be an ideal system to explore.

[Methods] The NSE technique has been traditionally used to determine membrane's elastic bending modulus, κ . However, the recent development of membrane theories and experimental techniques started to shed light on more detailed membrane properties. [7,8]

Recently, thickness fluctuations in lipid membranes have been successfully measured using NSE, [3,4,9] and this technique was shown to be potential means to access β , which characterizes the inter-leaflet coupling. [4] The bending fluctuations have been modeled by Zilman and Granek [10] as the intermediate scattering function decays following a stretched exponential function with a stretching exponent of 2/3. The decay rate $\Gamma(q)$, where q is the momentum transfer, follows q^3 for bending fluctuations, while the thickness fluctuations are seen as a peak in $\Gamma(q)/q^3$ with an underlying q^3 dependence as follows: [4]

$$\frac{\Gamma}{q^3} = 0.0069 \sqrt{\frac{k_B T}{\kappa} \frac{k_B T}{\eta}} + \frac{(\tau_{TF} q_0^3)^{-1}}{1 + (q - q_0)^2 \zeta^2} \quad (1)$$

where the first term indicates the contribution from the bending fluctuations and the second term represents the thickness fluctuation contributions. η is the solvent viscosity, τ_{TF} represents the relaxation time for the thickness fluctuations, q_0 denotes the peak location in Γ/q^3 representation which is identical to the dip location of the bilayer form factor measured by SANS, and ζ indicates the half width at half maximum (HWHM) of the Lorentz function. The fractional change in the thickness, σ_h , is ex-

pressed as $\sigma_h = \Delta h/h = 2(q_0\zeta)^{-1}$, where h represents the bilayer thickness. Neglecting changes of the molecular volume, σ_h is compensated for by the fractional change in the area, σ_A , as $\sigma_h^2 = \sigma_A^2$, and a simple statistical mechanical relation connects area compressibility modulus K_A and σ_h as $K_A = k_B T / \sigma_h^2 A_0$. [4,11] Therefore, the measurement of the thickness fluctuation amplitude yields to estimate K_A . On the other hand, in a thin elastic sheet theory, a relation between κ and K_A is formulated as $K_A = \beta\kappa/d_t^2$, where d_t is the thickness of the hydrocarbon region of the membrane. [2] These two independent measure of κ and K_A by the bending and thickness fluctuations, respectively, allows one to estimate a change in β if any.

[Results] We have performed an NSE experiment on the NGA-NSE and SANS experiment on the NG7, NIST, using dipalmitoylphosphatidylcholine (DPPC) bilayers with and without alkanes. We measured the cases for *n*-octane (C8), *n*-decane (C10), *n*-dodecane (C12) and *n*-tetradecane (C14). We independently measured the bending and thickness fluctuations by using protiated and alkanes in D₂O for the bending fluctuations, while the thickness fluctuation measurements were performed by employing tail-deuterated DPPC, deuterated *n*-alkanes and D₂O.

As the alkane length increased, κ became lower, which means that the membrane became more flexible. This trend is very interesting considering SANS results indicating that membrane thickness increases with increasing the alkane length. The thickness change is also supported by the results of thickness fluctuations (Fig. ??). The peak derived from thickness fluctuation shifted to lower- q with increasing alkane length. κ should be larger as membrane thickness becomes larger if the membrane viscosity and molecular volume are not changed by the incorporation. Therefore, the decrease in κ suggests the possibility of changes in them. As peak width ζ is inversely proportional to thickness fluctuation amplitude

($\sigma_h = 2(q_0\zeta)^{-1}$), the observed increase in ζ indicates that the thickness fluctuation is suppressed by *n*-alkanes. The results also show the alkane length dependence of ζ . It is possible that shorter alkane changes the membrane structure or viscosity more largely, resulting in the larger suppress.

- [1] J. Szöllösi, in *Mobility and proximity in biological membranes*, CRC Press (1994). Haracska, G. Bogdanovics, Z. Torok, I. Horvath, L. Vigh, *Int. J. Hyperthermia* **29**, 491 (2013).
- [2] D. Boal, in *Mechanics of the Cell*, 2nd Ed.; Cambridge University Press, 267 (2002).
- [3] A.C. Woodka, P.D. Butler, L. Porcar, B. Farago, M. Nagao, *Phys. Rev. Lett.* **109**, 058102 (2012).
- [4] M. Nagao, E.G. Kelley, R. Ashkar, R. Bradbury, P.D. Butler, *J. Phys. Chem. Lett.* **8**, 4679 (2017).
- [5] M. Hishida, A. Endo, K. Nakazawa, Y. Yamamura, K. Saito, *Chem. Phys. Lipids*, **188**, 61 (2015).
- [6] M. Hishida, R. Yanagisawa, H. Usuda, Y. Yamamura, K. Saito, *J. Chem. Phys.* **144**, 041103 (2016).
- [7] M.C. Watson, E.S. Penev, P.M. Welch, F.L.H. Brown, *J. Chem. Phys.* **135**, 244701 (2011).
- [8] J.F. Nagle, *Phys. Rev. E* **96**, 030401(R) (2017).
- [9] M. Nagao, *Phys. Rev. E* **80**, 031606 (2009).
- [10] A.G. Zilman, R. Granek, *Phys. Rev. Lett.* **77**, 4788 (1996).
- [11] M.P. Allen, D.J. Tildesley, *Computer Simulation of Liquids*, Clarendon Press, Oxford, 43-54 (1987).

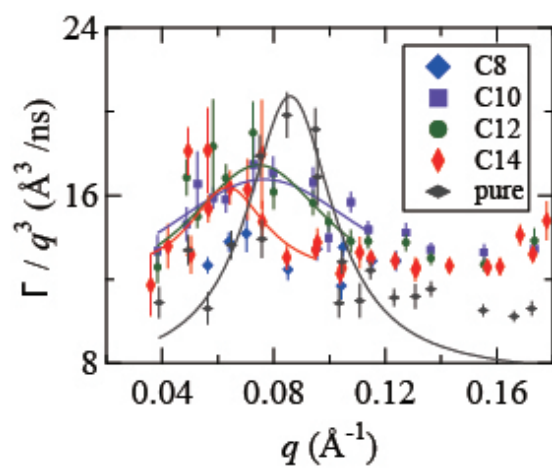


Fig. 1. $\Gamma(q)/q^3$ for DPPC with and without alkanes (C8 C10, C12 and C14). Red diamond: our unpublished previous result. Black diamond: result from [4].

Investigation of Microscopic Structural Changes in Poly(oligo-ethylene glycol methyl ether methacrylate)-Based Hydrogels

Takuma Kureha, Xiang Li
The Institute for Solid State Physics

Polymer hydrogels are soft and water-swollen materials. Physicochemical properties, such as polarity and softness of gels, can be changed greatly by the stimuli-responsiveness of hydrogels, which make hydrogels promising materials for the advanced applications, including controlled uptake/release and actuators. More recently, poly(oligo-ethylene glycol methyl ether methacrylate) (POEGMA)-based polymers have been developed as a new type of thermo-responsive polymer (Lutz et al., *Macromolecules* 2006, 39, 893-896.). They offer a potential alternative to the use of thermo-responsive polymers and PEG for a design of hydrogels for biomedical applications.

However, to the best of our knowledge, very few studies have been reported on the physical properties of POEGMA-based gels, especially for the volume transition during changes in temperature. So far, we have investigated the dynamics of POEGMA-based gels by dynamic light scattering (DLS) (Kureha et al., *Macromolecules* 2018, 51, 8932-8939). Here, the formation mechanism of hydrophobic domains in the gels was investigated from the slow mode in the correlation functions. The hydrophobic domains composed of polymer aggregation grew in the gels by rising temperature and they were copolymerization ratio dependent. The domain formation was suppressed as the copolymerization ratio of the longer side chain was increased.

In this study, in order to investigate the domain formation mechanism in the molecular level, we carried out a systematic study of network structural changes in POEGMA gels by small-angle neutron scattering (SANS) as a function of temperature.

SANS results of POEGMA gels show the peak (Fig. 1), which correspond to the characteristic distance between the hydrophobic domains. Moreover, with increasing temperature, the scattering contribution of the peak was gradually decreased, suggesting that the correlation of the distance between domains disappeared because the heterogeneity of the polymer network was increased due to the growth of domain.

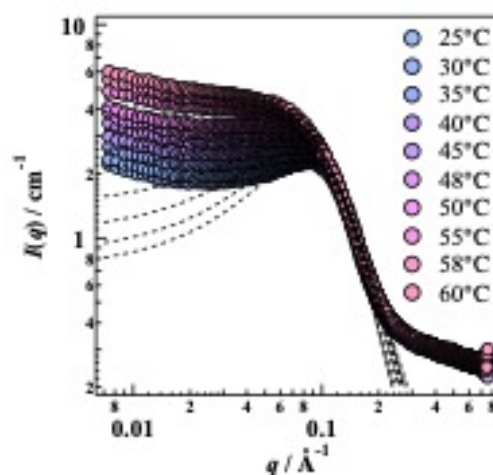


Fig. 1. Fig.1. Temperature dependence of SANS profiles of POEGMA-based gels.

USER-PROGRAM SUPPORT FOR OVERSEAS EXPERIMENTS

(2012 – 2018)

	海外施設名	装置名	所属機関	職位(学年)	申請者氏名	課題番号	装置	採択課題名	代表者所属	代表者氏名	旅程
1	ILL	D23	東京大学	教授	佐賀山 基	11533 (H23転送課題)	5G	マルチフェロイックMn3O4の高磁場領域におけるスピン配列の変化	東京大学	佐賀山 基	2012.06.22-06.29
2	ILL	FIGARO	九州大学	D2	堀 耕一郎	11665 (H23転送課題)	C3-1-2-3	混合液体と接触した高分子界面の凝集構造	九州大学	田中 敬二	2012.07.07-07.12
3	ISIS	Let	東京大学	准教授	益田 隆嗣	12573	C1-1	[Cu2(bza)4(py2)]nにおける吸着酸素分子の磁気相関	東京大学	左右田 稔	2012.05.17-05.26
4	ISIS	Let	東京大学	助教	左右田 稔	12573	C1-1	[Cu2(bza)4(py2)]nにおける吸着酸素分子の磁気相関	東京大学	左右田 稔	2012.05.17-05.29
5	ANSTO	ECHIDA	東京工業大学	D3	尾本 和樹	12723 他	T1-3	鉛フリー圧電体ニオブ酸銀系材料の結晶構造と誘電性 他	東京工業大学	八島 正知	2012.05.09-05.17
6	ILL	D11	お茶の水女子大学	教授	古川 はづき	12581	C1-2	新規Fe系超伝導BaFe2(AS,P)2の磁束研究	お茶の水女子大学	古川 はづき	2012.06.24-06.29
7	ANSTO	ECHIDA	東京工業大学	M2	原武 大樹	12723 他	T1-3	鉛フリー圧電体ニオブ酸銀系材料の結晶構造と誘電性 他	東京工業大学	八島 正知	2012.05.09-05.17
8	ANSTO	TAIPAN	東北大学	准教授	藤田 全基	12539	6G	新規T構造銅酸化物Pr2-xCaxCuO4における磁気相関のホールドープ効果	東北大学	藤田 全基	2012.05.29-06.05
9	ANSTO	TAIPAN	東北大学	D1	堤 健之	12539	6G	新規T構造銅酸化物Pr2-xCaxCuO4における磁気相関のホールドープ効果	東北大学	藤田 全基	2012.05.29-06.05
10	ILL	IN5	岡山大学	准教授	奥地 拓生	11648 (H23転送課題)	C3-1-1	水素ハイドレートのトンネル拡散過程	東京大学	山室 修	2012.07.26-08.02
11	ANSTO	ECHIDA	京都大学	助教	小林 洋治	12700	T1-3	異常高原子価を持つ(Ba,Sr)FeO3の磁気構造と相境界の解明	京都大学	陰山 洋	2012.06.27-07.04
12	ANSTO	ECHIDA	京都大学	D3	山本 隆文	12700	T1-3	異常高原子価を持つ(Ba,Sr)FeO3の磁気構造と相境界の解明	京都大学	陰山 洋	2012.06.27-07.04
13	FRM-II	PUMA	東北大学	M2	奈良 壮	12540,12680	6G,T1-2	反強磁性金属Mn3Siにおける高温スピン励起	東北大学	平賀 晴弘	2012.09.02-09.11
14	FRM-II	PUMA	東北大学	助教	平賀 晴弘	12540,12681	6G,T1-2	反強磁性金属Mn3Siにおける高温スピン励起	東北大学	平賀 晴弘	2012.09.02-09.11
15	ILL	IN5	東京電機大学	准教授	山室 憲子	11647 (H23転送課題)	C3-1-1	両性イオン適合溶質グリシンペタインの水溶液のダイナミクス	東京電機大学	山室 憲子	2012.07.23-08.03
16	HANARO	4CD	東北大学	M2	古川 圭作	12730	T2-2	マルチフェロイック物質(Bi,Eu)Mn2O5の圧力誘起磁気秩序と強誘電性	東北大学	木村 宏之	2012.06.14-06.19
17	HANARO	HRPD	東北大学	M2	萩谷 聡	12701	T1-3	混晶系マルチフェロイックス(1-x)BiFeO3-xPbTiO3のMPB近傍の結晶構造と磁気構造	東北大学	木村 宏之	2012.06.03-06.09
18	HANARO	40mSANS	東京大学	D2	西 健吾	12597	C1-2	温度応答性部位を有するTetraゲルの構造解析	東京大学	酒井 崇匡	2012.07.08-07.14
19	HANARO	40mSANS	東京大学	M2	橋本 憲	12606	C1-2	時分割SANS法によるイオン液体中のゲル化反応メカニズム解明	東京大学	柴山 充弘	2012.07.08-07.14
20	ILL	IN5	首都大学東京	准教授	門脇 広明	11567 (H23転送課題)	C1-1	量子スピニアイスの研究	首都大学東京	門脇 広明	2012.09.25-10.01
21	ILL	IN14	琉球大学	准教授	阿曾 尚文	11563 (H23転送課題)	C1-1	空間反転対称性のない超伝導体CeIrSi3の磁気励起	琉球大学	阿曾 尚文	2012.10.21-10.31
22	ANSTO	ECHIDA	京都大学	D3	山本 隆文	12699	T1-3	層間酸素を含んだ鉄平面4配位酸化物	京都大学	陰山 洋	2012.10.24-10.29
23	ILL	IN11	福岡大学	教授	山口 敏男	12629	C3-1-1	有機無機ハイブリッドメソポーラスシリカ中に閉じ込めた水とメタノールのダイナミクス	福岡大学	山口 敏男	2012.10.22-11.04
24	HANARO	HRPD	東京工業大学	M2	兼子 直人	12723 他	T1-3	鉛フリー圧電体ニオブ酸銀系材料の結晶構造と誘電性 他	東京工業大学	八島 正知	2012.11.21-11.26
25	HANARO	HRPD	東京工業大学	M2	原武 大樹	12723 他	T1-3	鉛フリー圧電体ニオブ酸銀系材料の結晶構造と誘電性 他	東京工業大学	八島 正知	2012.11.21(往路)

	海外施設名	装置名	所属機関	職位(学年)	申請者氏名	課題番号	装置	採択課題名	代表者所属	代表者氏名	旅程
26	HANARO	40mSANS	高エネ研	研究員	貞包 浩一朗	12596	C1-2	界面不活性の働きをする界面活性剤	高エネ研	貞包 浩一朗	2012.12.02(往路)
27	PSI	TriCS	東京大学	特任研究員	萩原 雅人	12694	T1-3	擬一次元鎖フラストレーション磁性体SrCo ₂ V ₂ O ₈ の中性子回折	東京大学	萩原 雅人	2012.10.20-10.27
28	ILL	D33	お茶の水女子大学	教授	古川 はづき	12581 12582	C1-2	新規Fe系超伝導BaFe ₂ (AS,P) ₂ の磁束研究 中性子小角散乱実験によるSr ₂ RuO ₄ の異常金属状態の研究	お茶の水女子大学	古川 はづき	2012.12.02-12.13
29	FRM-II	TOFTOF	東京大学	助教	古府 麻衣子	12626	C3-1-1	M(OH)(bdc-R) (M=Fe, Al, bdc=terephthalate, R=NH ₂ ,OH,(COOH) ₂)配位高分子の酸発生基によるプロトン伝導性の制御	京都大学	北川 宏	2013.02.03-02.12
30	FRM-II	TOFTOF	東京大学	M1	宮津 怜嗣	12626	C3-1-1	M(OH)(bdc-R) (M=Fe, Al, bdc=terephthalate, R=NH ₂ ,OH,(COOH) ₂)配位高分子の酸発生基によるプロトン伝導性の制御	京都大学	北川 宏	2013.02.03-02.12
31	ISIS	IRIS	東京大学	助教	古府 麻衣子	12632	C3-1-1	逆浸透膜表面における水のダイナミクス	東京大学	山室 修	2013.02.17-03.11
32	ISIS	IRIS	東京大学	准教授	山室 修	12632	C3-1-1	逆浸透膜表面における水のダイナミクス	東京大学	山室 修	2013.02.28-03.11

	海外施設名	装置名	所属機関	職位(学年)	申請者氏名	課題番号	装置	採択課題名	代表者所属	代表者氏名	旅程
1	NIST	HFBS	東京大学	教授	山室 修	13620	C3-1-1	H2-SF6/ハイドレート中の水素の拡散ダイナミクス	東京大学	古府 麻衣子	2013.05.28-06.11
2	NIST	HFBS	東京大学	助教	古府 麻衣子	13620	C3-1-1	H2-SF6/ハイドレート中の水素の拡散ダイナミクス	東京大学	古府 麻衣子	2013.05.28-06.11
3	HANARO	SANS	名古屋大学	准教授	高野 敦志	13604	C1-2	結び目を有する環状高分子の溶液中のコンフォメーション	名古屋大学	高野 敦志	2013.06.02-06.05
4	HANARO	SANS	名古屋大学	D1	土肥 侑也	13604	C1-2	結び目を有する環状高分子の溶液中のコンフォメーション	名古屋大学	高野 敦志	2013.06.02-06.05
5	ANSTO	ECHIDNA	東京工業大学	M2	江崎 勇一	13679	T1-3	新規AA'BO4型構造をもつ混合イオン伝導体の結晶構造とイオン伝導経路の解明	東京工業大学	藤井 孝太郎	2013.06.06-06.14
6	ANSTO	ECHIDNA	東京工業大学	M2	上田 孝志朗	13679	T1-3	新規AA'BO4型構造をもつ混合イオン伝導体の結晶構造とイオン伝導経路の解明	東京工業大学	藤井 孝太郎	2013.06.06-06.14
7	HANARO	40mSANS	東京大学	D2	草野 巧巳	13596	C1-2	燃料電池電極用触媒インクの構造解析	東京大学	柴山 充弘	2013.06.30-07.06
8	HANARO	40mSANS	東京大学	M2	廣井 卓思	13596	C1-2	燃料電池電極用触媒インクの構造解析	東京大学	柴山 充弘	2013.06.30-07.06
9	PSI	SINQ TASP	東京大学	助教	左右田 稔	13532, 13570	5G, C1-1	A2CoSi2O7(A=Ca and Ba)におけるエレクトロマグノン	東京大学	左右田 稔	2013.08.25-09.04
10	PSI	SINQ TASP	東京大学	M1	林田 翔平	13532, 13570	5G, C1-1	A2CoSi2O7(A=Ca and Ba)におけるエレクトロマグノン	東京大学	左右田 稔	2013.08.25-09.04
11	HZB	E4	東京理科大学	M2	玉造 博夢	12658 12659	T1-1	スピン格子結合系CuFeO2のスピン波分散関係の一軸応力変化 スピン誘導型強誘電体CuFeO2における磁気ビエゾ効果	東京理科大学	満田 節生	2013.09.17-10.06
12	HZB	E4	東京理科大学	M1	保坂 翔太	12658 12659	T1-1	スピン格子結合系CuFeO2のスピン波分散関係の一軸応力変化 スピン誘導型強誘電体CuFeO2における磁気ビエゾ効果	東京理科大学	満田 節生	2013.09.17-09.24
13	ORNL	SNS NSE	東京大学	教授	柴山 充弘	13612	C2-3-1	Tetra-PEG イオンゲル・ハイドロゲルの動的挙動の解析	東京大学	柴山 充弘	2013.08.12-08.19
14	ORNL	SNS NSE	東京大学	M2	廣井 卓思	13612	C2-3-1	Tetra-PEG イオンゲル・ハイドロゲルの動的挙動の解析	東京大学	柴山 充弘	2013.08.12-08.27
15	HANARO	HRPD	東京工業大学	助教	藤井 孝太郎	13699	T1-3	格子間酸素を利用したイオン伝導性セラミックスの結晶構造とイオン拡散経路	東京工業大学	八島 正知	2013.07.14-07.20
16	ORNL	SNS CNCS	東京大学	准教授	益田 隆嗣	13531, 13569	5G, C1-1	カゴメ格子・三角格子積層系YBaCo4O7の磁気励起	東京大学	左右田 稔	2013.08.21-08.27
17	ORNL	SNS CNCS	東京大学	助教	左右田 稔	13531, 13569	5G, C1-1	カゴメ格子・三角格子積層系YBaCo4O7の磁気励起	東京大学	左右田 稔	2013.08.18-08.24
18	PSI	SANS-1	お茶の水女子大学	教授	古川 はづき	13578	C1-2	希釈冷凍機温度領域におけるCeMn5(M=Co, Ir)の磁束の磁気形状因子の異常	お茶の水女子大学	古川 はづき	2013.09.04-09.18
19	PSI	SANS-1	お茶の水女子大学	D2	呉 麻美子	13578	C1-2	希釈冷凍機温度領域におけるCeMn5(M=Co, Ir)の磁束の磁気形状因子の異常	お茶の水女子大学	古川 はづき	2013.09.04-09.19
20	LLB	6T2	東北大学	准教授	岩佐 和晃	13543 13557, 13702	6G C1-1, T2-2	PrIr2Zn20における非Kramers二重項による四極子秩序の検証 DyFe2Zn20における異方性変化を伴う逐次磁気転移	東北大学	岩佐 和晃	2013.10.12-10.21
21	ANSTO	ECHIDNA	東京大学	D1	白 椽大	13559	C1-1	スピン・ネマティック相関の検出	東京大学	益田 隆嗣	2013.10.06-10.14
22	ANSTO	ECHIDNA	東京大学	M1	林田 翔平	13559	C1-1	スピン・ネマティック相関の検出	東京大学	益田 隆嗣	2013.10.06-10.14
23	ISIS	OSIRIS	慶應義塾大学	講師	千葉 文野	13615	C3-1-1	GeTe系の液液転移と個別原子拡散	慶應義塾大学	千葉 文野	2013.09.29-10.10
24	ISIS	OSIRIS	JAEA	主任研究員	服部 高典	13615	C3-1-1	GeTe系の液液転移と個別原子拡散	慶應義塾大学	千葉 文野	2013.09.29-10.10
25	ORNL	HFIR GP-SANS	お茶の水女子大学	D2	呉 麻美子	13576	C1-2	空間反転対称性の破れた超伝導体のヘリカル磁束格子の観測	お茶の水女子大学	古川 はづき	2013.10.07-10.14

	海外施設名	装置名	所属機関	職位(学年)	申請者氏名	課題番号	装置	採択課題名	代表者所属	代表者氏名	旅程
26	HANARO	FCD	東北大学	教授	木村 宏之	12730	T2-2	マルチフェロイック物質(Bi,Eu)Mn2O5の圧力誘起磁気秩序と強誘電性	東北大学	木村 宏之	2013.11.04-11.14
27	NIST	BT-7	首都大学東京	助教	高津 浩	13558	C1-1	量子スピニアイスの研究	首都大学東京	門脇 広明	2014.01.26-02.03
28	HANARO	18mSANS	立命館大学	助教	貞包 浩一朗	13589	C1-2	界面不活性の働きをする界面活性剤	立命館大学	貞包 浩一朗	2013.12.19-12.22
29	HANARO	18mSANS	立命館大学	M2	高木 寛和	13589	C1-2	界面不活性の働きをする界面活性剤	立命館大学	貞包 浩一朗	2013.12.19-12.23
30	FRM II	TOFTOF	大阪大学	准教授	金子 文俊	13617	C3-1-1	非晶性高分子の分子運動への超臨界二酸化炭素の影響	大阪大学	金子 文俊	2014.01.15-01.25
31	NIST	HFBS	東京大学	教授	山室 修	13627	C3-1-1	多孔性配位高分子MIL-55におけるプロトン伝導ダイナミクス	東京大学	山室 修	2013.12.01-12.10
32	NIST	HFBS	東京大学	M2	宮津 怜嗣	13627	C3-1-1	多孔性配位高分子MIL-55におけるプロトン伝導ダイナミクス	東京大学	山室 修	2013.12.01-12.10
33	HANARO	40mSANS	東京大学	M1	廣澤 和	13592	C1-2	PEG/PDMS相互連結相構造を有する高分子ゲルの構造解析	東京大学	酒井 崇匡	2014.01.05-01.11
34	HANARO	40mSANS	東京大学	M2	廣井 卓思	13592	C1-2	PEG/PDMS相互連結相構造を有する高分子ゲルの構造解析	東京大学	酒井 崇匡	2014.01.05-01.11
35	HANARO	SANS	名古屋大学	M2	木下 敬太	13604	C1-2	結び目を有する環状高分子の溶液中のコンフォメーション	名古屋大学	高野 敦志	2014.01.09-01.14
36	HANARO	SANS	名古屋大学	M2	小林 侑生	13604	C1-2	結び目を有する環状高分子の溶液中のコンフォメーション	名古屋大学	高野 敦志	2014.01.09-01.14
37	NIST	DCS	東京大学	助教	古府 麻衣子	13408	C3-1-1	AGNES(高分解能パルス冷中性子分光器) IRT課題	東京大学	古府 麻衣子	2014.01.16-01.23
38	NIST	DCS	東京大学	教授	山室 修	13408	C3-1-1	AGNES(高分解能パルス冷中性子分光器) IRT課題	東京大学	古府 麻衣子	2014.01.18-01.23
39	ANSTO	WOMBAT	京都大学	准教授	藤田 晃司	12693	T1-3	ニオブ酸リチウム型構造をもつ遷移金属酸化物の磁気構造	京都大学	藤田 晃司	2014.02.04-02.09
40	ANSTO	WOMBAT	京都大学	D1	河本 崇博	12693	T1-3	ニオブ酸リチウム型構造をもつ遷移金属酸化物の磁気構造	京都大学	藤田 晃司	2014.02.04-02.09
41	LLB	6T2	広島大学	准教授	松村 武	13547	6G	Ce0.5La0.5B6における磁気八極子秩序の検証	広島大学	松村 武	2014.02.25-03.11
42	ISIS	IRIS	東京大学	助教	古府 麻衣子	13626	C3-1-1	逆浸透膜表面での水のダイナミクス	東京大学	山室 修	2014.03.12-03.21
43	ISIS	IRIS	東京大学	研究員	根本 文也	13626	C3-1-1	逆浸透膜表面での水のダイナミクス	東京大学	山室 修	2014.03.12-03.21

	海外施設名	装置名	所属機関	職位(学年)	申請者氏名	課題番号	装置	採択課題名	代表者所属	代表者氏名	旅程
1	ORNL	SNS HYSPEC	東京大学	助教	左右田 稔	13570	C1-1	A2CoSi2O7(A=Ca and Ba)におけるエレクトロマグノン	東京大学	左右田 稔	2014.05.05-05.13
2	PSI	SINQ DMC, HRPT	物質・材料研究機構	研究員	長谷 正司	14806 14807	5G	偏極中性子を用いたCu3Mo2O9単結晶の磁気構造の決定 (CuZn)3Mo2O9単結晶の磁気反射の測定	物質・材料 研究機構	長谷 正司	2014.07.10-07.23
3	ORNL	SNS HYSPEC	東京大学	准教授	益田 隆嗣	13570	C1-1	A2CoSi2O7(A=Ca and Ba)におけるエレクトロマグノン	東京大学	左右田 稔	2014.05.05-05.10
4	ISIS	MERLIN	東京大学	准教授	益田 隆嗣	14559	C1-1	正方格子磁性体における新規磁気相の探索	東京大学	益田 隆嗣	2014.06.10-06.16
5	ISIS	MERLIN	東京大学	D2	白 椽大	14559	C1-1	正方格子磁性体における新規磁気相の探索	東北大学	白 椽大	2014.06.10-06.17
6	ISIS	MARI	東京大学	助教	左右田 稔	14522	5G	S=1/2正四面体をもつBa3Yb2Zn5O11の磁気励起	東京大学	左右田 稔	2014.07.16-07.23
7	NIST	NCNR	首都大学東京	准教授	門脇 広明	14564	C1-1	量子スピン液体の研究	首都大学東京	門脇 広明	2014.05.21-05.27
8	PSI	SANS-1	お茶の水女子大学	教授	古川 はづき	14573	C1-2	Fe系超伝導体の磁束研究	お茶の水女子大学	古川 はづき	2014.05.27-06.03
9	ANSTO	ECHIDNA	東京工業大学	M2	齋藤 千紘	14657	T1-3	新規ペロブスカイト関連AA'BO4型構造をもつ混合イオン伝導体の結晶構造とイオン伝導経路の解明	東京工業大学	藤井 孝太郎	2014.05.21-05.31
10	ANSTO	ECHIDNA	東京工業大学	D2	川村 圭司	14657	T1-3	新規ペロブスカイト関連AA'BO4型構造をもつ混合イオン伝導体の結晶構造とイオン伝導経路の解明	東京工業大学	藤井 孝太郎	2014.05.21-05.31
11	ANSTO	QUOKKA	立命館大学	助教	貞包 浩一朗	14592	C1-2	界面不活性の働きをする界面活性剤	立命館大学	貞包 浩一朗	2014.08.17-08.23
12	PSI	FOCUS	福岡大学	教授	山口 敏男	14609	C3-1-1	メソポーラス物質に閉じ込めたジオキサン-水二成分溶液中の水分子のダイナミクス	福岡大学	山口 敏男	2014.08.10-08.19
13	PSI	FOCUS	福岡大学	M2	浦部 俊雄	14609	C3-1-1	メソポーラス物質に閉じ込めたジオキサン-水二成分溶液中の水分子のダイナミクス	福岡大学	山口 敏男	2014.08.10-08.19
14	NIST	DCS	東京大学	教授	山室 修	14607	C3-1-1	H2-SF6ハイドレート中の水素の拡散ダイナミクス	東京大学	古府 麻衣子	2014.08.03-08.10
15	NIST	DCS	東京大学	助教	古府 麻衣子	14607	C3-1-1	H2-SF6ハイドレート中の水素の拡散ダイナミクス	東京大学	古府 麻衣子	2014.08.03-08.13
16	ISIS	MARI	東京大学	D2	白 椽大	14522	5G	S=1/2正四面体をもつBa3Yb2Zn5O11の磁気励起	東京大学	左右田 稔	2014.07.15-07.23
17	NIST	NSE	福岡大学	助教	吉田 亨次	14601	C2-3-1	リチウムイオン電解液の構造緩和	福岡大学	吉田 亨次	2014.09.05-09.13
18	NIST	NSE	名古屋大学	助教	山口 毅	14601	C2-3-1	リチウムイオン電解液の構造緩和	福岡大学	吉田 亨次	2014.09.17-09.27
19	ANSTO	ECHIDNA	東京理科大学	助教	萩原 雅人	14656	T1-3	一次元フラストレート鎖 AM(VO4)(OD) (A=Ca,Sr;M=Co,Ni)の磁気構造	東京理科大学	萩原 雅人	2014.08.17-08.25
20	ANSTO	ECHIDNA	東京理科大学	教授	元屋 清一郎	14656	T1-3	一次元フラストレート鎖 AM(VO4)(OD) (A=Ca,Sr;M=Co,Ni)の磁気構造	東京理科大学	萩原 雅人	2014.08.17-08.25
21	ANSTO	WONBAT	大阪府立大学	特別講師	山田 幾也	14902	T1-3	新規鉄ペロブスカイト酸化物の結晶構造・磁気構造の決定	大阪府立大学	山田 幾也	2014.08.10-08.16
22	ANSTO	WONBAT	大阪府立大学	M1	村上 誠	14902	T1-3	新規鉄ペロブスカイト酸化物の結晶構造・磁気構造の決定	大阪府立大学	山田 幾也	2014.08.10-08.16
23	ILL	IN4	東京大学	准教授	益田 隆嗣	14528	5G	NaBa2Mn3F11の磁気状態	東京大学	益田 隆嗣	2014.09.18-10.01
24	ILL	IN4	東京大学	M2	林田 翔平	14528	5G	NaBa2Mn3F11の磁気状態	東京大学	益田 隆嗣	2014.09.18-10.01
25	ANSTO	ECHIDNA	東京大学	M2	林田 翔平	14903	T1-3	正方格子反強磁性体A2FeGe2O7の磁気構造	東京大学	益田 隆嗣	2014.10.07-10.12

	海外施設名	装置名	所属機関	職位(学年)	申請者氏名	課題番号	装置	採択課題名	代表者所属	代表者氏名	旅程
26	ANSTO	QUOKKA	東京大学	D1	廣井 卓思	14587	C1-2	親油性高分子電解質ゲルの各種誘電率を持つ溶媒下での網目構造解析	東京大学	柴山 充弘	2014.08.26-09.03
27	ANSTO	QUOKKA	東京大学	M2	柄岡 沙希	14587	C1-2	親油性高分子電解質ゲルの各種誘電率を持つ溶媒下での網目構造解析	東京大学	柴山 充弘	2014.08.26-09.03
28	ANSTO	QUOKKA	京都大学	助教	大場 洋次郎	14900	C1-2	塑性変形による銅板中Cu粒子の変形挙動の解析	京都大学	大場 洋次郎	2014.11.24-12.06
29	ANSTO	QUOKKA	京都大学	助教	佐藤 信浩	14570	C1-2	中性子小角散乱法による多孔性放射線合成ゲルのナノ構造解析	京都大学	佐藤 信浩	2014.11.24-12.06
30	ANSTO	QUOKKA	豊橋技術科学大学	D3	足立 望	14570	C1-2	中性子小角散乱法による多孔性放射線合成ゲルのナノ構造解析	京都大学	佐藤 信浩	2014.11.24-12.06
31	NIST	NSE	東京大学	教授	山室 修	14611	C3-1-1	Dynamics of an ionic liquid C16mimPF6 in SmA liquid crystal and liquid phases	東京大学	山室 修	2014.10.06-10.23
32	NIST	NSE	東京大学	研究員	根本 文也	14611	C3-1-1	Dynamics of an ionic liquid C16mimPF6 in SmA liquid crystal and liquid phases	東京大学	山室 修	2014.10.06-10.19
33	NIST	HFBS	東京大学	助教	古府 麻衣子	14610	C3-1-1	New process of hydrogen diffusion in palladium hydrides	東京大学	山室 修	2014.10.06-10.23
34	NIST	HFBS	東京大学	M1	橋下 直樹	14610	C3-1-1	New process of hydrogen diffusion in palladium hydrides	東京大学	山室 修	2014.10.06-10.19
35	PSI	SANS-1	お茶の水女子大学	教授	古川 はづき	14573	C1-2	Fe系超伝導体の磁束研究	お茶の水女子大学	古川 はづき	2014.10.01-10.08
36	ANSTO	ECHIDNA	兵庫県立大学	助教	川崎 郁斗	14901	T1-3	中性子散乱によるSr1-xLaxRuO3のクラスターガラス相の研究	兵庫県立大学	川崎 郁斗	2014.11.29-12.08
37	ILL	IN8	総合科学研究機構	研究員	松浦 直人	14801	4G	ダイマーモット絶縁体 κ -(BEDT-TTF)2Cu[N(CN)2Cl]におけるマルチフェロイクスと電荷揺らぎ・分子格子ダイナミクス	総合科学研究機構	松浦 直人	2014.12.08-12.19
38	ANSTO	ECHIDNA	茨城大学	准教授	横山 淳	14901	T1-3	中性子散乱によるSr1-xLaxRuO3のクラスターガラス相の研究	兵庫県立大学	川崎 郁斗	2014.11.29-12.08
39	NIST	BT-1	京都大学	助教	山本 隆文	14650	T1-3	異常高原子価を持つ(Ba,Sr)FeO3の磁気構造と相境界の解明	京都大学	山本 隆文	2014.11.23-11.30
40	NIST	BT-1	京都大学	D1	竹入 史隆	14650	T1-3	異常高原子価を持つ(Ba,Sr)FeO3の磁気構造と相境界の解明	京都大学	山本 隆文	2014.11.23-11.30
41	ANSTO	ECHIDNA	東北大学	教授	佐藤 卓	14904	T1-3	S=2 籠目格子反強磁性体の磁気構造	東京工業大学	田中 秀数	2014.12.07-12.15
42	ANSTO	ECHIDNA	東京工業大学	M1	日比野 圭佑	14643	T1-3	層状ペロブスカイト型酸化物の結晶構造とイオン拡散経路	東京工業大学	八島 正知	2014.12.13-12.23
43	ILL	D23	お茶の水女子大学	教授	古川 はづき	14573	C1-2	Fe系超伝導体の磁束研究	お茶の水女子大学	古川 はづき	2014.11.13-11.18
44	ANSTO	ECHIDNA	東京工業大学	M1	山田 駿太郎	14643	T1-3	層状ペロブスカイト型酸化物の結晶構造とイオン拡散経路	東京工業大学	八島 正知	2014.12.13-12.23
45	NIST	NSE, SANS	首都大学東京	助教	川端 庸平	14579, 14602 14603	C1-2, C2-3-1 C2-3-1	クラフト転移で自発形成するベシクルの臨界ベシクル濃度近傍でのダイナミクス 界面活性剤2分子膜のゲル状態での膜内ダイナミクス	首都大学東京	川端 庸平	2015.01.22-02.06
46	LLB	6T2	東北大学	准教授	岩佐 和晃	14536, 14554	6G, C1-1	PrT2Zn20(T=Ru,Rh,Os,Ir)における非Kramers二重項基底状態のエントロピー解放過程	東北大学	岩佐 和晃	2015.02.20-03.03
47	NIST	NSE	東京大学	研究員	根本 文也	14905	C3-1-1	Collective dynamics of alkyl-methyl imidazolium based ionic liquids with liquid crystalline phase	東京大学	山室 修	2015.02.03-02.16
48	ORNL	HFIR GP-SANS	東京大学	M2	廣澤 和	14906	C1-2	イオン液体中における刺激応答性高分子の温度応答性相転移	東京大学	柴山 充弘	2015.03.04-03.10

	海外施設名	装置名	所属機関	職位(学年)	申請者氏名	課題番号	装置	採択課題名	代表者所属	代表者氏名	旅程
1	HZB	E4	東京理科大学	D2	玉造 博夢	15522	T1-1	スピン格子結合系における磁気相転移と電気分極の一軸応力制御	東京理科大学	満田 節生	2015.04.19-05.02
2	HZB	E4	東京理科大学	M2	中村 天風	15522	T1-1	スピン格子結合系における磁気相転移と電気分極の一軸応力制御	東京理科大学	満田 節生	2015.04.19-05.02
3	ANSTO	TAIPAN	東京大学	M1	尾山 拓彌	15523	5G	Magnetic structures of 1D frustrated chain compound NaCuMoO4(OH)	東京大学	益田 隆嗣	2015.04.26-05.05
4	ANSTO	TAIPAN	東京大学	特別研究員	浅井 晋一郎	15523	5G	Magnetic structures of 1D frustrated chain compound NaCuMoO4(OH)	東京大学	益田 隆嗣	2015.04.26-05.05
5	ANSTO	WOMBAT	東北大学	教授	藤田 全基	15631	T1-3	T構造銅酸化物の超伝導発現と結晶構造の関係	東北大学	藤田 全基	2015.05.03-05.07
6	ISIS	LET	東京大学	教授	山室 修	15589	C3-1-1	逆浸透膜表面における水のダイナミクス	東京大学	山室 修	2015.04.26-05.03
7	ISIS	LET	東京大学	助教	古府 麻衣子	15589	C3-1-1	逆浸透膜表面における水のダイナミクス	東京大学	山室 修	2015.04.26-05.03
8	ISIS	Osiris	東京大学	助教	左右田 稔	15590	C3-1-1	リラクサー磁性体LuFeCoO4におけるナドメインのダイナミクス	東京大学	左右田 稔	2015.07.11-07.22
9	PSI	HRPT	東京大学	特任研究員	浅井晋一郎	15807	T1-3	平面4配位構造を有する正方格子磁性体マンガン酸塩化物の磁気基底状態の研究	物質材料研究機構	辻本吉廣	2015.06.04-06.08
10	PSI	HRPT	物質材料研究機構	主任研究員	辻本 吉廣	15807	T1-3	平面5配位構造を有する正方格子磁性体マンガン酸塩化物の磁気基底状態の研究	物質材料研究機構	辻本吉廣	2015.06.04-06.07
11	ANSTO	QUOKKA	京都大学	教授	杉山 正明	15554	C1-2	小角中性子散乱による α -クリスタリンのサブユニット交換	京都大学	井上倫太郎	2015.05.27-06.04
12	ANSTO	QUOKKA	京都大学	准教授	井上倫太郎	15554	C1-2	小角中性子散乱による α -クリスタリンのサブユニット交換	京都大学	井上倫太郎	2015.05.27-06.04
13	ANSTO	ECHIDNA	東京工業大学	M2	白岩 大裕	15616	T1-3	層状ペロブスカイト型酸化物の結晶構造とイオン拡散経路	東京工業大学	八島正知	2015.05.30-06.08
14	ANSTO	ECHIDNA	東京工業大学	M1	日比野圭佑	15616	T1-3	層状ペロブスカイト型酸化物の結晶構造とイオン拡散経路	東京工業大学	八島正知	2015.05.30-06.08
15	HZB	E4	東京理科大学	D2	玉造 博夢	15900	T1-1	2等辺三角格子反強磁性体CoNb2O6における交換相互作用定数の一軸応力による制御	東京理科大学	満田 節生	2015.07.04-07.28
16	HZB	E4	東京理科大学	M1	郡川ひろ子	15900	T1-1	2等辺三角格子反強磁性体CoNb2O6における交換相互作用定数の一軸応力による制御	東京理科大学	満田 節生	2015.07.12-07.28
17	FRM-II	DNS	大阪大学	助教	中野岳仁	15516	5G	中性子回折によるアルカリ金属ナノクラスター強磁性体の研究	大阪大学	中野岳仁	2015.09.06-09.17
18	FRM-II	DNS	大阪大学	M1	梅本尚嗣	15516	5G	中性子回折によるアルカリ金属ナノクラスター強磁性体の研究	大阪大学	中野岳仁	2015.09.06-09.17
19	FRM-II	SPODI	東京大学	特任研究員	浅井晋一郎	15628	T1-3	Magnetic structures of frustrated magnets	東京大学	益田 隆嗣	2015.07.30-08.05
20	FRM-II	SPODI	東京大学	M1	吉田 俊也	15628	T1-3	Magnetic structures of frustrated magnets	東京大学	益田 隆嗣	2015.07.30-08.04
21	ANSTO	PELICAN	東京大学	准教授	益田隆嗣	15543	C-1-1	擬スピン 1/2 プリージングパイロクロア磁性体Ba3Yb2Zn5O11の非弾性中性子散乱研究	東京大学	益田 隆嗣	2015.08.05-08.15
22	PSI	TriCS	東京大学	助教	左右田 稔	15518	5G	マルチフェロイックスBa2CoGe2O7におけるエレクトロマグノンの偏極解析	東京大学	左右田 稔	2015.09.06-09.15
23	PSI	TriCS	東京大学	助教	左右田 稔	15519	5G	マルチフェロイックCa2CoSi2O7の磁場下における新規磁気相	東京大学	左右田 稔	2015.09.20-09.29
24	PSI	SANS-1	お茶の水女子大学	教授	古川はづき	15559 (14573)	C1-2	Fe系超伝導体の磁束研究	お茶の水女子大学	古川はづき	2015.06.23-06.29
25	ANSTO	PELICAN	東京大学	D3	白椽大	15543	C-1-1	擬スピン 1/2 プリージングパイロクロア磁性体Ba3Yb2Zn5O11の非弾性中性子散乱研究	東京大学	益田 隆嗣	2015.08.09-08.18

	海外施設名	装置名	所属機関	職位(学年)	申請者氏名	課題番号	装置	採択課題名	代表者所属	代表者氏名	旅程
26	PSI	TriCS	東京大学	M1	吉田俊也	15519	5G	マルチフェロイックCa ₂ CoSi ₂ O ₇ の磁場下における新規磁気相	東京大学	左右田 稔	2015.09.21-09.30
27	ANSTO	QUOKKA	東京大学	助教	Li Xiang	15568	C1-2	電場印加時のゲル内でのDNAの構造解析	東京大学	柴山 充弘	2015.08.17-08.23
28	ANSTO	QUOKKA	東京大学	D1	廣澤 和	15568	C1-2	電場印加時のゲル内でのDNAの構造解析	東京大学	柴山 充弘	2015.08.17-08.23
29	ANSTO	QUOKKA	京都大学	教授	大場洋次郎	15563	C1-2	HPT加工により発現する純鉄中の特異な磁気構造の解明	京都大学	大場洋次郎	2015.10.07-10.20
30	ANSTO	QUOKKA	豊橋技術科学大学	D2	山本康次郎	15563	C1-2	HPT加工により発現する純鉄中の特異な磁気構造の解明	京都大学	大場洋次郎	2015.10.07-10.20
31	ANSTO	QUOKKA	豊橋技術科学大学	研究員	足立 望	15901	C1-2	塑性変形により形成する金属ガラスの不均一構造解析	豊橋技術科学大学	足立 望	2015.10.07-10.20
32	ANSTO	QUOKKA	豊橋技術科学大学	准教授	戸高義一	15901	C1-2	塑性変形により形成する金属ガラスの不均一構造解析	豊橋技術科学大学	足立 望	2015.10.07-10.20
33	NIST	HFBS	東京大学	教授	山室 修	15902	C3-1-1	水/逆浸透膜系の遅いダイナミクス	東京大学	山室 修	2015.08.02-08.15
34	NIST	HFBS	東京大学	助教	古府 麻衣子	15902	C3-1-1	水/逆浸透膜系の遅いダイナミクス	東京大学	山室 修	2015.08.02-08.15
35	FRM-II	SANS-1 KWS-3	お茶の水女子大学	教授	古川はづき	15558 (14572) 14571	C1-2	空間反転対称性の破れた超伝導体のヘリカル磁束格子の観測 中性子小角散乱実験によるSr ₂ RuO ₄ の異常金属状態の研究	お茶の水女子大学	古川はづき	2015.07.27-08.09
36	FRM-II	SANS-1 KWS-3	お茶の水女子大学	D1	高橋 美郷	15558 (14572) 14571	C1-2	空間反転対称性の破れた超伝導体のヘリカル磁束格子の観測 中性子小角散乱実験によるSr ₂ RuO ₄ の異常金属状態の研究	お茶の水女子大学	古川はづき	2015.07.27-08.09
37	ANSTO	SIKA	東北大学	助教	鈴木謙介	15611	T1-2	Ai置換したLa ₂ 14系銅酸化物高温超伝導体のストライプ秩序と超伝導の研究	東北大学	鈴木謙介	2015.11.15-11.24
38	ANSTO	ECHIDNA	東北大学	助教	奥山 大輔	15621	T1-3	反転対称性の破れた磁性体Re ₅ Ru ₃ Al ₂ (Re=Ce,Pr,Nd)の磁気秩序構造	東北大学	奥山 大輔	2015.10.20-10.29
39	ANSTO	ECHIDNA	東北大学	D1	牧野 晃也	15621	T1-3	反転対称性の破れた磁性体Re ₅ Ru ₃ Al ₂ (Re=Ce,Pr,Nd)の磁気秩序構造	東北大学	奥山 大輔	2015.10.20-10.29
40	ANSTO	QUOKKA	京都大学	助教	佐藤信浩	15555	C1-2	放射線誘起反応に基づく機能性高分子多孔ゲルの合成と中性子小角散乱法による構造解析	京都大学	佐藤信浩	2015.10.22-11.02
41	ANSTO	QUOKKA	京都大学	教授	裏出令子	15555	C1-2	放射線誘起反応に基づく機能性高分子多孔ゲルの合成と中性子小角散乱法による構造解析	京都大学	佐藤信浩	2015.10.22-10.30
42	ANSTO	QUOKKA	京都大学	准教授	井上倫太郎	15577	C1-2	中性子小角散乱によるタンパク質凝縮物の構造解析	東京工業大学	野島達也	2015.10.22-11.02
43	HZB	V4	お茶の水女子大学	教授	古川はづき	15560 (14574)	C1-2	希釈冷凍機温度領域におけるCeCoIn ₅ の磁束構造の磁場方向依存性	お茶の水女子大学	古川はづき	2015.09.27-10.08
44	FRM-II	TOFTOF	東京大学	助教	古府 麻衣子	15588	C3-1-1	パラジウムナノ粒子中の水素原子の遅いダイナミクス	東京大学	山室 修	2015.09.26-10.07
45	FRM-II	TOFTOF	東京大学	M2	橋本直樹	15588	C3-1-1	パラジウムナノ粒子中の水素原子の遅いダイナミクス	東京大学	山室 修	2015.09.26-10.07
46	NIST	HFBS	東京大学	助教	古府 麻衣子	15904	C3-1-1	ROM-11.5D20の遅いダイナミクス	東京大学	山室 修	2015.10.18-10.25
47	ILL	IN5	首都大学東京	准教授	門脇広明	15545	C-1-1	量子スピン液体の研究	首都大学東京	門脇広明	2015.11.13-11.25
48	ILL	IN5	首都大学東京	M2	脇田美香	15545	C-1-1	量子スピン液体の研究	首都大学東京	門脇広明	2015.11.13-11.25
49	LLB	4F2	東北大学	准教授	岩佐和晃	15528	6G	Ce ₃ T ₄ Sn ₁₃ (T = Co, Rh) における磁気励起で見出す二重ギャップ電子状態	東北大学	岩佐和晃	2015.11.16-11.30
50	LLB	4F2	東北大学	M2	大友優香	15528	6G	Ce ₃ T ₄ Sn ₁₃ (T = Co, Rh) における磁気励起で見出す二重ギャップ電子状態	東北大学	岩佐和晃	2015.11.22-11.30

	海外施設名	装置名	所属機関	職位(学年)	申請者氏名	課題番号	装置	採択課題名	代表者所属	代表者氏名	旅程
51	ORNL	SNS CNCS	東京大学	助教	左右田 稔	15541	C-1-1	フェロイックスBa ₂ CoGe ₂ O ₇ における磁気異方性の電場制御	東京大学	左右田 稔	2015.12.13-12.21
52	ORNL	HFIR GP-SANS	お茶の水女子大学	D1	高橋 美郷	15559	C1-2	Fe系超伝導体の磁束研究	お茶の水女子大学	古川はづき	2015.11.15-11.25
53	NIST	NSE	東京大学	教授	山室 修	15587	C3-1-1	イミダゾリウム系イオン液体およびその液晶相の速いダイナミクス	東京大学	山室 修	2015.11.08-11.25
54	NIST	NSE	東京大学	助教	古府麻衣子	15587	C3-1-1	イミダゾリウム系イオン液体およびその液晶相の速いダイナミクス	東京大学	山室 修	2015.11.08-11.25
55	ANSTO	ECHIDNA	東京工業大学	助教	藤井孝太郎	15630	T1-3	新規ペロブスカイト関連AA'BO ₄ 型構造をもつ酸化物イオン伝導体の結晶構造とイオン伝導経路の解明	東京工業大学	藤井孝太郎	2015.11.21-12.01
56	HZB	E4	東京理科大学	助教	藤原 理賀	15903	T2-2	孤立四面体量子スピン系の新モデル物質K ₄ Cu ₄ OCl ₁₀ の磁気構造	東京理科大学	藤原 理賀	2016.01.08-01.21
57	HZB	E4	東京理科大学	M1	廣浦 晃	15903	T2-2	孤立四面体量子スピン系の新モデル物質K ₄ Cu ₄ OCl ₁₀ の磁気構造	東京理科大学	藤原 理賀	2016.01.08-01.21
58	ISIS	Wish	東京大学	D1	林田 翔平	15905	C1-1	カゴメ三角格子反強磁性体NaBa ₂ Mn ₃ F ₁₁ の磁気状態	東京大学	益田 隆嗣	2016.03.06-03.10

	海外施設名	装置名	所属機関	職位(学年)	申請者氏名	課題番号	装置	採択課題名	代表者所属	代表者氏名	旅程
1	ANSTO	PELICAN, SIKA	東京理科大学	助教	藤原 理賀	16900	C1-1	新一次元量子スピン系K ₂ Cu ₃ (SO ₄) ₃ の基底状態	東京理科大学	藤原 理賀	2016.04.05-04.16
2	ANSTO	QUOKKA	東京大学	助教	Li Xiang	16541 16560	C1-2	電場下での荷電性高分子の構造,高分子イオン液体溶液系における温度応答性相分離に関する熱力学的研	東京大学	Li Xiang	2016.04.28-05.09
3	ANSTO	QUOKKA	東京大学	特任研究員	守島 健	16541 16560	C1-2	電場下での荷電性高分子の構造,高分子イオン液体溶液系における温度応答性相分離に関する熱力学的研	東京大学	Li Xiang	2016.04.28-05.09
4	ANSTO	QUOKKA	東京大学	M2	廣澤 和	16541 16560	C1-2	電場下での荷電性高分子の構造,高分子イオン液体溶液系における温度応答性相分離に関する熱力学的研	東京大学	廣澤 和	2016.04.28-05.09
5	ANSTO	ECHIDNA	物質・材料研究機構	主任研究員	辻本 吉廣	16808	T1-3	新規正方格子磁性体Sr ₂ CrO ₃ (X = F & Cl) の磁気構造解析	物質・材料研究機構	辻本 吉廣	2016.05.18-05.26
6	ANSTO	ECHIDNA	東京大学	特別研究員	浅井 晋一郎	16808	T1-3	新規正方格子磁性体Sr ₂ CrO ₃ (X = F & Cl) の磁気構造解析	物質・材料研究機構	辻本 吉廣	2016.05.18-05.26
7	ORNL	SNS CORELLI	東京理科大学	嘱託教授	元屋 清一郎	16903	4G 他	時間分割中性子散乱測定による磁気構造変化過程の実時間追跡	東京理科大学	元屋 清一郎	2016.04.18-04.27
8	ANSTO	ECHIDNA	東京工業大学	助教	藤井孝太郎	16595	T1-3	層状ペロブスカイト型酸化物の結晶構造とイオン拡散経路	東京工業大学	八島 正知	2016.05.28-06.04
9	LLB	6T2, G41	茨城大学	教授	岩佐 和晃	16523, 16533 16524, 16534	T1-3	Ce ₃ T ₄ Sn ₁₃ (T = Co, Rh) におけるカイラルフェルミオンの磁気励起 PrT ₂ X ₂ O (T = Ru, Rh, Os, Ir, X = Al, Zn)における2チャンネル近藤効果	茨城大学	岩佐和晃	2016.06.04-06.14
10	NIST	NSE	東北大学	准教授	南部 雄亮	16570	C2-3-1	鉄系梯子型物質BaFe ₂ Se ₃ の中性子スピエンコー	東北大学	南部 雄亮	2016.07.19-08.04
11	ANSTO	QUOKKA	京都大学	准教授	井上 倫太郎	16547	C1-2	末端残基の切断がαクリスタリンのサブユニット交換に及ぼす影響	京都大学	井上 倫太郎	2016.05.31-06.07
12	ANSTO	QUOKKA	京都大学	教授	杉山 正明	16547	C1-2	末端残基の切断がαクリスタリンのサブユニット交換に及ぼす影響	京都大学	井上 倫太郎	2016.05.31-06.05
13	ANSTO	QUOKKA	東京工業大学	D1	日比野圭佑	16595	T1-3	層状ペロブスカイト型酸化物の結晶構造とイオン拡散経路	東京工業大学	八島 正知	2016.05.28-06.04
14	NIST	VSANS	高エネルギー加速器研究機構	博士研究員	根本文也	16562	C1-2	Structure of imidazolium-based ionic liquid under shear flow	高エネルギー加速器研究機構	根本文也	2016.07.13-07.20
15	ORNL	HFIR WAND	鹿児島大学	助教	重田 出	16606	T1-3	ホイスラー合金Ru ₂ Cr ₂ Siの反強磁性状態	鹿児島大学	重田 出	2016.06.28-07.06
16	ORNL	HFIR WAND	愛媛大学	教授	瀧崎 員弘	16606	T1-3	ホイスラー合金Ru ₂ Cr ₂ Siの反強磁性状態	鹿児島大学	重田 出	2016.06.28-07.06
17	ANSTO	QUOKKA	京都大学	助教	長田裕也	16567	C1-2	小角中性子散乱によるポリ(キノキサリン-2,3-ジイル)のらせん反転メカニズムの解明	京都大学	長田裕也	2016.06.18-06.27
18	ANSTO	QUOKKA	京都大学	教授	杉山正明	16567	C1-2	小角中性子散乱によるポリ(キノキサリン-2,3-ジイル)のらせん反転メカニズムの解明	京都大学	長田裕也	2016.06.19-06.26
19	HZB	E4	東京理科大学	M3	玉造 博夢	16904	T1-1	マルチフェロイックCuFeO ₂ における強誘電性の一軸応力制御	東京理科大学	満田 節生	2016.07.03-07.22
20	HZB	E4	東京理科大学	D1	逸見 龍太	16904	T1-1	マルチフェロイックCuFeO ₂ における強誘電性の一軸応力制御	東京理科大学	満田 節生	2016.07.03-07.22
21	ANSTO	SIKA, PELICAN	総合科学研究機構中性子科学センター	研究員	飯田 一樹	16802	C1-1	S = 3/2パーフェクトカゴメ系Li ₂ Cr ₃ SbO ₈ の磁気相関	総合科学研究機構中性子科学センター	飯田 一樹	2016.11.05-11.15
22	ANSTO	SIKA, PELICAN	北海道大学	助教	吉田篤行	16802	C1-1	S = 3/2パーフェクトカゴメ系Li ₂ Cr ₃ SbO ₈ の磁気相関	総合科学研究機構中性子科学センター	飯田 一樹	2016.11.05-11.15
23	ORNL	HFIR CTAX	東北大学	D2	牧野晃也	16905	4G	Chiral magnetic structure determination in non-centrosymmetric Pr ₅ Ru ₃ Al ₂	東北大学	奥山大輔	2016.06.19-07.02
24	ILL	D33	お茶の水女子大学	教授	古川はづき	16551	C1-2	Fe系超伝導体の磁束研究	お茶の水女子大学	古川はづき	2016.07.05-07.12
25	ANSTO	TAIPAN, WONBAT	岡山大学	教授	池田 直	16906	5G	偏極中性子回折による鉄過剰育成したYbFe _{2+x} O ₄ の磁気相関の研究	CROSS	加倉井 和久	2016.07.31-08.17

	海外施設名	装置名	所属機関	職位(学年)	申請者氏名	課題番号	装置	採択課題名	代表者所属	代表者氏名	旅程
26	ANSTO	TAIPAN, WONBAT	岡山大学	M1	鳥谷 友之	16906	5G	偏極中性子回折による鉄過剰育成したYbFe _{2+x} O ₄ の磁気相関の研究	CROSS	加倉井 和久	2016.07.31-08.17
27	ANSTO	SIKA	東北大学	准教授	南部 雄亮	16912	C1-1	スピントロニクス物質YIGの低エネルギー磁気励起	東北大学	南部 雄亮	2016.10.16-10.24
28	ANSTO	QUOKKA	東京大学	研究員	中川 慎太郎	16556 16907	C1-2	4分岐ポリマーの末端架橋により合成されるモデル高分子電解質ゲルの構造非膨潤性ハイドロゲルの構造に関する研究	東京大学	島 健 / 中川 慎太郎	2016.08.18-08.30
29	ANSTO	QUOKKA	東京大学	助教	Li Xiang	16556 16907	C1-2	4分岐ポリマーの末端架橋により合成されるモデル高分子電解質ゲルの構造非膨潤性ハイドロゲルの構造に関する研究	東京大学	島 健 / 中川 慎太郎	2016.08.18-08.30
30	ANSTO	QUOKKA	東京大学	研究員	守島 健	16556 16907	C1-2	4分岐ポリマーの末端架橋により合成されるモデル高分子電解質ゲルの構造非膨潤性ハイドロゲルの構造に関する研究	東京大学	島 健 / 中川 慎太郎	2016.08.18-08.30
31	ORNL	SNS CNCS	総合科学研究機構中性子科学センター	研究員	飯田 一樹	16908	C1-1	kapelasiliteにおける量子スピン液体状態の磁気励起	総合科学研究機構中性子科学センター	飯田 一樹	2016.12.11-12.18
32	ORNL	HFIR C-TAX	お茶の水女子大学	M2	高橋 美郷	16503	4G	強磁性超伝導体における磁性と超伝導の研究	お茶の水女子大学	古川はづき	2016.08.04-08.17
33	ORNL	SNS CORELLI	東京大学	助教	左右田 稔	16909	5G	カゴメ・三角格子を持つLuBaCo ₄ O ₇ の磁気散乱	東京大学	左右田 稔	2016.09.19-09.27
34	ANSTO	QUOKKA	物質材料研究機構	主任研究員	間宮 広明	16910	C1-3	新規ニッケルフリーオーステナイト系ODS鋼中のナノ析出粒子の研究	物質材料研究機構	間宮 広明	2016.10.12-10.20
35	ANSTO	QUOKKA	物質材料研究機構	D2	KOWALSKA, Agata	16910	C1-3	新規ニッケルフリーオーステナイト系ODS鋼中のナノ析出粒子の研究	物質材料研究機構	間宮 広明	2016.10.12-10.20
36	ANSTO	ECHIDNA	東京大学	D2	林田 翔平	16911	5G	マルチフェロイック物質CeFe ₃ (BO ₃) ₄ の磁気構造	東京大学	益田隆嗣	2016.12.13-12.18
37	ANSTO	ECHIDNA	東京大学	M1	加藤 大揮	16911	5G	マルチフェロイック物質CeFe ₃ (BO ₃) ₄ の磁気構造	東京大学	益田隆嗣	2016.12.13-12.18
38	ANSTO	QUOKKA	京都大学	助教	大場洋次郎	16554	C1-2	HPT加工により発現する巨大磁気異方性の起源	京都大学	大場洋次郎	2016.11.02-11.09
39	ANSTO	QUOKKA	京都大学	特任助教	足立 望	16566	C1-2	HPT加工した純鉄の磁気構造に及ぼす高密度格子欠陥の影響	京都大学	足立 望	2016.11.02-11.08
40	ANSTO	QUOKKA	豊橋技術科学大学	准教授	戸高 義一	16566	C1-2	HPT加工した純鉄の磁気構造に及ぼす高密度格子欠陥の影響	京都大学	足立 望	2016.11.02-11.09
41	ANSTO	SIKA	東北大学	M2	沖野友貴	16912	C1-1	スピントロニクス物質YIGの低エネルギー磁気励起	東北大学	南部 雄亮	2016.10.16-10.24
42	ORNL	HFIR WAND	岡山大学	M1	鳥谷 友之	16918	T1-3	鉄欠損を制御したLuFe ₂ O ₄ の磁気基底状態の研究	岡山大学	池田 直	2016.11.25-12.08
43	ORNL	SNS CNCS	北海道大学	助教	吉田敏行	16908	C1-1	kapelasiliteにおける量子スピン液体状態の磁気励起	総合科学研究機構中性子科学センター	飯田 一樹	2016.12.11-12.18
44	FRM-II	KWS-3	お茶の水女子大学	教授	古川はづき	16549	C1-2	中性子小角散乱実験によるSr ₂ RuO ₄ の異常金属状態の研究	お茶の水女子大学	古川はづき	2016.10.25-11.01
45	HZB	E4	東京理科大学	D1	逸見龍太	16917	T1-1	一軸応力による2等辺三角格子反強磁性体O ₆ Nb ₂ O ₆ の交換相互作用定数の制御	東京理科大学	満田 節生	2017.01.16-01.30
46	ANSTO	PELICAN	東京大学	研究員	浅井 晋一郎	16914	5G	吸着酸素磁性の磁気励起	東京大学	益田隆嗣	2016.12.05-12.18
47	ANSTO	ECHIDNA	東京工業大学	M1	中村圭吾	16604	T1-3	新規ペロブスカイト関連AA'BO ₄ 型構造をもつ酸化物イオン伝導体の結晶構造とイオン伝導経路の解明	東京工業大学	藤井孝太郎	2016.12.06-12.16
48	ANSTO	ECHIDNA	東京工業大学	M2	海野航	16604	T1-3	新規ペロブスカイト関連AA'BO ₄ 型構造をもつ酸化物イオン伝導体の結晶構造とイオン伝導経路の解明	東京工業大学	藤井孝太郎	2016.12.06-12.16
49	PSI	SINQ HRPT	物質・材料研究機構	グループリーダー	長谷 正司	16801	5G	磁場中の中性子回折を利用したCu ₃ (P ₂ O ₆ OD) ₂ の基底状態の研究	物質・材料研究機構	長谷 正司	2016.12.06-12.14
50	ORNL	SNS HYSPEC	東北大学	M2	沖野友貴	16915	C3-1-1	スピントロニクス物質YIGの偏極中性子非弾性散乱	東北大学	南部 雄亮	2016.11.22-12.03

	海外施設名	装置名	所属機関	職位(学年)	申請者氏名	課題番号	装置	採択課題名	代表者所属	代表者氏名	旅程
51	ANSTO	PELICAN	東京大学	助教	左右田 稔	16914	5G	吸着酸素磁性の磁気励起	東京大学	益田隆嗣	2016.12.05-12.18
52	ORNL	HFIR PTAX	お茶の水女子大学	M2	高橋 美郷	15505	4G	強磁性超伝導体における磁性と超伝導の研究	お茶の水女子大学	古川はづき	2017.01.12-01.22
53	ANSTO	QUOKKA	東京大学	研究員	中川 慎太郎	16919	C1-2	均一な網目構造を有する温度応答性ハイドロゲルの構造	東京大学	中川 慎太郎	2017.03.14-03.23
54	ANSTO	QUOKKA	東京大学	助教	Li Xiang	16919	C1-2	均一な網目構造を有する温度応答性ハイドロゲルの構造	東京大学	中川 慎太郎	2017.03.14-03.23

	海外施設名	装置名	所属機関	職位(学年)	申請者氏名	課題番号	装置	採択課題名	代表者所属	代表者氏名	旅程
1	ANSTO	ECHIDNA	東北大学	助教	那波 和宏	17584	T1-3	バイロクロア構造を有するNa ₃ Mn(CO ₃) ₂ Clの磁気構造	東北大学	那波 和宏	2017.04.23-05.01
2	ORNL	SNS CORELLI	総合科学研究機構 中性子科学センター	研究員	飯田一樹	17806	C1-1	La ₅ Mo ₄ O ₁₆ における長時間磁化緩和と悪魔の階段	総合科学研究機構 中性子科学センター	飯田一樹	2017.05.02-05.08
3	ORNL	SNS CORELLI	J-PARC	研究主幹	梶本 亮一	17806	C1-1	La ₅ Mo ₄ O ₁₆ における長時間磁化緩和と悪魔の階段	総合科学研究機構 中性子科学センター	飯田一樹	2017.05.02-05.09
4	ISIS	IRIS	東北大学	教授	佐藤 卓	17501	4G	近藤籠目格子CeRhSnの量子臨界磁気揺動	東北大学	佐藤 卓	2017.04.30-05.07
5	ISIS	IRIS	東北大学	M1	高橋 満	17501	4G	近藤籠目格子CeRhSnの量子臨界磁気揺動	東北大学	佐藤 卓	2017.04.30-05.12
6	NIST	DCS	日本原子力研究開発機構	研究員	古府 麻衣子	17563	C3-1-1	柔軟性結晶相をもつイオン液体の速いダイナミクス	東京大学	山室 修	2017.04.11-04.18
7	NIST	DCS	東京大学	M2	櫛井 真実	17563	C3-1-1	柔軟性結晶相をもつイオン液体の速いダイナミクス	東京大学	山室 修	2017.04.10-04.22
8	ORNL	SNS CORELLI	東京大学	特任研究員	吉田 雅洋	17507	4G	多段メタ磁性転移を示す空間反転対称性の破れたCePdSi ₃ における磁気構造の決定	東京大学	吉田 雅洋	2017.04.08-04.15
9	ORNL	SNS CORELLI	東京大学	M2	植田 大地	17507	4G	多段メタ磁性転移を示す空間反転対称性の破れたCePdSi ₃ における磁気構造の決定	東京大学	吉田 雅洋	2017.04.06-04.15
10	ANSTO	ECHIDNA	東北大学	助教	奥山 大輔	17584	T1-3	バイロクロア構造を有するNa ₃ Mn(CO ₃) ₂ Clの磁気構造	東北大学	那波 和宏	2017.04.23-05.01
11	FRM-II	TOFTOF	東京大学	M2	櫛井 真実	17562	C3-1-1	配位高分子ホスト[CuZn(CN) ₄]-に包接されたK+水溶液のダイナミクス	東京大学	山室 修	2017.06.25-07.03
12	FRM-II	TOFTOF	東京大学	教授	錦織 紳一	17562	C3-1-1	配位高分子ホスト[CuZn(CN) ₄]-に包接されたK+水溶液のダイナミクス	東京大学	山室 修	2017.06.25-07.03
13	ANSTO	QUOKKA	京都大学	助教	長田 裕也	17556	C1-2	アルカン溶媒中でらせん反転を示すポリ(キノキサリン-2,3-ジイル)の小角中性子散乱による構造解明	京都大学	長田 裕也	2017.04.28-05.05
14	ANSTO	QUOKKA	京都大学	教授	杉山 正明	17556	C1-2	アルカン溶媒中でらせん反転を示すポリ(キノキサリン-2,3-ジイル)の小角中性子散乱による構造解明	京都大学	長田 裕也	2017.04.28-05.05
15	ANSTO	Wombat	物質・材料研究機構	グループリーダー	長谷正司	17803	5G	スピン1/2テトラマー物質CuInVO ₅ の磁気構造の決定	物質・材料研究機構	長谷正司	2017.05.29-06.04
16	ANSTO	Wombat	上智大学	D2	江袋佑太	17803	5G	スピン1/2テトラマー物質CuInVO ₅ の磁気構造の決定	物質・材料研究機構	長谷正司	2017.05.29-06.04
17	ISIS	GEM	東京大学	教授	山室 修	17579	T1-3	Pd/Ruナノ合金の構造	東京大学	山室 修	2017.05.25-06.02
18	ISIS	GEM	京都大学	特定助教	草田康平	17579	T1-3	Pd/Ruナノ合金の構造	東京大学	山室 修	2017.05.25-06.02
19	ORNL	HFJR HB-3A	東京大学	特任研究員	浅井晋一郎	17514	5G	マルチフェロイック物質RFe ₃ (BO ₃) ₄ (R=Ce,Sm)	東京大学	益田 隆嗣	2017.06.15-06.25
20	LLB	5C1	茨城大学	教授	岩佐 和晃	17519	6G	Ce ₃ T ₄ Sn ₁₃ (T = Co, Rh, Ru) に現れるカイラルフェルミオンによる磁気構造と励起	茨城大学	岩佐 和晃	2017.06.17-06.30
21	FRM-II	MLZ	東北大学	外国人特別研究員	Johannes Reim	17568	T1-1	Switching the magnetic order in CaBaCo ₂ Fe ₂ O ₇ using magnetic field	東北大学	Johannes Reim	2017.08.06-08.20
22	ORNL	HFJR HB-3A	東京大学	M1	長谷川 舜介	17514	5G	マルチフェロイック物質RFe ₃ (BO ₃) ₄ (R=Ce,Sm)	東京大学	益田 隆嗣	2017.06.16-06.25
23	ANSTO	QUOKKA	京都大学	准教授	井上倫太郎	17537	C1-2	Crowding環境下におけるアルファクリスタリンのサブユニット動態	京都大学	井上倫太郎	2017.05.21-05.27
24	ANSTO	QUOKKA	京都大学	教授	杉山 正明	17537	C1-2	Crowding環境下におけるアルファクリスタリンのサブユニット動態	京都大学	井上倫太郎	2017.05.21-05.27
25	NIST	NSE	日本原子力研究開発機構	研究副主幹	中川洋	17809	C2-3-1	マルチドメイン蛋白質MurDのATP依存的な機能性ドメイン運動	日本原子力研究開発機構	中川洋	2017.07.05-07.14

	海外施設名	装置名	所属機関	職位(学年)	申請者氏名	課題番号	装置	採択課題名	代表者所属	代表者氏名	旅程
26	NIST	NSE	東北大学	准教授	南部 雄亮	17559	C2-3-1	鉄系梯子型超伝導物質BaFe2S3の中性子スピネコー	東北大学	南部 雄亮	2017.08.31-09.10
27	ANSTO	QUOKKA	東京大学	M2	吉川 祐輔	17547	C1-2	小角中性子散乱によるDNAモジールゲルの構造解析	東京大学	Xiang Li	2017.09.08-09.16
28	ANSTO	QUOKKA	東京大学	D3	廣澤 和	17901	C1-2	小角中性子散乱による反応率臨界ゲルクラスターの構造解析	東京大学	Xiang Li	2017.09.11-09.20
29	ANSTO	QUOKKA	東京大学	M1	乗富 貴子	17901	C1-2	小角中性子散乱による反応率臨界ゲルクラスターの構造解析	東京大学	Xiang Li	2017.09.11-09.20
30	NIST	NSE	筑波大学	助教	菱田 真史	17902	C2-3-1	脂質膜の粘弾性に及ぼすアルカンの効果	筑波大学	菱田 真史	2017.08.22-09.05
31	NIST	NSE	筑波大学	D1	臼田 初穂	17902	C2-3-1	脂質膜の粘弾性に及ぼすアルカンの効果	筑波大学	菱田 真史	2017.08.22-09.05
32	HZB	E4	東京理科大学	教授	満田 節生	17903	T1-1	2等辺Ising 三角格子磁性体CoNb2O6 における一軸応力による鎖間交換相互作用の制御	東京理科大学	満田 節生	2017.08.07-08.18
33	HZB	E4	東京理科大学	D2	逸見 龍太	17903	T1-1	2等辺Ising 三角格子磁性体CoNb2O6 における一軸応力による鎖間交換相互作用の制御	東京理科大学	満田 節生	2017.08.07-08.18
34	ANSTO	QUOKKA	東京大学	M2	渡辺 延幸	17900	C1-2	小角中性子散乱(SANS)法による高分子ゲル網目均一性の定量的評価	東京大学	Xiang Li	2017.09.05-09.13
35	PSI	ZEBRA	東京大学	D2	林田翔平	17515	5G	CsFeCl3における圧力誘起磁気秩序状態の磁気構造	東京大学	益田 隆嗣	2017.08.22-09.09
36	ANSTO	QUOKKA	東京大学	M1	辻 優依	17547	C1-2	小角中性子散乱によるDNAモジールゲルの構造解析	東京大学	Xiang Li	2017.09.08-09.16
37	ORNL	SNS CORELLI	東京大学	特任研究員	吉田 雅洋	17507 17904	4G	多段メタ磁性転移を示す空間反転対称性の破れたCePdSi3における磁気構造の決定 多段メタ磁性転移を示す空間反転対称性の破れたCePtSi3における磁気構造の決定	東京大学	吉田 雅洋	2017.08.28-09.12
38	ORNL	SNS CORELLI	東京大学	M2	植田 大地	17507 17904	4G	多段メタ磁性転移を示す空間反転対称性の破れたCePdSi3における磁気構造の決定 多段メタ磁性転移を示す空間反転対称性の破れたCePtSi3における磁気構造の決定	東京大学	吉田 雅洋	2017.08.28-09.12
39	NIST	HFBS	東京大学	教授	山室 修	17564	C3-1-1	超高エントロピー液体C6C10-テトラフェニルポリフィリンの長いアルキル鎖ダイナミクス	東京大学	山室 修	2017.08.17-08.27
40	NIST	HFBS	東京大学	M2	櫛井 真実	17564	C3-1-1	超高エントロピー液体C6C10-テトラフェニルポリフィリンの長いアルキル鎖ダイナミクス	東京大学	山室 修	2017.08.17-08.27
41	PSI	ZEBRA	東京大学	教授	益田隆嗣	17513	5G	マルチフェロイック物質Ba2MnGe2O7の磁気モーメントの電場制御	東京大学	益田 隆嗣	2017.08.30-09.07
42	ANSTO	QUOKKA	京都大学	助教	守島 健	17900	C1-2	小角中性子散乱(SANS)法による高分子ゲル網目均一性の定量的評価	東京大学	Xiang Li	2017.09.05-09.11
43	FRM-II	SANS-1	お茶の水女子大学	D1	鏡田 奈央	17546	C1-2	トポロジカル超伝導体の磁束格子	お茶の水女子大学	古川 はづき	2017.08.15-08.24
44	NIST	NSE	日本原子力研究開発機構	研究員	古府 麻衣子	17810	C3-1-1	Zn-Ln-Zn単分子磁石のスピンダイナミクス	日本原子力研究開発機構	古府 麻衣子	2017.09.06-09.13
45	ANSTO	QUOKKA	物質・材料研究機構	主幹研究員	間宮 広明	17808	C1-2	中性子小角散乱測定による耐熱超合金中の超微細析出物の評価	物質・材料研究機構	間宮 広明	2017.10.08-10.13
46	PSI	ZEBRA	東京大学	M1	長谷川 舜介	17513	5G	マルチフェロイック物質Ba2MnGe2O7の磁気モーメントの電場制御	東京大学	益田 隆嗣	2017.08.22-09.09
47	ANSTO	QUOKKA	東北大学	助教	奥山 大輔	17578	T1-3	Powder diffraction experiment on chiral magnetic Re5Ru3Al2	東北大学	奥山大輔	2017.10.14-10.21
48	ANSTO	QUOKKA	東北大学	外国人特別研究員	Johannes Reim	17578	T1-3	Powder diffraction experiment on chiral magnetic Re5Ru3Al2	東北大学	奥山大輔	2017.10.15-10.20
49	ORNL	HFIR HB-3A SNS CORELLI	理化学研究所	研究員	左右田 稔	17905 17512	5G	ワイル半金属候補物質NdGaSiの磁気構造 フラストレーションをもつ正方格子C20H19F6N5Pにおける磁気秩序	理化学研究所	左右田 稔	2017.11.26-12.09
50	ANSTO	ECHIDNA	東京工業大学	特任助教	丹羽 栄貴	17576	T1-3	層状ペロブスカイト型酸化物の結晶構造とイオン拡散経路	東京工業大学	八島 正知	2017.11.11-11.21

	海外施設名	装置名	所属機関	職位(学年)	申請者氏名	課題番号	装置	採択課題名	代表者所属	代表者氏名	旅程
51	ANSTO	ECHIDNA	東京工業大学	M1	辻口峰史	17576	T1-3	層状ペロブスカイト型酸化物の結晶構造とイオン拡散経路	東京工業大学	八島 正知	2017.11.11-11.21
52	LLB	4F2	茨城大学	教授	岩佐 和晃	17519	6G	Ce ₃ T ₄ Sn ₁₃ (T = Co, Rh, Ru) に現れるカイラルフェルミオンによる磁気構造と励起	茨城大学	岩佐 和晃	2017.12.09-12.17
53	ORNL	HFIR CTAX	東北大学	M1	高橋 満	17524	C1-1	近藤籠目格子CeRhSnの量子臨界磁気揺動	東北大学	佐藤 卓	2017.11.26-12.07
54	ANSTO	ECHIDNA	東北大学	教授	佐藤 卓	17500	4G	磁性準結晶中の隠れた磁気秩序の探索	東北大学	佐藤 卓	2017.12.04-12.10
55	NIST	NG7	東北大学	助教	奥山 大輔	17548	C1-2	Current driven motion of skyrmions in helical magnets	東北大学	奥山大輔	2018.01.23-01.31
56	NIST	NG7	東北大学	教授	佐藤 卓	17548	C1-2	Current driven motion of skyrmions in helical magnets	東北大学	奥山大輔	2018.01.25-01.30
57	FRM- II	SANS- I	お茶の水女子大学	D1	鏡田 奈央	17546	C1-2	トポロジカル超伝導体の磁束格子	お茶の水女子大学	古川 はづき	2018.02.13-02.21
58	FRM- II	MIRA	お茶の水女子大学	教授	古川 はづき	17504	4G	強磁性超伝導体における磁性と超伝導の研究	お茶の水女子大学	古川 はづき	2018.03.12-03.20
59	FRM- II	MIRA	お茶の水女子大学	M3	高橋 美郷	17504	4G	強磁性超伝導体における磁性と超伝導の研究	お茶の水女子大学	古川 はづき	2018.03.12-03.20
60	ANSTO	WONBAT	東京大学	特任研究員	浅井晋一郎	17906	5G	マグネトブランバイト型コバルト酸化物SrCo ₁₂ O ₁₉ の電荷-磁気秩序	東京大学	浅井晋一郎	2018.03.14-03.19
61	ANSTO	WONBAT	東京大学	M1	菊地帆高	17906	5G	マグネトブランバイト型コバルト酸化物SrCo ₁₂ O ₁₉ の電荷-磁気秩序	東京大学	浅井晋一郎	2018.03.14-03.19

	海外施設名	装置名	所属機関	職位(学年)	申請者氏名	課題番号	装置	採択課題名	代表者所属	代表者氏名	旅程
1	NIST	CHRNS	筑波大学	助教	菱田 真史	18560	C2-3-1	リン脂質膜の粘弾性および単層膜間カップリングに対するアルカンの効果:鎖長依存性	筑波大学	菱田 真史	2018.05.10-05.23
2	NIST	CHRNS	筑波大学	D1	白田 初穂	18560	C2-3-1	リン脂質膜の粘弾性および単層膜間カップリングに対するアルカンの効果:鎖長依存性	筑波大学	菱田 真史	2018.05.10-05.23
3	ANSTO	QUOKKA	東京大学	M2	栗富 貴子	18901	C1-2	金属貯蔵原子模倣 dendrimer の構造解析	東京大学	Li Xiang	2018.05.16-05.25
4	ANSTO	QUOKKA	東京大学	M2	辻 優依	18902	C1-2	均一構造を持つ高分子ゲルにおける架橋点間相関の視覚化	東京大学	Li Xiang	2018.05.13-05.21
5	ANSTO	QUOKKA	東京大学	助教	Li Xiang	18901	C1-2	金属貯蔵原子模倣 dendrimer の構造解析	東京大学	Li Xiang	2018.05.13-05.25
						18902	C1-2	均一構造を持つ高分子ゲルにおける架橋点間相関の視覚化			
6	ORNL	HFIR WAND	東北大学	M2	高橋 満	18574	T1-3	新奇量子カゴメ格子系 Yb ₃ Ni ₁₁ Ge ₄ の短距離スピン相関	東北大学	佐藤 卓	2018.05.12-05.20
7	ANSTO	ECHIDNA	東京工業大学	M2	井上 遼太	18584	T1-3	新規酸化物イオン伝導体の結晶構造解析とイオン伝導経路の解明	東京工業大学	藤井 孝太郎	2018.06.23-07.03
8	ANSTO	ECHIDNA	東京工業大学	M2	松井 将洋	18584	T1-3	新規酸化物イオン伝導体の結晶構造解析とイオン伝導経路の解明	東京工業大学	藤井 孝太郎	2018.06.23-07.03
9	ANSTO	BILBY	名古屋工業大学	准教授	山本 勝宏	18900	C1-2	中性子散乱法によるブロック共重合体の連続ダブルワーク型相分離構造内における添加物の分布状態解析	名古屋工業大学	山本 勝宏	2018.05.31-06.08
10	ANSTO	BILBY	北九州市立大学	教授	秋葉 勇	18900	C1-2	中性子散乱法によるブロック共重合体の連続ダブルワーク型相分離構造内における添加物の分布状態解析	名古屋工業大学	山本 勝宏	2018.05.31-06.08
11	ILL	IN16B	首都大学東京	准教授	門脇 広明	18534	C1-1	量子スピン液体の研究	首都大学東京	門脇 広明	2018.05.27-06.01
12	ORNL	HFIR CG-2	お茶の水女子大学	M1	篠原 加奈依	18548	C1-2	(Ce,Nd)CoIn ₅ のスピン密度波と超伝導の関係	お茶の水女子大学	古川 はづき	2018.06.17-06.24
13	ISIS	WISH	物質・材料研究機構	主任研究員	寺田 典樹	18800	4G	DyMnO ₃ の高圧力相の磁気秩序の探索	物質・材料研究機構	寺田 典樹	2018.06.25-07.02
14	ORNL	HFIR RELI	東京大学	D3	植田 大地	18508	4G	多段メタ磁性転移を示す空間反転対称性の破れた Ce 系化合物 Ce ₂ TSi ₃ (T = Pd, Pt) における磁気構造の決定	東京大学	益田 隆嗣	2018.06.21-07.01
15	HZB	E4	東京理科大学	教授	満田 節生	18903	T1-1	一軸応力による2等辺三角格子反強磁性体 CoNb ₂ O ₆ の磁区成長過程の制御	東京理科大学	満田 節生	2018.06.30-07.16
16	HZB	E4	東京理科大学	M1	下田 雄太郎	18903	T1-1	一軸応力による2等辺三角格子反強磁性体 CoNb ₂ O ₆ の磁区成長過程の制御	東京理科大学	満田 節生	2018.06.30-07.16
17	PSI	Eiger	物質・材料研究機構	グループリーダー	長谷 正司	18804	5G	磁場中の中性子回折を利用した Cu ₃ (P ₂ O ₆ OD) ₂ の基底状態の研究	物質・材料研究機構	長谷 正司	2018.08.25-09.01
18	NIST	NCNR	首都大学東京	准教授	門脇 広明	17532	C1-1	量子スピン液体の研究	首都大学東京	門脇 広明	2018.08.06-08.15
19	NIST	NCNR	東北大学	教授	佐藤 卓	17532	C1-1	量子スピン液体の研究	首都大学東京	門脇 広明	2018.08.06-08.15
20	ORNL	HIFR HB-1	お茶の水女子大学	M2	鏡田 奈央	18507	4G	トポロジカル超伝導体の非弾性散乱	お茶の水女子大学	古川 はづき	2018.08.09-08.19
21	ANSTO	QUOKKA	京都大学	准教授	井上 倫太郎	18542	C1-2	CV-SANS による DNA 存在下での制限分解酵素の解析	京都大学	井上 倫太郎	2018.07.25-07.31
22	ANSTO	QUOKKA	京都大学	教授	杉山 正明	18542	C1-2	CV-SANS による DNA 存在下での制限分解酵素の解析	京都大学	井上 倫太郎	2018.07.25-07.31
23	ILL	IN20	物質・材料研究機構	主任研究員	寺田 典樹	18800	4G	DyMnO ₃ の高圧力相の磁気秩序の探索	物質・材料研究機構	寺田 典樹	2018.09.23-10.05
24	ANSTO	SIKA	東北大学	教授	佐藤 卓	18527	C1-1	磁気スカーミオン格子におけるトポロジカルマグノンの探索	東北大学	佐藤 卓	2018.10.16-10.26
25	ANSTO	SIKA	東北大学	D1	Seno Aji	18527	C1-1	磁気スカーミオン格子におけるトポロジカルマグノンの探索	東北大学	佐藤 卓	2018.10.16-10.30

	海外施設名	装置名	所属機関	職位(学年)	申請者氏名	課題番号	装置	採択課題名	代表者所属	代表者氏名	旅程
26	ANSTO	ECHIDNA	東京大学	助教	浅井 晋一郎	18904	5G	メイプルリーフ化合物MgMn3O7・3D2Oの磁気秩序	東京大学	浅井 晋一郎	2018.08.26-08.31
27	ORNL	HFIR HB-2A	東北大学	M2	村崎 遼	18587	T1-3	擬スピン1/2/バイロクロア反強磁性体Na3Co(CO3)2Clの磁気秩序	東北大学	那波 和宏	2018.09.02-09.07
28	ORNL	HIFR CG-3	東京大学	M1	大平 征史	18539	C1-2	SANS・DSC同時測定による2本鎖DNAにより架橋されたモデル物理ゲルの構造解析	東京大学	Li Xiang	2018.09.23-09.30
29	ORNL	HFIR HB-1	東京大学	M2	長谷川 舜介	18519	5G	マルチフェロイック物質Ba2CoGe2O7の磁気モーメントの完全電場制御	東京大学	益田 隆嗣	2018.09.10-09.26
30	ILL	IN15	理化学研究所	研究員	左右田 稔	18812	C2-3-1	磁気スキルミオンMnSi1-xGexにおけるダイナミクス	理化学研究所	左右田 稔	2018.10.16-10.26
31	PSI	DMC	明治大学	教授	安井 幸夫	18578	T1-3	量子スピンの三量体構造をもつNa2Cu3Ge4O12の磁気構造	明治大学	安井 幸夫	2018.11.28-12.04
32	PSI	DMC	明治大学	M1	菅麻 隆成	18578	T1-3	量子スピンの三量体構造をもつNa2Cu3Ge4O12の磁気構造	明治大学	安井 幸夫	2018.11.28-12.04
33	PSI	SINQ	理化学研究所	研究員	左右田 稔	18546	C1-2	空間反転対称性の破れた超伝導体のヘリカル磁東格子の観測	お茶の水女子大学	古川 はづき	2018.11.19-11.27
34	ORNL	BL-14B HYSPEC	お茶の水女子大学	M1	藤原 加奈依	18908	C1-1	Ce(Co,Rh)In5のネスティングと超伝導発現機構	お茶の水女子大学	古川 はづき	2019.01.21-01.29
35	ISIS	GEM	名古屋工業大学	教授	羽田 政明	18579	T1-3	PdRuナノ粒子の構造と触媒活性	東京大学	山室 修	2019.02.10-02.17
36	ISIS	GEM	京都大学	助教	草田 康平	18579	T1-3	PdRuナノ粒子の構造と触媒活性	東京大学	山室 修	2019.02.10-02.18
37	ANSTO	QUOKKA	東京大学	研究員	呉羽 拓真	18905	C1-2	生体適合性ホ ¹ リオリコ ² エチレンク ³ リコールメタクリレート ⁴ の微細構造変化の調査	東京大学	呉羽 拓真	2019.02.26-03.06
38	ANSTO	QUOKKA	東京大学	助教	Li Xiang	18905	C1-2	生体適合性ホ ¹ リオリコ ² エチレンク ³ リコールメタクリレート ⁴ の微細構造変化の調査	東京大学	呉羽 拓真	2019.02.26-03.03
39	FRM- II	PUMA	大阪大学	D1	森 仁志	18801	4G	熱電材料Mg3Sb2のフォノンダイナミクス	産業技術総合研究所	李 哲虎	2019.02.11-02.20
40	FRM- II	PUMA	広島大学	助教	長谷川 巧	18801	4G	熱電材料Mg3Sb2のフォノンダイナミクス	産業技術総合研究所	李 哲虎	2019.02.11-02.21
41	NIST	NG-7	東北大学	助教	奥山 大輔	18907	C1-2	MnSi における変動電流下の磁気スキルミオンのダイナミクス	東北大学	奥山 大輔	2019.03.17-03.27
42	NIST	NG-7	東北大学	教授	佐藤 卓	18907	C1-2	MnSi における変動電流下の磁気スキルミオンのダイナミクス	東北大学	奥山 大輔	2019.03.18-03.23
43	ANSTO	ECHIDNA	東北大学	教授	佐藤 卓	18909	T1-3	歪んだ籠目格子遷歴磁性体Yb3Ru4Al12 の磁気構造	東北大学	佐藤 卓	2019.03.24-04.02
						18910	T1-3	Ga-Pd-Tb 2/1 近似結晶の磁気構造			
44	ANSTO	ECHIDNA	東北大学	助教	壁谷 典幸	18909	T1-3	歪んだ籠目格子遷歴磁性体Yb3Ru4Al12 の磁気構造	東北大学	佐藤 卓	2019.03.26-04.02
45	ANSTO	BILBY	北九州市立大学	研究員	藤井 翔太	18912	C1-2	完全に単分散な逆ミセルの構造可視化	北九州市立大学	藤井 翔太	2019.03.20-03.31
46	ANSTO	BILBY	京都大学	助教	西村 智貴	18911	C1-2	SANS測定による分子透過性ベシクルのPoly(propylene oxide)層中の水含量の決定	京都大学	西村 智貴	2019.03.20-03.29
47	ANSTO	BILBY	名古屋工業大学	准教授	山本 勝宏	18911	C1-2	SANS測定による分子透過性ベシクルのPoly(propylene oxide)層中の水含量の決定	京都大学	西村 智貴	2019.03.20-03.31

PUBLICATIONS AND DISSERTATIONS

(2010 – 2019)

Published by:
Neutron Science Laboratory,
Institute for Solid State Physics,
University of Tokyo
106-1, Shirakata, Tokai,
Ibaraki 319-1106,
JAPAN

This list is generated automatically from our database at: 2019/08/16 11:35:56 JST.
Visit our [on-line database](#) for updated information.

Publications

2019

- Magnetic states of coupled spin tubes with frustrated geometry in CsCrF₄
Hagihala M., Hayashida S., Avdeev M., Manaka H., Kikuchi H., Masuda T.
npj Quantum Materials **4** (2019) 14-1-9
- Nano-structure of organic-inorganic layered hybrids characterized by small-angle scattering of X-rays and neutrons
Harada M.
Materials Letters **253** (2019) 102-104
- Coexisting spin resonance and long-range magnetic order of Eu in EuRbFe₄As₄
Iida K., Nagai Y., Ishida S., Ishikado M., Murai N., Christianson A. D., Yoshida H., Inamura Y., Nakamura H., Nakao A., Munakata K., Kagerbauer D., Eisterer M., Kawashima K., Yoshida Y., Eisaki H., Iyo A.
Phys. Rev. B **100** (2019) 14506-14506
- Progress in High Resolution Chopper Spectrometer HRC by improving collimator and Fermi chopper
Itoh S., Yokoo T., Masuda T., Asai S., Saito H., Kawana D., Sugiura R., Asami T., Ihata Y.
Physica B **568** (2019) 76-80
- Spin correlations of quantum spin liquid and quadrupole-ordered states of Tb_{2+x}Ti_{2-x}O_{7+y}
Kadowaki H., Wakita M., Fak B., Ollivier J., Ohira-Kawamura S., Nakajima K., Lynn J. W.
Phys. Rev. B **99** (2019) 14406-14406
- Neutron scattering studies of static and dynamic correlation lengths in alkali metal borate glasses
Kojima S., Novikov V.N., Kofu M., Yamamuro O.
J. Non-Cryst. Solids **518** (2019) 18-23
- Sinusoidally modulated magnetic structure of Kramers local moments in CePd₅Al₂
Onimaru T., Inoue Y. F., Ishida A., Umeo K., Oohara Y., Sato T. J., Adroja D. T., Takabatake T.

- Controlling the stoichiometry of the triangular lattice antiferromagnet $\text{Li}_{1+x}\text{Zn}_{2-y}\text{Mo}_3\text{O}_8$
Sandvik K. E., Okuyama D., Nawa K., Avdeev M., Sato T. J.
J. Solid State Chem. **271** (2019) 216-221
- Precision polymer network science with tetra-PEG gels—a decade history and future
Shibayama M., Li X., Sakai T.
Colloid Polym. Sci. **297** (2019) 1-12
- 梯子型鉄系化合物 BaFe_2S_3 における圧力誘起超伝導
Yamauchi T., Hirata Y., Takahashi H., Nambu Y., Sato T. J., Ohgushi K.
固体物理 **54** (2019) 27-42
- Oxide-ion Diffusion Mechanism and Oxygen Deficiency δ of Hexagonal Perovskite-Related Oxide $\text{Ba}_3\text{MoNb}_{0.5-\delta}$
Yashima M., Tsujiguchi T., Fujii K., Niwa E., Nishioka S., Hester J. R., Maeda K.
J. Mater. Chem. A **7** (2019) 13910-13916

2018

- Cluster-Based Haldane State in an Edge-Shared Tetrahedral Spin-Cluster Chain: Fedotovite $\text{K}_2\text{Cu}_3(\text{SO}_4)_3$
Fujihala M., Sugimoto T., Tohyama T., Mitsuda S., Mole R. A., Yu D. H., Yano S., , Inagaki Y., Morodomi H., Kawae T., Sagayama H., Kumai R., Murakami Y., Tomiyasu K., Matsuo A., Kindo K.
Phys. Rev. Lett. **120** (2018) 77201-77201
- Discovery and development of BaNdInO_4 - A brief review -
Fujii K., Yashima M.
J. Ceram. Soc. Jpn. **126** (2018) 852-859
- Crystal Growth and Neutron Scattering Study of Spin Correlations of the T'-Structured $\text{Pr}_{2-x}\text{Ca}_x\text{CuO}_4$
Fujita M., Tsutsumi K., Miura T., Danilkin S.
Journal of Physics, Vol. 969 (The Institute of Physics, Sweden, 2018) pp. 12070-12070
- Ion Gel Network Formation in an Ionic Liquid Studied by Time-Resolved Small-Angle Neutron Scattering
Hashimoto K., Fujita K., Nishi K., Shibayama M.
J. Phys. Chem. B **122** (2018) 9419-9424
- Magnetic order in the rare-earth ferroborate $\text{CeFe}_3(\text{BO}_3)_4$
Hayashida S., Asai S., Kato D., Hasegawa S., Avdeev M., Cao H., Masuda T.
Phys. Rev. B **98** (2018) 224405-1-9
- Magnetic state selected by magnetic dipole interaction in the kagome antiferromagnet $\text{NaBa}_2\text{Mn}_3\text{F}_{11}$
Hayashida S., Ishikawa H., Okamoto Y., Okubo T., Hiroi Z., Avdeev M., Manuel P., Hagihala M., Soda M., Masuda T.
Phys. Rev. B **97** (2018) 54411-1-7
- Pressure-induced quantum phase transition in the quantum antiferromagnet CsFeCl_3
Hayashida S., Zaharko O., Kurita N., Tanaka H., Hagihala M., Soda M., Itoh S., Uwatoko Y., Masuda T.
Phys. Rev. B **97** (2018) 140405-1-4
- High resolution chopper spectrometer HRC and neutron Brillouin scattering

Itoh S., Yokoo T., Masuda T., Yoshizawa H., Soda M., Ibuka S., Ikeda Y., Yoshida M., Hawai T., Kawana D., Sugiura R., Asami T., Kawamura Y., Shinozaki T., Ihata Y. AIP Conf. Proc., Vol. 1969 (AIP, U.S.A, 2018) pp. 50002–50002

- Improvement for Neutron Brillouin Scattering Experiments on High Resolution Chopper Spectrometer HRC
Itoh S., Yokoo T., Masuda T., Yoshizawa H., Soda M., Yoshida M., Hawai T., Kawana D., Sugiura R., Asami T., Ihata Y.
J. Phys.: Conf. Series, Vol. 1021 (IOP Publishing, U. K., 2018) pp. 12028–12028
- Continuum Excitation and Pseudospin Wave in Quantum Spin-Liquid and Quadrupole Ordered States of $Tb_{2+x}Ti_{2-x}O_{7+y}$
Kadowaki H., Wakita M., Fak B., Ollivier J., Ohira-Kawamura S., Nakajima K., Takatsu H., Tamai M.
J. Phys. Soc. Jpn. **87** (2018) 64704–64704
- YUI and HANA: control and visualization programs for HRC in J-PARC
Kawana D., Soda M., Yoshida M., Ikeda Y., Asami T., Sugiura R., Yoshizawa H., Masuda T., Hawai T., Ibuka S., Yokoo T., Itoh S.
Journal of Physics: Conference Series, Vol. 1021 (IOP Publishing, London, 2018) pp. 12014–4
- Two inherent crossovers of the diffusion process in glass-forming liquids
Kofu M., Faraone A., Tyagi M., Nagao M., Yamamuro O.
Phys. Rev. E **98** (2018) 42601–42606
- Small-angle scattering study of tetra-poly(acrylic acid) gels
Morishima K., Li X., Oshima K., Mitsukami Y., Shibayama M.
J. Chem. Phys. **149** (2018) 163301–1–8
- Insight into the microscopic structure of module-assembled thermoresponsive conetwork hydrogels
Nakagawa S., Shibayama M., Kamata H., Sakai T., Gilbert E.
Macromolecules **51** (2018) 6645–6652
- Degenerate ground state in the classical pyrochlore antiferromagnet $Na_3Mn(CO_3)_2Cl$
Nawa K., Okuyama D., Avdeev M., Nojiri H., Yoshida M., Ueta D., Yoshizawa H., Sato T. J.
Phys. Rev. B **98** (2018) 144426–1–8
- Neutron scattering studies on short- and long-range layer structures and related dynamics in imidazolium-based ionic liquids
Nemoto F., Kofu M., Nagao M., Ohishi K., Takata S., Suzuki J., Yamada T., Shibata K., Ueki T., Kitazawa Y., Watanabe M., Yamamuro O.
J. Chem. Phys. **149** (2018) 54502–1–11
- Characterization of microstructure using Bragg edge and energy-resolved small-angle neutron scattering
Oba Y., Morooka S., Ohishi K., Suzuki J., Tsuchiyama T., Gilbert E. P.
Proceedings of the 5th International Symposium on Steel Science (ISSS 2017), Ed(s). Ii S., Furuhashi, T., Tsuchiyama T., and Miyamoto G. (The Iron and Steel Institute of Japan, Japan, 2018) pp. 151–154
- Neutron Diffraction Studies on Valence Ordering Compound YbPd
Oyama K., Sugishima M., Tanabe K., Mitsuda A., Wada H., Ohoyama K., Matsukawa T., Yoshida Y., Hoshikawa A., Ishigaki T., Iwasa K.
J. Phys. Soc. Jpn. **87** (2018) 114705–1–6
- Gels: From Soft Matter to BioMatte
Shibayama M., Li X., Sakai T.
Ind. Eng. Chem. Res. **57** (2018) 1121–1128
- Polarization analysis of magnetic excitation in multiferroic $Ba_2CoGe_2O_7$
Soda M., Chang L., Matsumoto M., Garlea V. O., Roessli B., White J. S., Kawano-Furukawa H., Masuda T.

- Crystalline Electric Field Level Scheme of the Non-Centrosymmetric CePtSi₃
Ueta D., Kobuke T., Yoshida M., Yoshizawa H., Ikeda Y., Itoh S., Yokoo T.
Physica B **536** (2018) 21-23
- Magnetic structure of a non-centrosymmetric CePtSi₃
Ueta D., Yoshida M., Ikeda Y., Liu Y., Hong T., Masuda T., Yoshizawa H.
AIP Advances **8** (2018) 115006-1-5
- Neutron Spin Resonance in the 112-Type Iron-Based Superconductor
Xie T., Gong D., Ghosh H., Ghosh A., Soda M., Masuda T., Itoh S., Bourdarot F.,
Regnault L.-P., Danilkin S., Li S., Luo H.
Phys. Rev. Lett. **120** (2018) 137001-1-7
- Magnetic and thermodynamic studies on the charge and spin ordering in the highly-
doped La_{2-x}Sr_xCoO₄
Yoshida M., Ueta D., Ikeda Y., Yokoo T., Itoh S., Yoshizawa H.
Physica B **536** (2018) 338-341

2017

- Powder neutron diffraction in one-dimensional frustrated chain compound
NaCuMoO₄(OD)
Asai S., Oyama T., Soda M., Rule K., Nawa K., Hiroi Z., Masuda T.
Journal of Physics: Conference Series, Vol. 828 (IOP Publishing, U. K., 2017) pp.
12006-12006
- Spin dynamics in the stripe-ordered buckled honeycomb lattice antiferromagnet
Ba₂NiTeO₆
Asai S., Soda M., Kasatani K., Ono T., Garlea V. O., Winn B., Masuda T.
Phys. Rev. B **96** (2017) 104414-1-6
- Magnetic excitations from the two-dimensional interpenetrating Cu framework in
Ba₂Cu₃O₄Cl₂
Babkevich P., Shaik N. E., Lancon D., Kikkawa A., Enderle M., Ewings R. A., Walker
H. C., Adroja D. T., Manuel P., Khalyavin D. D., Taguchi Y., Tokura Y., Soda M.,
Masuda T., Ronnow H. M.
Phys. Rev. B **96** (2017) 14410-1-12
- Possible Tomonaga-Luttinger spin liquid state in the spin-1/2 inequilateral
diamond-chain compound K₃Cu₃AlO₂(SO₄)₄
Fujihala M., Koorikawa H., Mitsuda S., Morita K., Tohyama T., Tomiyasu K., Koda
A., Okabe H., Itoh S., Yokoo T., Ibuka S., Tadokoro M., Itoh M., Sagayama H.,
Kumai R., Murakami Y.
Scientific Reports **7** (2017) 16785-1-6
- New Oxide-Ion Conductor SrYbInO₄ with Partially Cation-Disordered CaFe₂O₄-Type
Structure
Fujimoto A., Yashima M., Fujii K., Hester J.R.
J. Phys. Chem. C **121** (2017) 21272-21280
- Neutron Scattering Study in Breathing Pyrochlore Antiferromagnet Ba₃Yb₂Zn₅O₁₁
Haku T., Soda M., Sera M., Kimura K., Taylor J., Itoh S., Yokoo T., Matsumoto Y.,
Yu D., Mole R. A., Takeuchi T., Nakatsuji S., Kono Y., Sakakibara T., Chang L. -
J., Masuda T.
Journal of Physics: Conference Series, Vol. 828 (IOP Publishing, U. K., 2017) pp.
12018-12018
- Fast-forming hydrogel with ultralow polymeric content as an artificial vitreous
body

Hayashi K., Okamoto F., Hoshi S., Katashima T., Zujur D. C., Li X., Shibayama M., Gilbert E. P., Chung U., Ohba S., Osika T., Sakai T.
Nature Biomedical Engineering **1** (2017) 44-1-7

- Decisive test of the ideal behavior of tetra-PEG gels
Horkay F., Nishi K., Shibayama M.
J. Chem. Phys. **146** (2017) 164905-1-8
- Impurity effects in the microscopic elastic properties of polycrystalline Mg-Zn-Y alloys with a synchronized long-period stacking ordered phase
Hosokawa S., Kimura K., Yamasaki M., Kawamura Y., Yoshida K., Inui M., Tsutsui S., Baron A. Q. R., Kawakita Y., Itoh S.
J. Alloys Compounds **695** (2017) 426-432
- Damped spin-wave excitations in the itinerant antiferromagnet γ -Fe_{0.7}Mn_{0.3}
Ibuka S., Itoh S., Yokoo T., Endoh Y.
Phys. Rev. B **95** (2017) 224406-1-7
- Spin Resonance in the New-Structure-Type Iron-Based Superconductor CaKFe₄As₄
Iida K., Ishikado M., Nagai Y., Yoshida H., Christianson A. D., Murai N., Kawashima K., Yoshida Y., Eisaki H., Iyo A.
J. Phys. Soc. Jpn. **86** (2017) 93703-93703
- Time-of-Flight Elastic and Inelastic Neutron Scattering Studies on the Localized 4d Electron Layered Perovskite La₅Mo₄O₁₆
Iida K., Kajimoto R., Mizuno Y., Kamazawa K., Inamura Y., Hoshikawa A., Yoshida Y., Matsukawa T., Ishigaki T., Kawamura Y., Ibuka S., Yokoo T., Itoh S., Katsufuji T.
J. Phys. Soc. Jpn. **86** (2017) 64803-1-6
- 金属強磁性体SrRuO₃のスピン波におけるワイルフェルミオン
Itoh S., Endoh Y., Yokoo T., Ibuka S., Park J. G., Kaneko Y., Takahashi K. S., Tokura Y., Nagaosa N.
波紋, vol. 27 (日本中性子科学会, 東京都, 2017) pp. 67-70
- Evidence for antiferromagnetic-type ordering of f-electron multipoles in PrIr₂Zn₂₀
Iwasa K., Matsumoto K. T., Onimaru T., Takabatake T., Mignot J.-M., Gukasov A.
Phys. Rev. B **95** (2017) 155106-1-10
- Crystal-electric-field excitations and spin dynamics in Ce₃Co₄Sn₁₃ semimetallic chiral-lattice phase
Iwasa K., Otomo Y., Suyama K., Tomiyasu K., Ohira-Kawamura S., Nakajima K., Mignot J. M.
Phys. Rev. B **95** (2017) 195156-195156
- Effect of interlamellar interactions on shear induced multilamellar vesicle formation
Kawabata Y., Bradbury R., Kugizaki S., Weigandt K., Melnichenko Y. B., Sadakane K., Yamada N. L., Endo H., Nagao M., Seto H.
J. Chem. Phys. **147** (2017) 34905-1-10
- SANS Study on Critical Polymer Clusters of Tetra-Functional Polymers
Li X., Hirose K., Sakai T., Gilbert E. P., Shibayama M.
Macromolecules **50** (2017) 3655-3661
- Magnetic properties of DyPdSn single crystal
Li Y., Andoh Y., Kurisu M., Nakamoto G., Tsutaoka T., Kawano S.
J. Alloys Compd. **692** (2017) 961-965
- Thermal stability and irreversibility of skyrmion-lattice phases in Cu₂OSeO₃
Makino K., Reim J. D., Higashi D., Okuyama D., Sato T. J., Nambu Y., Gilbert E. P., Booth N., Seki S., Tokura Y.
Phys. Rev. B **95** (2017) 134412-1-10

- Microscopic Structure of the “Nonswellable” Thermoresponsive Amphiphilic Conetwork
Nakagawa S., Li X., Kamata H., Sakai T., Gilbert E. P., Shibayama M.
Macromolecules **50** (2017) 3388–3395
- Materials and Life Science Experimental Facility (MLF) at the Japan Proton Accelerator Research Complex II: Neutron Scattering Instruments
Nakajima K., Kawakita Y., Itoh S., Abe J., Aizawa K., Aoki H., Endo H., Fujita M., Funakoshi K., Wu G., Harada M., Harjo S., Hattori T., Hino M., Honda T., Hoshikawa A., Ikeda K., Ino T., Ishigaki T., Ishikawa Y., Iwase H., Kai T., Kajimoto R., Kamiyama T., Kaneko N., Kawana D., Kawamura S., Kawasaki T., Kimura A., Kiyanagi R., Kojima K., Kusaka K., Lee S., Machida S., Masuda T., Mishima K., Mitamura K., Nakamura M., Nakamura S., Nakao A., Oda T., Ohhara T., Ohishi K., Ohshita H., Oikawa K., Otomo T., Sano A., Shibata K., Shinohara T., Soyama K., Suzuki J., Suzuya K., Takahara A., Takata S., Takeda M., Toh Y., Torii S., Torikai N., Yamada N. L., Yamada T., Yamazaki D., Yokoo T., Yonemura M., Yoshizawa H.
Quantum Beam Sci. **1** (2017) 9–1–59
- Energy-resolved small-angle neutron scattering from steel
Oba Y., Morooka S., Ohishi K., Suzuki J., Takata S., Sato N., Inoue R., Tsuchiyama T., Gilbert E. P., Sugiyama M.
J. Appl. Crystallogr. **50** (2017) 334–339
- Impact of minute-time-scale kinetics on the stabilization of the skyrmion-lattice in Cu₂OSeO₃
Reim J. D., Makino K., Higashi D., Nambu Y., Okuyama D., Sato T. J., Gilbert E. P., Booth N., Seki S.
J. Phys.: Conf. Ser. **828** (2017) 12004–1–7
- Materials and Life Science Experimental Facility at the Japan Proton Accelerator Research Complex III: Neutron Devices and Computational and Sample Environments
Sakasai K., Satoh S., Seya T., Nakamura T., Toh K., Yamagishi H., Soyama K., Yamazaki D., Maruyama R., Oku T., Ino T., Kira H., Hayashida H., Sakai K., Itoh S., Suzuya K., Kambara W., Kajimoto R., Nakajima K., Shibata K., Nakamura M., Otomo T., Nakatani T., Inamura Y., Suzuki J., Ito T., Okazaki N., Moriyama K., Aizawa K., Kawamura S., Watanabe M.
Quantum Beam Sci. **1** (2017) 10–1–35
- Inelastic and quasi-elastic neutron scattering spectrometers in J-PARC
Seto H., Itoh S., Yokoo T., Endo H., Nakajima K., Shibata K., Kajimoto R., Ohira-Kawamura S., Nakamura M., Kawakita Y., Nakagawa H., Yamada T.
Bioch. Biophys. Acta **1861** (2017) 3651–3660
- Crystal Structure and Oxide-Ion Conductivity of Ba_{1+x}Nd_{1-x}InO_{4-x/2}
Shiraiwa M., Fujii K., Esaki Y., Kim S.J., Lee S., Yashima M.
J. Electrochem. Soc. **164** (2017) F1392–F1399
- Magnetic Structure and Dielectric State in the Multiferroic Ca₂CoSi₂O₇
Soda M., Hayashida S., Yoshida T., Akaki M., Hagiwara M., Avdeev M., Zaharko O., Masuda T.
J. Phys. Soc. Jpn. **86** (2017) 64703–1–5
- Dielectric Property and Diffuse Scattering in Relaxor Magnet LuFeCoO₄
Soda M., Masuda T.
Journal of Physics: Conference Series, Vol. 828 (IOP Publishing, U. K., 2017) pp. 12001–12001
- A layered wide-gap oxyhalide semiconductor with an infinite ZnO₂ square planar sheet: Sr₂ZnO₂Cl₂
Su Y., Tsujimoto Y., Miura A., Asai S., Avdeev M., Ogino H., Ako M., Belik A. A., Masuda T., Uchikoshi T., Yamaura K.
Chem. Commun. **53** (2017) 3826–3826–3829
- Cubic lead perovskite PbMoO₃ with anomalous metallic behavior
Takatsu H., Hernandez O., Yoshimune W., Prestipino C., Yamamoto T., Tassel C., Kobayashi Y., Batuk D., Shibata Y., Abakumov A. M., Brown C. M., Kageyama H.

- Spin-lattice-coupling-mediated magnetoferroelectric phase transition induced by uniaxial pressure in multiferroic $\text{CuFe}_{1-x}\text{M}_x\text{O}_2$ ($\text{M} = \text{Ga}, \text{Al}$)
Tamatsukuri H., Mitsuda S., Nakamura T., Takata K., Nakajima T., Prokes K., Yokaichiya F., Kiefer K.
Phys. Rev. B **95** (2017) 174108-1-9
- Decoupling Between the Temperature-Dependent Structural Relaxation and Shear Viscosity of Concentrated Lithium Electrolyte
Yamaguchi T., Yoshida K., Yamaguchi T., Nagao M., Faraone A., Seki S.
J. Phys. Chem. B **121** (2017) 8767-8773
- 熱測定と中性子散乱の相補利用による新規物質研究
Yamamuro O.
熱測定 **44** (2017) 117-123
- Calorimetric and Neutron Scattering Studies on Glass Transitions and Ionic Diffusions in Imidazolium-based Ionic Liquids
Yamamuro O., Kofu M.
IOP Conf. Ser.: Mater. Sci. Eng. **196** (2017) 12001-1-4

2016

- Nanometer-Size Effect on Hydrogen Sites in Palladium Lattice
Akiba H., Kofu M., Kobayashi H., Kitagawa H., Ikeda K., Otomo T., Yamamuro O.
J. Am. Chem. Soc. **138** (2016) 10238-10243
- Magnetic ordering of the buckled honeycomb lattice antiferromagnet $\text{Ba}_2\text{NiTeO}_6$
Asai S., Soda M., Kasatani K., Ono T., Avdeev M., Masuda T.
Phys. Rev. B **93** (2016) 24412-24412
- LiNbO_3 -Type InFeO_3 : Room-Temperature Polar Magnet without Second-Order Jahn-Teller Active Ions
Fujita K., Kawamoto T., Yamada I., Hernandez O., Hayashi N., Akamatsu H., Lafargue-Dit-Hauret W., Rocquefelte X., Fukuzumi M., Manuel P., Studer A. J., Knee C. S., Tanaka K.
Chem. Mater. **28** (2016) 6644-6655
- Low-energy excitations and ground-state selection in the quantum breathing pyrochlore antiferromagnet $\text{Ba}_3\text{Yb}_2\text{Zn}_5\text{O}_{11}$
Haku T., Kimura K., Matsumoto Y., Soda M., Sera M., Yu D., Mole R.A., Takeuchi T., Nakatsuji S., Kono Y., Sakakibara T., Chang L. J., Masuda T.
Phys. Rev. B **93** (2016) 220407-220407
- Crystal Field Excitations in the Breathing Pyrochlore Antiferromagnet $\text{Ba}_3\text{Yb}_2\text{Zn}_5\text{O}_{11}$
Haku T., Soda M., Sera M., Kimura K., Itoh S., Yokoo T., Masuda T.
J. Phys. Soc. Jpn. **85** (2016) 34721-34721
- Crystal field excitations on $\text{NdFe}_3(\text{BO}_3)_4$ investigated by inelastic neutron scattering
Hayashida S., Soda M., Itoh S., Yokoo T., Ohgushi K., Kawana D., Masuda T.
J. Phys.: Conf. Ser., Vol. 746 (IOP Publishing, UK, 2016) pp. 12059-12059
- Mechanism of Heat-induced Gelation for Ovalbumin and Its N-terminus Cleaved Form
Hiroi T., Okazumi Y., Littrell K. C., Narita Y., Tanaka N., Shibayama M.
Polymer **93** (2016) 152-158
- Fabrication and Structural Characterization of Module-Assembled Amphiphilic Conetwork Gels

- Hiroi T., Kondo S., Sakai T., Gilbert E. P., Han Y. -S., Kim T. -H., Shibayama M.
Macromolecules **49** (2016) 4940-4947
- SANS Study on Solvated Structure and Molecular Interactions of a Thermo-responsive Polymer in a Room Temperature Ionic Liquid
 Hiroi T., Fujita K., Ueki T., Kitazawa Y., Littrell K. C., Watanabe M., Shibayama M.
Phys. Chem. Chem. Phys. **18** (2016) 17881-17889
 - Inelastic Neutron Scattering Study of Stripe and Overdoped Checkerboard Ordering in Layered Nickel Oxide $\text{Nd}_{2-x}\text{Sr}_x\text{NiO}_4$
 Ikeda Y., Suzuki S., Nakabayashi T., Yoshizawa H., Yokoo T., Itoh S.
J. Phys. Soc. Jpn. **85** (2016) 23701-1-5
 - New insight into the dynamical system of αB -crystallin oligomers
 Inoue R., Takata T., Fujii N., Ishii K., Uchiyama S., Sato N., Oba Y., Kato K., Fujii N., Sugiyama M.
Sci. Rep. **6** (2016) 0-0
 - Weyl fermions and spin dynamics of metallic ferromagnet SrRuO_3
 Itoh S., Endoh Y., Yokoo T., Ibuka S., Park J.-G., Kaneko Y., Takahashi K. S., Tokura Y., Nagaosa N.
Nature Communications **7** (2016) 11788-1-8
 - 高分解能チョッパー分光器による物質のダイナミクスの研究
 Itoh S., Ibuka S., Yokoo T., Masuda T., Yoshizawa H., Sato T. J.
RADIOISOTOPES, Vol. 65 (公益社団法人 日本アイソトープ協会, 東京都, 2016) pp. 535-544
 - Instrument developments and neutron Brillouin scattering experiments on HRC
 Itoh S., Yokoo T., Ibuka S., Masuda T., Yoshizawa H., Soda M., Ikeda Y., Asami T., Sugiura R., Kawana D., Shinozaki T., Ihata Y.
 Proceedings of the 21st meeting of the international collaboration on advanced neutron sources (ICANS-21)., Vol. 48 (Japan Atomic Energy Agency, Tokai, Japan, 2016) pp. 298-305
 - Muon Spin Relaxation and Neutron Diffraction Studies of Cluster-Glass States in $\text{Sr}_{1-x}\text{La}_x\text{RuO}_3$
 Kawasaki I., Fujimura K., Watanabe K., Avdeev M., Tenya K., Yokoyama M.
J. Phys. Soc. Jpn. **85** (2016) 54701-1-8
 - Magnetic Reversal of Electric Polarization with Fixed Chirality of Magnetic Structure in a Chiral-Lattice Helimagnet MnSb_2O_6
 Kinoshita M., Seki S., Sato T. J., Nambu Y., Hong T., Matsuda M., Cao H. B., Ishiwata S., Tokura Y.
Phys. Rev. Lett. **117** (2016) 47201-1-5
 - イオン液体の階層的構造およびダイナミクス
 Kofu M.
 波紋, Vol. 26 (日本中性子科学会, 東京都, 2016) pp. 95-99
 - Hydrogen diffusion in bulk and nanocrystalline palladium: A quasielastic neutron scattering study
 Kofu M., Hashimoto N., Akiba H., Kobayashi H., Kitagawa H., Tyagi M., Faraone A., Copley J. R. D., Lohstroh W., Yamamuro O.
Phys. Rev. B **94** (2016) 64303-64303
 - イミダゾリウム系イオン液体の階層的・ガラスダイナミクス
 Kofu M., Yamamuro O.
 日本結晶学会誌, Vol. 58 (日本結晶学会, 東京都, 2016) pp. 18-23
 - Magnetic structure of the $S=1/2$ quasi-two-dimensional square-lattice Heisenberg antiferromagnet $\text{Sr}_2\text{CuTeO}_6$
 Koga T., Kurita N., Avdeev M., Danilkin S., Sato T. J., Tanaka H.

- "Simultaneous evidence for Pauli paramagnetic effects and multiband superconductivity in KFe₂As₂ by small-angle neutron scattering studies of the vortex lattice"
Kuhn J.S., Kawano-Furukawa H., Jellyman E., Riyat R., Forgan M. E., Ono M., Kihou K., Lee H. C., Hardy F., Adelman P., Wolf Th., Meingast C., Gavilano J., Eskildsen R. M.
Phys. Rev. B **93** (2016) 104527-1-8
- ZnTaO₂N: Stabilized High-Temperature LiNbO₃-type Structure
Kuno Y., Tassel C., Fujita K., Batuk D., Abakumov A. M., Shitara K., Kuwabara A., Moriwake H., Watabe D., Ritter C., Brown C. M., Yamamoto T., Takeiri F., Abe R., Kobayashi Y., Tanaka K., Kageyama H.
J. Am. Chem. Soc. **138** (2016) 15950-15955
- Incommensurate Magnetic Structure in the Cubic Noncentrosymmetric Ternary Compound Pr₅Ru₃Al₂
Makino K., Okuyama D., Avdeev M., Sato T. J.
J. Phys. Soc. Jpn. **85** (2016) 73705-1-5
- Topochemical Nitridation with Anion Vacancy-assisted N₃-/O₂- Exchange
Mikita R., Aharen T., Yamamoto T., Takeiri F., Ya T., Yoshimune W., Fujita K., Yoshida S., Tanaka K., Batuk D., Abakumov A. M., Brown C. M., Kobayashi Y., Kageyama H.
J. Am. Chem. Soc. **138** (2016) 3211-3217
- Topochemical Nitridation with Anion Vacancy-assisted N₃-/O₂- Exchange
Mikita R., Aharen T., Yamamoto T., Takeiri F., Ya T., Yoshimune W., Fujita K., Yoshida S., Tanaka K., Kobayashi Y., Kageyama H.
J. Am. Chem. Soc. **138** (2016) 3211-3217
- HfMnSb₂: Metal Ordered NiAs-type Pnictide with a Conical Spin Order
Murakami T., Yamamoto T., Tassel C., Takatsu H., Ritter C., Ajiro Y., Kageyama H.
Angew. Chem. Int. Ed. **55** (2016) 9877-9880
- Magnetic scattering in the simultaneous measurement of small-angle neutron scattering and Bragg edge transmission from steel
Oba Y., Morooka S., Ohishi K., Sato N., Inoue R., Adachi N., Suzuki J., Tsuchiyama T., Gilbert E. P., Sugiyama M.
J. Appl. Crystallogr. **49** (2016) 1659-1664
- Hydrothermal Synthesis, Crystal Structure, and Superconductivity of a Double-Perovskite Bi Oxide
Rubel M. H. K., Takei T., Kumada N., Ali M. M., Miura A., Tadanaga K., Oka K., Azuma M., Yashima M., Fujii K., Magome E., Moriyoshi C., Kuroiwa Y., Hester J., Avdeev M.
Chem. Mater. **28** (2016) 459-465
- 中性子散乱とソフトマター
Shibayama M.
物性科学ハンドブック -概念・現象・物質-, Ed(s). 東京大学物性研究所 (朝倉書店, 東京, 2016) pp. 876-926
- Continuous control of local magnetic moment by applied electric field in multiferroics Ba₂CoGe₂O₇
Soda M., Hayashida S., Roessli B., Mansson M., White J. S., Matsumoto M., Shiina R., Masuda T.
Phys. Rev. B **94** (2016) 94418-94418-94418
- Dielectric and Magnetic Properties in Relaxor Magnet LuFeCoO₄
Soda M., Masuda T.
J. Phys. Soc. Jpn. **85** (2016) 34713-34713

- Quadrupole Order in the Frustrated Pyrochlore $Tb_{2+x}Ti_{2-x}O_7$
Takatsu H., Onoda S., Kittaka S., Kasahara A., Kono Y., Sakakibara T., Kato Y., Fak B., Ollivier J., Lynn J. W., Taniguchi T., Wakita M., Kadowaki H.
Phys. Rev. Lett. **116** (2016) 217201-1-6
- High Pressure Synthesis of Layered Iron Oxyselenide $BaFe_2Se_2O$ with Strong Magnetic Anisotropy
Takeiri F., Matsumoto Y., Yamamoto T., Hayashi N., Li Z., Tohyama T., Tassel C., Ritter C., Narumi Y., Hagiwara M., Kageyama H.
Phys. Rev. B **94** (2016) 184426-1-6
- Uniaxial pressure effects on spin-lattice coupled phase transitions in a geometrical frustrated magnet $CuFeO_2$
Tamatsukuri H., Aoki S., Mitsuda S., Nakajima T., Itabashi T., Hosaka S., Ito S., Yamasaki Y., Nakano H., Prokes K., Kiefer K.
Phys. Rev. B **94** (2016) 174402-1-7
- High Pressure Synthesis of a Manganese Oxyhydride with Partial Anion Order
Tassel C., Goto Y., Watabe D., Tang Y., Lu H., Kuno Y., Takeiri F., Yamamoto T., Aharen T., Brown C. M., Hester J., Kobayashi Y., Kageyama H.
Angew. Chem. Int. Ed. **55** (2016) 9667-9670
- Selective and Low Temperature Transition Metal Intercalation in the Layered Tellurides
Yajima T., Koshiko M., Zhang Y., Oguchi T., Yu W., Kato D., Kobayashi Y., Orikasa Y., Yamamoto T., Uchimoto Y., Green M. A., Kageyama H.
Nature Communications **7** (2016) 13809-1-8
- Neutron Diffraction Study of Quadruple Perovskite $SrCu_3Fe_3O_{12}$
Yamada I., Murakami M., Mori S., Irifune T.
AIP Conference Proceedings, Vol. 1763 (American Institute of Physics, USA, 2016) pp. 50002-50002
- Impact of Lanthanoid Substitution on the Structural and Physical Properties of the Infinite Layer Iron Oxide
Yamamoto T., Ohkubo H., Tassel C., Hayashi N., Kawasaki S., Okada T., Yagi T., Hester J., Avdeev M., Kobayashi Y., Kageyama H.
Inorg. Chem. **55** (2016) 12093-12099
- Collective dynamics measurement of liquid methanol by inelastic neutron scattering
Yoshida K., Yamaguchi T., Yokoo T., Itoh S.
J. Mol. Liquids **222** (2016) 395-397

2015

- Improved oxide-ion conductivity of $NdBaInO_4$ by Sr doping
Fujii K., Shiraiwa M., Esaki Y., Yashima M., Kim S. J., Lee S.
J. Mater. Chem. A **3** (2015) 11985-11990
- Magnetic structure and Dzyaloshinskii-Moriya interaction in the $S = 1/2$ helical-honeycomb antiferromagnet $\alpha-Cu_2V_2O_7$
Gitgeatpong G., Zhao Y., Avdeev M., Piltz R. O., Sato T. J., Matan K.
Phys. Rev. B **92** (2015) 24423-1-10
- Magnetic structure of the spin-1/2 frustrated quasi-one-dimensional antiferromagnet $Cu_3Mo_2O_9$: Appearance of a partially disordered state
Hase M., Kuroe H., Pomjakushin V. Yu., Keller L., Tamura R., Terada N., Matsushita Y., Doenni A., Sekine T.
Phys. Rev. B **92** (2015) 54425-1-7
- Temperature and composition phase diagram in the iron-based ladder compounds

- Ba_{1-x}Cs_xFe₂Se₃
 Hawai T., Nambu Y., Ohgushi K., Du F., Hirata Y., Avdeev M., Uwatoko Y., Sekine Y., Fukazawa H., Ma J., Chi S., Ueda Y., Yoshizawa H., Sato T. J.
 Phys. Rev. B **91** (2015) 184416-1-11
- Inelastic Neutron Scattering on Multiferroics NdFe₃(BO₃)₄
 Hayashida S., Soda M., Itoh S., Yokoo T., Ohgushi K., Kawana D., Masuda T.
 Physics Procedia **75** (2015) 127-133
 - Magnetic model in multiferroic NdFe₃(BO₃)₄ investigated by inelastic neutron scattering
 Hayashida S., Soda M., Itoh S., Yokoo T., Ohgushi K., Kawana D., Ronnow H. M., Masuda T.
 Phys. Rev. B **92** (2015) 54402-54402
 - Investigations on average and local structures of Li(Li_{1/6}Mn_{1/2}Ni_{1/6}Co_{1/6})O₂ by the pair distribution function and the density functional theory
 Idemoto Y., Akatsuka K., Kitamura N.
 J. Power Sources **299** (2015) 280-285
 - Crystal and electronic structures, thermodynamic stability, and cathode performance of Li(Ni, Co, M)O₂ (M = Cu, Zn)
 Idemoto Y., Tsukada Y., Kitamura N.
 Solid State Ionics **279** (2015) 6-10
 - Transport and Thermodynamic Studies of Stripe and Checkerboard Ordering in Layered Nickel Oxides R_{2-x}Sr_xNiO₄ (R = La and Nd)
 Ikeda Y., Suzuki S., Nakabayashi T., Yoshizawa H., Yokoo T., Itoh S.
 J. Phys. Soc. Jpn. **84** (2015) 23706-1-5
 - Characterization of Ferromagnetic Order in CePd₂P₂
 Ikeda Y., Yoshizawa H., Konishi S., Araki S., Kobayashi T.C., Yokoo T., Itoh S.
 Characterization of Ferromagnetic Order in CePd₂P₂, Vol. 592 (J. Phys: Conf. Ser., Japan, 2015) pp. 12013-6
 - Phase Behavior of Block Copolymers in Selective Supercritical Solvent
 Ito M., Ito K., Shibayama M., Sugiyama K., Yokoyama H.
 Macromolecules **48** (2015) 3590-3597
 - チョッパー分光器(2)-非弾性散乱実験の観測領域の拡大に向けて-
 Itoh S., Ohoyama K.
 波紋, Vol. 25 (日本中性子科学会, 東京都, 2015) pp. 52-59
 - Science from the Initial Operation of HRC
 Itoh S., Yokoo T., Masuda T., Yoshizawa H., Soda M., Ikeda Y., Ibuka S., Kawana D., Sato T. J., Nambu Y., Kuwahara K., Yano S., Akimitsu J., Kaneko Y., Tokura Y., Fujita M., Hase M., Iwasa K., Hiraka H., Fukuda T., Ikeuchi K., Yoshida K., Yamaguchi T., Ono K., Endoh Y.
 JPS Conf. Proc., Vol. 8 (JPS, Japan, 2015) pp. 34001-34001
 - Nd-ion substitution effect on f-electron multipole order of PrRu₄P₁₂
 Iwasa K., Yonemoto A., Takagi S., Itoh S., Yokoo T., Ibuka S., Sekine C., Sugawara H.
 Physics Procedia **75** (2015) 179-186
 - Composite spin and quadrupole wave in the ordered phase of Tb_{2+x}Ti_{2-x}O_{7+y}
 Kadowaki H., Takatsu H., Taniguchi T., Fak B., Ollivier J.
 SPIN **5** (2015) 154003-1-8
 - Structural Origin of the Anisotropic and Isotropic Thermal Expansion of K₂NiF₄-Type LaSrAlO₄ and Sr₂TiO₄
 Kawamura K., Yashima M., Fujii K., Omoto K., Hibino K., Yamada S., Hester J. R., Avdeev M., Miao P., Torii S., Kamiyama T.
 Inorg. Chem. **54** (2015) 3896-3904

- Inelastic neutron scattering study on boson peaks of imidazolium-based ionic liquids
Kofu M., Inamura Y., Moriya Y., Podlesnyak A., Ehlers G., Yamamuro O.
J. Mol. Liq **210** (2015) 164-168
- Quasielastic neutron scattering studies on glass-forming ionic liquids with imidazolium cations
Kofu M., Tyagi M., Inamura Y., Miyazaki K., Yamamuro O.
J. Chem. Phys. **143** (2015) 234502-1-10
- Reliable hydrogel with mechanical 'fuse link' in an aqueous environment
Kondo S., Hiroi T., Han Y. S., Kim T.H., Shibayama M., Chung U., Sakai T.
Adv. Mater. **27** (2015) 7407-7411
- Intermultiplet transitions in filled skutterudite SmFe₄P₁₂
Konno S., Suzuki A., Nihei K., Kuwahara K., Kawana D., Yokoo T., Itoh S.
International Conference on Strongly Correlated Electron Systems 2014 (SCES2014), Vol. 592 (Journal of Physics: Conference Series, Japan, 2015) pp. 12029-6
- Structure evolution of catalyst ink for fuel cell in drying process investigated by CV-SANS
Kusano T., Hiroi T., Amemiya K., Ando M., Takahashi T., Shibayama M.
Polym. J. **47** (2015) 546-556
- Hydride in BaTiO_{2.5}H_{0.5}: A Labile Ligand in Solid State Chemistry
Masuda N., Kobayashi Y., Hernandez O., Bataille T., Paofai S., Suzuki H., Ritter C., Ichijo N., Noda I., Takegoshi K., Tassel C., Yamamoto T., Kageyama H.
J. Am. Chem. Soc. **137** (2015) 15315-15321
- Hydride in BaTiO_{2.5}H_{0.5}: A Labile Ligand in Solid State Chemistry
Masuda N., Kobayashi Y., Hernandez O., Bataille T., Paofai S., Suzuki H., Ritter C., Ichijo N., Noda Y., Tassel C., Yamamoto T., Kageyama H.
J. Am. Chem. Soc. **137** (2015) 15315-15321
- 2次元正方格子反強磁性体Ba₂CoGe₂₀₇におけるスピン・ネマティック相互作用の観測
Masuda T.
Radioisotopes **64** (2015) 765-774
- マルチフェロイック物質Ba₂CoGe₂₀₇におけるスピン・ネマティック相互作用の観測
Masuda T., Soda M.
固体物理 **50** (2015) 111-122
- Spin Fluctuations from Hertz to Terahertz on a Triangular Lattice
Nambu Y., Gardner J. S., MacLaughlin D. E., Stock C., Endo H., Jonas S., Sato T. J., Nakatsuji S., Broholm C.
Phys. Rev. Lett. **115** (2015) 12720-1-5
- Thermal and Structural Studies of Imidazolium-Based Ionic Liquids with and without Liquid-Crystalline Phases: The Origin of Nanostructure
Nemoto F., Kofu M., Yamamuro O.
J. Phys. Chem. B **119** (2015) 5028-5034
- Structural Analysis of Lipophilic Polyelectrolyte Solutions and Gels in Low-Polar Solvents
Nishi K., Tochioka S., Hiroi T., Yamada T., Kokado K., Kim T. H., Gilbert E., Sada K., Shibayama M.
Macromolecules **48** (2015) 3613-3621
- Gelation Kinetics and Polymer Network Dynamics of Homogeneous Tetra-PEG Gels
Shibayama M., Nishi K., Hiroi T.
Macromol. Symp. **348** (2015) 9-13
- Pressure-induced superconductivity in the iron-based ladder material BaFe₂S₃

- Takahashi H., Sugimoto A., Nambu Y., Yamauchi T., Hirata Y., Kawakami T., Avdeev M., Matsubayashi K., Du F., Kawashima C., Soeda H., Nakano S., Uwatoko Y., Ueda Y., Sato T. J., Ohgushi K.
Nature Mater. **14** (2015) 1008–1012
- MnTaO₂N: Polar LiNbO₃-type Oxynitride with a Helical Spin Order
 Tassel C., Kun Y., Goto Y., Yamamoto T., Brown C., Hester J., Fujita K., Higashi M., Abe R., Tanaka K., Kobayashi Y., Kageyama H.
Angew. Chem. Int. Ed. **54** (2015) 516–521
 - MnTaO₂N: Polar LiNbO₃-type Oxynitride with a Helical Spin Order
 Tassel C., Kuno Y., Goto Y., Yamamoto T., Brown C., Hester J., Fujita K., Higashi M., Abe R., Tanaka K., Kobayashi Y., Kageyama H.
Angew. Chem. Int. Ed. **54** (2015) 516–521
 - A Labile Hydride Strategy for the Synthesis of Heavily Nitridized BaTiO₃
 Yajima T., Takeiri F., Aidzu K., Akamatsu H., Fujita K., Ohkura M., Yoshimune W., Lei S., Gopalan V., Tanaka K., Brown C. M., Green M. A., Yamamoto T., Kobayashi Y., Kageyama H.
Nature Chemistry **7** (2015) 1017–1023
 - A Labile Hydride Strategy for the Synthesis of Heavily Nitridized BaTiO₃
 Yajima T., Takeiri F., Aidzu K., Akamatsu H., Fujita K., Ohkura M., Yoshimune W., Lei S., Gopalan V., Tanaka K., Yamamoto T., Kobayashi Y., Kageyama H.
Nat. Chem. **7** (2015) 1017–1023
 - Relationship between Structural Relaxation, Shear Viscosity, and Ionic Conduction of LiPF₆ / Propylene Carbonate Solutions
 Yamaguchi T., Yonezawa T., Yoshida K., Yamaguchi T., Nagao M., Faraone A., Seki S.
J. Phys. Chem. B **119** (2015) 15675–15682
 - 中性子散乱で観たイオン液体の階層的構造とダイナミクス
 Yamamuro O., Nemoto F., Kofu M.
高圧力の科学と技術, vol. 25 (日本高圧力学会, 東京都, 2015) pp. 200–207
 - Invited Review: Some recent developments in the atomic-scale characterization of structural and transport properties of ceria-based catalysts and ionic conductors
 Yashima M.
Catal. Today **253** (2015) 3–19
 - Chapter 3. Crystal Structure, Structural Disorder and Oxide-Ion Diffusional Pathway of Fluorite-Type Oxides and Fluorite-Related Phases
 Yashima M.
New Research Trends of Fluorite-Based Oxide Materials: From Basic Chemistry and Materials Science to Engineering Applications (Nova Science Publisher, New York, 2015) pp. 59–77
 - 中性子とx線回折法を含む多面的アプローチによるセラミック材料の結晶構造, 電子密度分布とイオン拡散経路の研究
 Yashima M.
日本結晶学会誌 **57** (2015) 13–19
 - 新しい層状構造を有する酸化物イオン伝導体の発見
 Yashima M., Fujii K.
パリテイ **30** (2015) 19–21
 - Crystal structure analysis and design of ceramic materials for clean energy
 Yashima M., Fujii K.
Fine Ceramics Report **33** (2015) 88–93

- Weak Ferromagnetic Ordering Disordered by Rh³⁺ Ions for LaCo_{0.8}Rh_{0.2}O₃
Asai S., Okazaki R., Terasaki I., Yasui Y., Igawa N., Kakurai K.
JPS Conf. Proc. (JPS, Japn, 2014) pp. 14034–14034
- Crystal structure and electrical conductivity of new mixed conductor Nd₂-
XBaXInO_{4.5-X/2}
Esaki Y., Fuji K., Omoto K., Yashima M., Ishigaki T., Hoshikawa A., Hester J. R.
NSL News Letter, ISSP joint research on neutron scattering in facilities abroad
(The institute for Solid State Physics, Japan, 2014) pp. 124–124
- New Perovskite-Related Structure Family of Oxide-Ion Conducting Materials NdBaInO₄
Fujii K., Esaki Y., Omoto K., Yashima M., Hoshikawa A., Ishigaki T., Hester J.R.
Chem. Mater. **26** (2014) 2488–2491
- Discovery of the new structure family of oxide-ion conducting material
Fujii K., Yashima M.
Ceramics **49** (2014) 615–615
- Discovery of the new structure family of oxide-ion conductor NdBaInO₄
Fujii K., Yashima M.
Parity **29** (2014) 35–37
- Experimental confirmation of spin gap in antiferromagnetic alternating spin 3/2
chain substances RCrGeO₅ (R=Y or 154Sm) by inelastic neutron scattering
experiments
Hase M., Soda M., Masuda T., Kawana D., Yokoo T., Itoh S., Matsuo A., Kindo K.,
Kohno M.
Phys. Rev. B **90** (2014) 24416–24416
- Multiscale Dynamics of Inhomogeneity-Free Polymer Gels
Hiroi T., Ohl M., Sakai T., Shibayama M.
Macromolecules **47** (2014) 763–770
- Anisotropic inplane spin correlation in the parent and Co-doped BaFe₂As₂: a
neutron scattering study
Ibuka S., Nambu Y., Yamazaki T., Lumsden M. D., Sato T. J.
Physica C **507** (2014) 25–30
- Investigation into properties of highly functional oxides using quantum beam and
thermodynamic measurement
Idemoto Y.
J. Ceram.Soc. Jpn **122** (2014) 839–845
- Development of Cathode Material for Li Ion Battery Using Neutron, Synchrotron X-
ray Sources and Theoretical Calculation
Idemoto Y.
J. Ceram.Soc. Jpn **49** (2014) 926–930
- Relationship between the local dynamics and gas permeability of polyacetylenes
containing polymethylated indan/tetrahydronaphtalene moieties
Inoue R., Kanaya T., Hu Y., Masuda T., Nishida K., Yamamuro O.
Polymer **55** (2014) 182–186
- Spin Waves in Ferromagnetic Phase of MnP
Itoh S., Yano S., Yokoo T., Satoh S., Kawana D., Kousaka Y., Akimitsu J., Endoh Y.
J. Phys.: Conf. Series, Vol. 502 (IOP Publishing, U. K., 2014) pp. 12044–12044
- Neutron Brillouin Scattering Experiments with Pulsed Neutrons on High Resolution
Chopper Spectrometer HRC
Itoh S., Yokoo T., Kawana D., Kaneko Y., Tokura Y., Fujita M., Yoshida K., Saito
K., Inami N., Takeichi Y., Ono K., Endoh Y.
J. Phys.: Conf. Ser., Vol. 502 (IOP Publishing, U. K., 2014) pp. 12043–12043

- Neutron scattering study on f-electron states in PrCu₄Au
Iwasa K., Kobayashi H., Saito K., Tomiyasu K., Zhang S., Isikawa Y., Mignot J.-M., Andre G., Kawana D., Kolesnikov A. I., Savici A. T., Granroth G. E.
Proc. Int. Conf. Strongly Correlated Electron Systems (SCES2013), Vol. 3, Ed(s).
Kenji Ishida (JPS Conf. Proc., Tokyo, 2014) pp. 11075–11075
- SANSおよびSAXSによるフェノール樹脂硬化物の構造解析
Izumi A., Nakao T., Iwase H., Shibayama M.
波紋 **24** (2014) 11–14
- A Room-Temperature Polar Ferromagnet ScFeO₃ Transformed from a High-Pressure Orthorhombic Perovskite Phase
Kawamaoto T., Fujita K., Yamada Y., Matoba T., Kim S. J., Gao P., Pan X., Findlay S. D., Tassel C., Kageyama H., Irifune T., Tanaka K.
J. Am. Chem. Soc. **136** (2014) 15291–15299
- Room-Temperature Polar Ferromagnet ScFeO₃ Transformed from a High-Pressure Orthorhombic Perovskite Phase
Kawamoto T., Fujita K., Yamada I., Matoba T., Kim S. J., Gao P., Pan X., Findlay C., Tassel C., Kageyama H., Studer A. J., Hester J., Irifune T., Tanaka K.
J. Am. Chem. Soc. **136** (2014) 15291–15299
- イミダゾリウム系イオン液体の不均一ダイナミクス
Kofu M., Yamamuro O.
波紋, vol. 24 (日本中性子科学会, 東京都, 2014) pp. 126–131
- 原子炉における小角散乱装置
Koizumi S., Shibayama M., Kumada Y., Yamaguchi D., Furusaka M.
波紋 **24** (2014) 141–150
- 中性子小角散乱を用いた分子集合体の解析
Kusano T., Shibayama M.
Colloid & Interface Communication **39** (2014) 16–18
- Ghost modes and continuum scattering in the dimerized distorted kagome lattice antiferromagnet Rb₂Cu₃SnF₁₂
Matan K., Nambu Y., Zhao Y., Sato T. J., Fukumoto Y., Ono T., Tanaka H., Broholm C., Podlesnyak A., Ehlers G.
Phys. Rev. B **89** (2014) 24414–1–7
- Appearance of Antiferromagnetic Dipole Order in Ce_{0.5}La_{0.5}B₆ with Pr Ion Doping
Matsumura T., Kunimori K., Kondo A., Soejima K., Tanida H., Mignot J.-M., Iga F., Sera M.
J. Phys. Soc. Jpn. **83** (2014) 94724–1–7
- Proton Dynamics of Two Dimensional Oxalate-Bridged Coordination Polymers
Miyasu S., Kofu M., Nagoe A., Yamada T., Sadakiyo M., Yamada T., Kitagawa H., Tyagi M., Sakai V. G., Yamamuro O.
Phys. Chem. Chem. Phys. **16** (2014) 17295–17304
- Proton Dynamics of Two Dimensional Oxalate-Bridged Coordination Polymers
Miyatsu S., Kofu M., Nagoe A., Yamada T., Sadakiyo M., Yamada T., Kitagawa H., Tyagi M., Garcia-Sakai V., Yamamuro O.
Phys. Chem. Chem. Phys. **16** (2014) 17295–17304
- “Vortex lattice structure in BaFe₂(As_{0.67} P_{0.33})₂ via small-angle neutron scattering”
Morisaki-Ishii R., Kawano-Furukawa H., Cameron S. A., Lemberger L., Blackburn E., Holmes T. A., Forgan M. E., DeBeer-Schmitt M. L., Littrell K., Nakajima M., Kihou K., Lee H. C., Iyo A., Eisaki H., Uchida S., White S. J., Dewhurst D. C., Gavigano L. J., Zolliker M.

- "Vortex lattice structure in BaFe₂(As_{0.67}P_{0.33})₂ via small-angle neutron scattering"
Morisaki-Ishii R., Kawano-Furukawa H., Cameron S. A., Lemberger L., Blackburn E., Holmes T. A., Forgan M. E., DeBeer-Schmitt M. L., Littrell K., Nakajima M., Kihou K., Lee H. C., Iyo A., Eisaki H., Uchida S., White S. J., Dewhurst D. C., Gavilano L. J., Zolliker M.
Phys. Rev. B **90** (2014) 125116-1-9
- Neutron magnetic scattering study in manganite thin film system
Nakao H., Yamada H., Sawa A., Iwasa K., Okamoto J., Sudayama T., Yamasaki Y., Murakami Y.
Solid State Commun. **185** (2014) 18-20
- Small-Angle Neutron Scattering Study on Defect-Controlled Polymer Networks
Nishi K., Asai H., Fujii K., Han Y.S., Kim T.H., Sakai T., Shibayama M.
Macromolecules **47** (2014) 1801-1809
- Origin of anisotropic thermal expansion in CaYAlO₄
Omoto K., Yashima M.
Appl. Phys. Express **7** (2014) 1-4
- Structural Origin of the Anisotropic Thermal Expansion of a K₂NiF₄-Type Oxide CaErAlO₄ through Interatomic Distances
Omoto K., Yashima M., Hester J. R.
Chem. Lett. **43** (2014) 515-517
- Observation of spin-wave dispersion in Nd-Fe-B magnets using neutron Brillouin scattering
Ono K., Inami N., Saito K., Takeichi Y., Yano M., Shoji T., Manabe A., Kato A., Kaneko Y., Kawana D., Yokoo T., Itoh S.
J. Appl. Phys. **115** (2014) 1-3
- Large Negative Quantum Renormalization of Excitation Energies in the Spin-1/2 Kagome Lattice Antiferromagnet Cs₂Cu₃SnF₁₂
Ono T., Matan K., Nambu Y., Sato T. J., Katayama K., Hirata S., Tanaka H.
J. Phys. Soc. Jpn. **83** (2014) 43701-1-5
- Emergence of reentrant metal-nonmetal transition in Pr_{0.85}Ce_{0.15}Ru₄P₁₂ and Pr(Ru_{0.95}Rh_{0.05})₄P₁₂
Saito K., Laulhe C., Sato T., Hao L., Mignot J. M., Iwasa K.
Phys. Rev. B **89** (2014) 75131-75131
- Small-angle Neutron Scattering of Polysaccharide Hydrogels
Shibayama M.
Polysaccharide hydrogels: characterization and biomedical applications, Ed(s). Matricardi P.; Alhaique F.; Coviello T. (Pan Stanford Publishing Pte. Ltd., Singapore, 2014) pp. 254-264
- SANS Studies on Catalyst Ink of Fuel Cell
Shibayama M., Matsunaga T., Kusano T., Amemiya K., Kobayashi N., Yoshida T.
J. Appl. Polym. Sci. **131** (2014) 39842-1-7
- Spin-Nematic Interaction in the Multiferroic Compound Ba₂CoGe₂O₇
Soda M., Matsumoto M., Mansson M., Kawamura S. O., Nakajima K., Shiina R., Masuda T.
Phys. Rev. Lett. **112** (2014) 127205-127205
- Thermo-reversible Solid-like and Liquid-like Behaviors of Carboxyl-terminated Telechelic Poly(ethylene-butylene) Neutralized by Octadecylamine
Takada A., Saeki K., Murata S., Motoyama Y., Takano A., Yamamoto H., Takahashi Y.
Nihon Reoroji Gakkaishi (J. Soc. Rheol., Japan) **42** (2014) 33-38
- Magnetic structure of the conductive triangular-lattice antiferromagnet PdCrO₂

Takatsu H., Nenert G., Kadowaki H., Yoshizawa H., Enderle M., Yonezawa S., Maeno Y., Kim J., Tsuji N., Takata M., Zhao Y., Green M., Broholm C.
Phys. Rev. B **89** (2014) 104408-1-12

- Direct Synthesis of Chromium Perovskite Oxyhydride with a High Magnetic Transition Temperature
Tassel C., Goto Y., Kuno Y., Hester J., Green M., Kobayashi Y., Kageyama H.
Angew. Chem. Int. Ed. **53** (2014) 10377-10380
- Direct Synthesis of Chromium Perovskite Oxyhydride with a High Magnetic Transition Temperature
Tassel C., Goto Y., Kuno Y., Hester J., Green M., Kobayashi Y., Kageyama H.
Angew. Chem. Int. Ed. **53** (2014) 10377-10380
- Crystal structure and electrical conductivity of LaSr₂Ga₁₁O₂₀
Ueda K., Omoto K., Fujii K., Yashima M., Ishigaki T., Kim S. J., Lee S.
NSL News Letter, ISSP joint research on neutron scattering in facilities abroad (The institute for Solid State Physics, Japan, 2014) pp. 124-124
- Charge-Order Melting in Charge-Disproportionated Perovskite CeCu₃Fe₄O₁₂
Yamada I., Etani H., Murakami M., Hayashi N., Kawakami T., Mizumaki M., Ueda S., Abe H., Liss K.-D., Studer A., Ozaki T., Mori S., Takahashi R., Irifune T.
Inorg. Chem. **53** (2014) 11794-11801
- 連載講座「中性子散乱による原子・分子のダイナミクスの観測」Ⅲ-2 中性子非弾性散乱法による固体表面での分子分光
Yamamuro O., Kofu M.
RADIOISOTOPES, Vol. 63 (公益社団法人 日本アイソトープ協会, 東京都, 2014) pp. 453-459
- High Temperature Powder Diffractometry and Structure-Property Correlation of Materials at High Temperatures
Yashima M.
日本の結晶学(Ⅱ) (日本結晶学会, 東京, 2014) pp. 140-141
- Crystal structure research on the ceramic materials for the clean energy using overseas facility
Yashima M., Fujii K., Omoto K., Fumi U., Kaneko N., Haratake D., Ueda K., Esaki Y., Hibino K., Yamada S.
NSL News Letter, ISSP joint research on neutron scattering in facilities abroad (The institute for Solid State Physics, Japan, 2014) pp. 12-18
- Spin and Hole Dynamics in Carrier-Doped Quantum Haldane Chain
Yokoo T., Itoh S., Ibuka S., Yoshizawa H., Akimitsu J.
Spin and Hole Dynamics in Carrier-Doped Quantum Haldane Chain, Vol. 568 (J. Phys: Conf. Ser., Japan, 2014) pp. 42035-4
- Dynamical Properties of Spins and Holes in Carrier Doped Quantum Haldane Chain
Yokoo T., Itoh S., Kawana D., Yoshizawa H., Akimitsu J.
Dynamical Properties of Spins and Holes in Carrier Doped Quantum Haldane Chain, Vol. 502, Ed(s). 502 (2014) 012045 (J. Phys: Conf Ser., Japan, 2014) pp. 12045-4

2013

- Recent Developments of Instruments in a Spallation Neutron Source at J-PARC and Those Prospects in the Future
Arai M., Kajimoto R., Nakamura M., Inamura Y., Nakajima K., Shibata K., Takahashi N., Suzuki J., Takata S., Yamada T., Itoh S.
J. Phys. Soc. Jpn. **82** (2013) SA024-SA024

- Structural Study on the UCST-type Phase Separation of Poly(N-isopropylacrylamide) in Ionic Liquid
Asai H., Ueki T., Sawamura S., Nakamura Y., Kitazawa Y., Watanabe M., Han Y. S., Kim T. H., Shibayama M.
Macromolecules **46** (2013) 1101-1106
- Thermal behavior, structure, and dynamics of low-temperature water confined in mesoporous organosilica by differential scanning calorimetry, X-ray diffraction, and quasi-elastic neutron scattering
Aso M., Ito K., Sugino H., Yoshida K., Yamada T., Yamamuro O., Inagaki S., Yamaguchi T.
Pure Appl. Chem. **85** (2013) 289-305
- Thermal behaviour, structure and dynamics of low-temperature water confined in mesoporous organosilica by differential scanning calorimetry, X-ray diffraction and quasi-elastic neutron scattering
Aso M., Ito K., Sugino H., Yoshida K., Yamada T., Yamamuro O., Inagaki S., Yamaguchi T.
Pure Appl. Chem. **85** (2013) 289-305
- Uptake of water in as-spun poly(methyl methacrylate) thin films.
Atarashi H., Hirai T., Hori K., Hino M., Morita H., Serizawa T., Tanaka K.
RSC Adv. **3** (2013) 3516-3519
- Experimental Visualization of the Diffusional Pathway of Oxide Ions in a Layered Perovskite-type Cobaltite $\text{PrBaCo}_2\text{O}_5+\square$
Chen Y.-C., Yashima M., Pena J., Kilner J. A.
Chem. Mater. **25** (2013) 2638-2641
- Spin-Stripe Density Varies Linearly With the Hole Content in Single-Layer $\text{Bi}_{2+x}\text{Sr}_{2-x}\text{CuO}_6+y$ Cuprate Superconductors
Enoki M., Fujita M., Nishizaki T., Iikubo S., Singh D. K., Chang S., Tranquada J. M., Yamada K.
Phys. Rev. Lett. **110** (2013) 17004-1-4
- Dual Structure of Low-Energy Spin Fluctuations in $\text{La}_{1.80}\text{Sr}_{0.14}\text{Ce}_{0.06}\text{CuO}_4$
Enoki M., Fujita M., Yamada K.
J. Phys. Soc. Jpn. **82** (2013) 82-114707-114707
- イオン液体を媒体とする高分子溶液の構造研究
Fujii K.
Hamon **178** (2013) 127-130
- Ho-doping effect on incommensurate magnetic order in $\text{La}_{1.88}\text{Sr}_{0.12}\text{CuO}_4$,
Fujita M., Enoki M., Tsutsumi K., Iikubo S., Yamada K.
Ho-doping effect on incommensurate magnetic order in $\text{La}_{1.88}\text{Sr}_{0.12}\text{CuO}_4$, Vol. 62
(J. Korean Phys. Soc., Korea, 2013) pp. 1840-1843
- 1次元フラストレート強磁性鎖のスピン密度波とBond Nematic相関
Hagihala M., Masuda T.
波紋 **23** (2013) 14-18
- SANS, Infrared, and ^7Li and ^{23}Na NMR Studies on Phase Separation of Alkali Halide-Acetonitrile-Water Mixtures by Cooling
Haramaki H., Shimomura T., Umecky T., Takamuku T.
J. Phys. Chem. B **117** (2013) 2438-2448
- Field-Induced Ferromagnetism of Fe^{4+} -Perovskite System, $\text{Sr}_{1-x}\text{Ba}_x\text{FeO}_3$ ($0 < x < 1$)
Hayashi N., Yamamoto T., Kitada A., Matsuo A., Kindo K., Hester J., Kageyama H., Takano M.
J. Phys. Soc. Jpn. **82** (2013) 113702-1-4
- Neutron Brillouin Scattering with Pulsed Spallation Neutron Source - Spin-Wave Excitations from Ferromagnetic Powder Samples

- Itoh S., Endoh Y., Yokoo T., Kawana D., Kaneko Y., Tokura Y., Fujita M.
J. Phys. Soc. Jpn. **82** (2013) 43001-1-4
- Neutron Brillouin Scattering on High Resolution Chopper Spectrometer, HRC
 Itoh S., Yokoo T., Kawana D., Endoh Y.
J. Phys. Soc. Jpn. **82** (2013) SA034-SA034
 - Progress in High Resolution Chopper Spectrometer, HRC
 Itoh S., Yokoo T., Kawana D., Yoshizawa H., Masuda T., Soda M., Sato T. J., Satoh S., Sakaguchi M., Muto S.
J. Phys. Soc. Jpn. Suppl. A **82** (2013) 33-1-6
 - Progress in High Resolution Chopper Spectrometer, HRC
 Itoh S., Yokoo T., Yoshizawa H., Masuda T., Soda M., Sato T. J., Sakaguchi M., Muto S.
J. Phys. Soc. Jpn. **82** (2013) SA033-SA033
 - Well-Defined Crystal Field Splitting Schemes and Non-Kramers Doublet Ground States of f Electrons in PrT₂Zn₂₀ (T = Ir, Rh, and Ru)
 Iwasa K., Kobayashi H., Onimaru T., Matsumoto K. T., Nagasawa N., Ohira-Kawamura S., Kikuchi T., Inamura Y., Nakajima K.
J. Phys. Soc. Jpn. **82** (2013) 43707-1-5
 - Structural and electrochemical properties of hydrogen titanium oxides
 Kataoka K., Kijima N., Akimoto J.
Solid State Ionics **252** (2013) 109-115
 - Ion-Exchange Synthesis, Crystal Structure, and Physical Properties of Hydrogen Titanium Oxide H₂Ti₃O₇
 Kataoka K., Kijima N., Akimoto J.
Inorg. Chem. **52** (2013) 13861-13864
 - Control of magnetic interaction and ferroelectricity by nonmagnetic Ga substitution in multiferroic YMn₂O₅
 Kimura H.
Phys. Rev. B **87** (2013) 104414-1-8
 - An Oxyhydride of BaTiO₃ Exhibiting Hydride Exchange and Electronic Conductivity
 Kobayashi Y., Kageyama H., , , , , , , Hernandez O., Sakaguchi T., Yajima T., Roisnel T., Tsujimoto Y., Morita M., Noda Y., Mogami Y., Kitada A., Ohkura M., Hosokawa S., Li Z., Hayashi K., Kusano Y., Kim J. E., Tsuji N., Fujiwara A., Matsushita Y., Yoshimura K., Takegoshi K., Inoue M., Takano M.
Nat. Matter. **11** (2013) 507-511
 - Magnetic relaxations in a Tb-based single molecule magnet studied by quasielastic neutron scattering
 Kofu M., Kajiwara T., Gardner J. S., Simeoni G. G., Tyagi M., Nakajima K., Ohira-Kawamura S., Nakano M., Yamamuro O.
Chem. Phys. **427** (2013) 147-152
 - Hyperfine structure of magnetic excitations in a novel Tb based single molecule magnet studied by high-resolution neutron spectroscopy
 Kofu M., Kajiwara T., Nakano M., Nakajima K., Ohira-Kawamura S., Kikuchi T., Inamura Y., Yamamuro O.
Phys. Rev. B **88** (2013) 64405-64405
 - Heterogeneous Slow Dynamics of Imidazolium Based Ionic Liquids Studied by Neutron Spin Echo
 Kofu M., Nagao M., Ueki T., Kitazawa Y., Nakamura Y., Sawamura S., Watanabe M., Yamamuro O.
J. Phys. Chem. B **117** (2013) 2773-2781
 - Small-angle Neutron Scattering Study on Aggregation of 1-Alkyl-3-methylimidazolium-based Ionic Liquids in Aqueous Solution
 Kusano T., Fujii K., Tabata M., Shibayama M.

- Negative magnetostrictive magnetoelectric coupling of BiFeO₃
Lee S.
Phys. Rev. B **88** (2013) 60103–1–5
- In Situ Small-angle X-ray and Neutron Scattering Measurements on a Blend of Deuterated and Hydrogenated Polyethylenes during Uniaxial Drawing
Matsuba G., Ito C., Zhao Y., Inoue R., Nishida K., Kanaya T.
Polym. J. **45** (2013) 293–299
- Damped soft phonons and diffuse scattering in (Bi_{1/2}Na_{1/2})TiO₃
Matsuura M., Iida H., Hirota K., Ohwada K., Noguchi Y., Miyayama M.
Phys. Rev. B **87** (2013) 64109–64118
- Structure of Concentrated Aqueous Urea Solutions Involving Alkali Metal Salts by Neutron Diffraction with ¹⁴N/¹⁵N, ⁶Li/⁷Li and ³⁵Cl/³⁷Cl Isotopic Substitution Methods
Miyazaki T., Kameda Y., Amo Y., Usuki T.
Bull. Chem. Soc. Jpn. **86** (2013) 104–111
- SANS and DLS Study of Tacticity Effects on Hydrophobicity and Phase Separation of Poly(N-isopropylacrylamide)
Nishi K., Hiroi T., Hashimoto K., Fujii K., Han Y. S., Kim T. H., Katsumoto Y., Shibayama M.
Macromolecules **46** (2013) 6225–6232
- Residual-Charge Induced Memory Effect of Electric Polarization in Multiferroic CuFe_{1-x}Ga_xO₂ as Seen via Polarized Neutron Diffraction
Nakajima T., Mitsuda S., Yamazaki H., Matsuura M.
J. Phys. Soc. Jpn. **82** (2013) 24706–1–7
- T_c Enhancement by Aliovalent Anionic Substitution in Superconducting BaTi₂(Sb_{1-x}Sn_x)₂O
Nakano K., Yajima T., Takaeiri F., Green M. A., Hester J., Kobayashi Y., Kageyama H.
J. Phys. Soc. Jpn. **82** (2013) 74707–1–5
- Interplay among spin, orbital, and lattice degrees of freedom in a frustrated spinel Mn₃O₄
Nii Y., Sagayama H., Umetsu H., Abe N., Taniguchi K., Arima T.
Phys. Rev. B **87** (2013) 195115–1–7
- Muon Spin Relaxation and Electron/Neutron Diffraction Studies of BaTi₂(As_{1-x}Sb_x)₂O: Absence of Static Magnetism and Superlattice Reflections
Nozaki Y., Nakano K., Yajima T., Kageyama H., Frandsen B., Liu L., Cheung S., Goko T., Uemura Y. J., Brown C. M.
Phys. Rev. B **88** (2013) 214506–1–5
- Field-induced Evolution of Magnetic Ordering under Field in the Quantum Spin System (CuBr)Sr₂Nb₃O₁₀ with a 1/3 Magnetization Plateau
Ritter C., Yusuf S. M., Bera A. K., Goto Y., Tassel C., Kageyama H., Lopez A. A., Attfield J. P.
Phys. Rev. B **88** (2013) 104401–1–7
- Membrane formation by preferential solvation of ions in mixture of water, 3-methylpyridine, and sodium tetrphenylborate
Sadakane K., Nagao M., Endo H., Seto H.
J. Chem. Phys. **139** (2013) 234905–234905
- Lithium insertion and extraction properties of hollandite-type K_xTiO₂ with different K content in the tunnel space
Sakao M., Kijima N., Akimoto J., Okutani T.
Solid State Ionics **243** (2013) 22–29

- On the superconducting Symmetry of Fe-based Systems -Impurity Effects Studies and Neutron Scattering measurements-
Sato M., Kobayashi Y., Kawamata T., Yasui Y., Suzuki K., Itoh M., Kajimoto R., Ikeuchi K., Arai M., Bourges P.
J. Korean Phys. Soc., Vol. 62 (Spring Link, UK, 2013) pp. 1726-1733
- 中性子散乱を用いた構造解析手法
Shibayama M.
ソフトマテリアルの高機能化, Ed(s). ゴム協会 (ポスティコーポレーション, Tokyo, 2013) pp. 1-10
- SANS, ATR-IR, and 1D- and 2D-NMR Studies on Mixing States of Imidazolium-based Ionic Liquid and Aryl Solvents
Shimomura T., Inoue S., Kadohata S., Umecky T., Takamuku T.
Phys. Chem. Chem. Phys. **15** (2013) 20565-20576
- Viscoelastic Properties of Low Molecular Weight Symmetric Poly(styrene-b-2-vinylpyridine)s in the Ordered and Disordered States under Steady Shear Flow
Takahashi Y., Fang L., Takano A., Torikai N., Matsushita Y.
Nihon Reoroji Gakkaishi (Journal of the Society of Rheology, Japan) **41** (2013) 2-83-91
- Long-range order and spin-liquid states of polycrystalline $Tb_{2+x}Ti_{2-x}O_{7+y}$
Taniguchi T., Kadowaki H., Takatsu H., Fak B., Ollivier J., Yamazaki T., Sato T. J., Yoshizawa H., Shimura Y., Sakakibara T., Hong T., Goto K., Yaraskavitch L. R., Kycia J. B.
Phys. Rev. B **87** (2013) 60408-1-5
- Sr_2FeO_3 with Stacked Infinite Chains of FeO_4 Square Planes
Tassel C., Seinberg L., Hayashi N., Ganesanpotti S., Ajiro Y., Kobayashi Y., Kageyama H.
Inorg. Chem. **52** (2013) 6906-6912
- Physical properties of double perovskite-type barium neodymium osmate Ba_2NdOsO_6
Wakeshima M., Hinatsu Y., Ohoyama K.
J. Solid State Chem. **197** (2013) 236-241
- Synthesis and Physical Properties of the New Bismuthides $BaTi_2Bi_2O$ and $(SrF)_2Ti_2Bi_2O$ with a d1 Square Net
Yajima T., Nakano K., Takaeiri F., Hester J., Yamamoto T., Kobayashi Y., Tsuji N., Kim J. E., Fujiwara A., Kageyama H.
J. Phys. Soc. Jpn. **82** (2013) 13703-1-4
- Phase Transition and Dynamics of Water Confined in Hydroxyethyl Copper Rubeanate Hydrate
Yamada T., Yamada T., Tyagi M., Nagao M., Kitagawa H., Yamamuro O.
QENS/WINS 2012 (J. Phys. Soc. Jpn., Japan, 2013) pp. 10-10
- 連載講座「中性子散乱による原子・分子のダイナミクスの観測」Ⅲ 原子・分子のダイナミクス「液体・非晶質・表面／界面」
Yamamuro O.
RADIOISOTOPES, Vol. 62 (公益社団法人 日本アイソトープ協会, 東京都, 2013) pp. 691-701
- Magnetic excitations in ferromagnetic phase of MnP
Yano S., Itoh S., Yokoo T., Satoh S., Kawana D., Kousaka Y., Akimitsu J., Endoh Y.
J. Magn. Magn. Mater. **347** (2013) 33-38
- セリア-ジルコニア固溶体の結晶構造と触媒活性
Yashima M.
マテリアルインテグレーション **26** (2013) 7-11
- Chapter 1: Crystal and Electronic Structures, Structural Disorder, Phase

Transformation, and Phase Diagram of Ceria-Zirconia and Ceria-Based Materials
Yashima M.

Catalysis by Ceria and Related Materials 2nd Edition, Ed(s). A. Trovarelli and P. Fornasiero (Imperial College Press, London, 2013) pp. 1-45

- Crystal Structure, Optical Properties and Electronic Structure of Calcium Strontium Tungsten Oxynitrides $CaxSr_{1-x}WO_{2N}$
Yashima M., Fumi U., Nakano H., Omoto K., Hester J. R.
J. Phys. Chem. C **117** (2013) 18529-18539
- Crystal Structure and Oxide-Ion Diffusion of Nano-Crystalline, Compositionally Homogeneous Ceria-Zirconia $Ce_{0.5}Zr_{0.5}O_2$ up to 1176 K
Yashima M., Sekikawa T., Sato D., Nakano H., Omoto K.
Cryst. Growth Des. **13** (2013) 829-837
- フラストレートした1次元量子スピン磁性体で誘起される強誘電転移と新奇量子磁気状態
Yasui Y.
日本中性子科学会誌 **23** (2013) 1-44-49

2012

- Structural Analysis of High Performance Ion-gel Comprising Tetra-PEG Network
Asai H., Fujii K., Ueki T., Sakai T., Chung U., Watanabe M., Han Y., Kim T., Shibayama M.
Macromolecules **45** (2012) 3902-3909
- Magnetic Phase Diagram of YVO_3 and $TbVO_3$ under High Pressure
Bizen D., Nakao H., Iwasa K., Murakami Y., Osakabe T., Fujioka J., Miyasaka S., Tokura Y.
J. Phys. Soc. Jpn. **81** (2012) 24715-1-6
- Diffuse scattering anisotropy and inhomogeneous lattice deformations in the lead magnoniobate relaxor PMN above the Burns temperature
Burkovsky R. G., Filimonov A. V., Rudskoy A. I., Hirota K., Matsuura M., Vakhrushev S. B.
Phys. Rev. B **85** (2012) 94108-94114
- Crystal Structure, Oxygen Deficiency and Oxygen Diffusion Path of Perovskite-type Lanthanum Cobaltites $La_{0.4}Ba_{0.6}CoO_{3-\delta}$ and $La_{0.6}Sr_{0.4}CoO_{3-\delta}$
Chen Y.-C., Yashima M., Ohta T., Ohoyama K., Yamamoto S.
J. Phys. Chem. C **116** (2012) 8-5246-5254
- Short-range correlations and persistent spin fluctuations in the undistorted kagome lattice Ising antiferromagnet $Co_3Mg(OH)_6Cl$,
Phys. Rev. B: Condens. Matter Mater. Phys., **85**, 012402 (2012).
Fijihala M., Zheng X.G., Oohara Y., Morodomi H., Kawae T., Matsuo A., Kindo K.
Phys. Rev. B **85** (2012) 12402-1-5
- High-performance ion gel with Tetra-PEG network
Fujii K., Asai H., Ueki T., Sakai T., Imaizumi S., Chung U., Watanabe M., Shibayama M.
Soft Matter **8** (2012) 1756-1759
- Plastically deformed Ge-crystal wafers as elements for neutron focusing monochromator.
Hiraka H., Ohkubo K., Furusaka M., Kiyonagi Y., Yamada K., Morihista K., Nakajima K.
Nucl. Instrum. Methods Phys. Res. A **693** (2012) 166-169
- Investigation on Crystal and Electronic Structures of $0.5Li_2MnO_3$ -

- 0.5LiMnxNixCo(1-2x)O2 (x = 1/3, 5/12) Samples Heat-Treated under Vacuum Reducing Conditions
Idemoto Y., Kashima T., Kitamura N.
Electrochemistry **80** (2012) 791-799
- 中性子,放射光を駆使したリチウムイオン電池正極材料の平均・局所構造, 熱力学的安定性と電池特性
Idemoto Y., Kitamura N.
電池技術 **24** (2012) 19-27
 - Relationship between the Local Dynamics and Gas Permeability of Para-Substituted Poly(1-chloro-2-phenylacetylenes)
Inoue R., Kanaya T., Masuda T., Nishida K., Yamamuro O.
Macromolecules **45** (2012) 6008-6014
 - T0 chopper developed at KEK
Itoh S., Ueno K., Ohkubo R., Sagehashi H., Funahashi Y., Yoko T.
Nucl. Instrum. Methods Phys. Res. A **661** (2012) 86-92
 - Fermi chopper developed at KEK
Itoh S., Ueno K., Yokoo T.
Nucl. Instrum. Methods Phys. Res. A **661** (2012) 58-63
 - Performance of High Resolution Chopper Spectrometer (HRC)
Itoh S., Yokoo T., Kawana D., Yano S., Satoh S., Sato T. J., Masuda T., Yoshizawa H.
Proceedings of the 20th Meeting of the International Collaboration on Advanced Neutron (ICANS-XX) (Bariloche Atomic Centre, Argentine, 2012) pp. 416-421
 - Large area window on vacuum chamber surface for neutron scattering instruments
Itoh S., Yokoo T., Ueno K., Suzuki J., Teraoku T., Tsuchiya M.
Nucl. Instrum. Methods Phys. Res. A **670** (2012) 1-5
 - Quantum Renormalization Effect in One-Dimensional Heisenberg Antiferromagnets
Itoh S., Yokoo T., Yano S., Kawana D., Tanaka H., Endoh Y.
J. Phys. Soc. Jpn. **81** (2012) 84706-1-7
 - Magnetic Excitation in Totally Symmetric Staggered Ordered Phase of PrFe4P12
Iwasa K., Hao L., Kohgi M., Kuwahara K., Mignot J.-M., Sugawara H., Aoki Y., Matsuda T. D., Sato H.
J. Phys. Soc. Jpn. **81** (2012) 94711-1-9
 - Neutron scattering study on magnetic ordering in a partially rare-earth filled skutterudite PrxFe4Sb12
Iwasa K., Orihara T., Saito K., Tomiyasu K., Murakami Y., Sugawara H., Kuwahara K., Kimura H., Kiyonagi R., Ishikawa Y., Noda Y., Aoki Y., Sato H., Kohgi M.
International Conference on Strongly Correlated Electron Systems 2011 (SCES2011), Vol. 391 (Journal of Physics: Conference Series, UK, 2012) pp. 1-4
 - Optimization of thickness of a ZnS/6LiF scintillator for a high-resolution detector installed on a focusing small-angle neutron scattering spectrometer (SANS-U)
Iwase H., Katagiri M., Shibayama M.
J. Appl. Crystallogr. **45** (2012) 507-512
 - Structural analysis of cured phenolic resins using complementary small-angle neutron and X-ray scattering and scanning electron microscopy
Izumi A., Nakao T., Iwase H., Shibayama M.
Soft Matter **8** (2012) 8438-8445
 - 溶液中での重水素化ノボラックのコンフォメーション
Izumi A., Toshio N., Shibayama M.
ネットワークポリマー **33** (2012) 204-208

- Structures and Low-energy Excitations of Amorphous Gas Hydrates
Kikuchi T., Inamura Y., Onoda-Yamamuro N., Yamamuro O.
J. Phys. Soc. Jpn. **81** (2012) 94604-94604
- Crystal structure and thermoelectric properties of $K_xBa_{8-x}Zn_yGe_{46-y}$ clathrates
Kishimoto K., Sasaki Y., Koyanagi T., Ohyama K., Akai K.
J. Appl. Phys. **111** (2012) 93716-1-8
- Quadruple-Layered Perovskite (CuCl)Ca₂NaNb₄O₁₃
Kitada A., Tsujimoto Y., Yamamoto T., Kobayashi Y., Narumi Y., Kindo K., Aczel A. A., Luke G. M., Kageyama H., Uemura Y. J., Kiuchi Y., Ueda Y., Yoshimura K., Ajiro Y.
J. Solid State Chem. **185** (2012) 10-17
- An Oxyhydride of BaTiO₃ Exhibiting Hydride Exchange and Electronic Conductivity
Kobayashi Y., Kaageyama H., , , , , , , Hernandez O., Sakaguchi T., Yajima T., Roisnel T., Tsujimoto Y., Morita M., Noda Y., Mogami Y., Kitada A., Ohkura M., Hosokawa S., Li Z., Hayashi K., Kusano Y., Kim J. E., Tsuji N., Fujiwara A., Matsushita Y., Yoshimura K., Takegoshi K., Inoue M., Takano M.
Nat. Matter. **11** (2012) 507-511
- Microscopic insights into Ion Gel dynamics using neutron spectroscopy
Kofu M., Someya T., Tatsumi S., Ueno K., Ueki T., Watanabe M., Matsunaga T., Shibayama M., Garcia-Sakai V., Tyagi M., Yamamuro O.
Soft Matter **8** (2012) 7888-7897
- Structural and Rheological Studies on Growth of Salt-Free Wormlike Micelles Formed by Star-Type Trimeric Surfactants
Kusano T., Iwase H., Yoshimura T., Shibayama M.
Langmuir **28** (2012) 16798-16806
- Relationship between crystal structure and superconductivity in iron-based superconductors
Lee C. H., Kihou K., Iyo A., Kito H., Eisaki H.
Solid State Commun. **152** (2012) 644-648
- Study of Neutron Diffraction on 154SmRu₄P₁₂ Single Crystal
Lee C. H., Tsutsui S., Kihou K., Sugawara H., Yoshizawa H.
J. Phys. Soc. Jpn. **81** (2012) 63702-1-4
- Ni-substitution effects on the spin dynamics and superconductivity in La_{1.85}Sr_{0.15}CuO₄
Matsuura M., Fujita M., Hiraka H., Kofu M., Kimura H., Wakimoto S., Perring T. G., Frost C. D., Yamada K.
Phys. Rev. B **86** (2012) 134529-1-8
- Hydration properties and compressive strength development of Low Heat Cement
Mori K., Fukunaga T., Sugiyama M., Iwase K., Oishi K., Yamamuro O.
J. Phys. Chem. Solids **73** (2012) 1274-1277
- Direct Observation of Supercooled Water in Mortar Materials by Quasi-elastic Neutron Scattering
Mori K., Iwase K., Sugiyama M., Fukunaga T., Yamamuro O.
Trans. Mater. Res. Soc. Jpn. **37** (2012) 139-142
- Neutron scattering studies of Ti-Cr-V bcc alloy with the residual hydrogen and deuterium
Mori K., Iwase K., Sugiyama M., Kofu M., Yamamuro O., Onodera Y., Otomo T., Fukunaga T.
J. Phys.: Conference Series **340** (2012) 12103-1-5
- Small-Angle Neutron Scattering Study on Specific Polymerization Loci Induced by Copolymerization of Polymerizable Surfactant and Styrene during Miniemulsion Polymerization

- Motokawa R., Taniguchi T., Sasaki Y., Enomoto Y., Murakami F., Kasuya M., Kohri M., Nakahira T.
Macromolecules **45** (2012) 9435-9444
- Microscopic Investigation on Morphologies of Bilayer Gel Structure in the Mixed Polyoxyethylene-Type Nonionic Surfactant Systems
 Nagai Y., Kawabata Y., Kato T.
J. Phys. Chem. B **116** (2012) 12558-12566
 - Magnetic interactions in the multiferroic phase of $\text{CuFe}_{1-x}\text{Ga}_x\text{O}_2$ ($x = 0.035$) refined by inelastic neutron scattering with uniaxial-pressure control of domain structure
 Nakajima T., Mitsuda S., Haraldsen J. T., Fishman R. S., Hong T., Terada N., Uwatoko Y.
Phys. Rev. B **85** (2012) 144405-1-7
 - Uniaxial-Pressure Control of Magnetic Phase Transitions in a Frustrated Magnet $\text{CuFe}_{1-x}\text{Ga}_x\text{O}_2$ ($x = 0, 0.018$)
 Nakajima T., Mitsuda S., Takahashi K., Yoshitomi K., Masuda K., Kaneko C., Honma Y., Kobayashi S., Kitazawa H., Kosaka M., Aso N., Uwatoko Y., Terada N., Wakimoto S., Takeda M., Kakurai K.
J. Phys. Soc. Jpn. **81** (2012) 94710-1-8
 - Direct Observation by Neutron Diffraction of Antiferromagnetic Ordering in s Electrons Confined in Regular Nanospace of Sodalite
 Nakano T., Matsuura M., Hanazawa A., Hirota K., Nozue Y.
Phys. Rev. Lett. **109** (2012) 167208-1-4
 - Stress Relaxation and Hysteresis of Nanocomposite Gel Investigated by SAXS and SANS Measurement
 Nishida T., Obayashi A., Haraguchi K., Shibayama M.
Polymer **53** (2012) 4533-4538
 - Development of a non-adiabatic two-coil spin flipper for a polarised thermal neutron diffractometer with a ^3He spin filter
 Ohoyama K., Tsutsumi K., Ino T., Hiraka H., Yamaguchi Y., Kira H., Oku T., Sakaguchi Y., Arimoto Y.
Nucl. Instrum. Meth. Phys. Res. A. **680** (2012) 75-81
 - Pressure Effects on Cononsolvency Behavior of Poly(N-isopropylacrylamide) in water/DMSO Mixed Solvents
 Osaka N., Shibayama M.
Macromolecules **45** (2012) 2171-2174
 - Oxyhydrides of $(\text{Ca}, \text{Sr}, \text{Ba})\text{TiO}_3$ perovskite solid solution
 Sakaguchi T., Kobayashi Y., Yajima T., Ohkura M., Tassel C., Takeiri F., Mitsuoka S., Ohokubo H., Kageyama H., Yamamoto T., Kim J., Tsuji N., Fujihara A., Matsushita Y., Hester J., Andeev M., Ohoyama K.
Inorg. Chem. **51** (2012) 11371-11376
 - Study of Magnetic Excitation Spectra of Several Fe-Pnictide Systems
 Sato M., Kawamata T., Kobayashi Y., Yasui Y., Iida T., Suzuki K., Itoh M., Moyoshi T., Motoya K., Kajimoto R., Nakamura M., Inamura Y., Arai M.
J. Phys.: Conf. Ser., Vol. 400 (IOP Publishing, UK, 2012) pp. 22105-22105
 - Ferroquadrupolar ordering in $\text{PrTi}_2\text{Al}_{20}$
 Sato T. J., Ibuka S., Nambu Y., Yamazaki T., Hong T., Sakai A., Nakatsuji S.
Phys. Rev. B **86** (2012) 184419-1-8
 - 中性子による材料評価・構造解析
 Shibayama M.
表面科学 **33** (2012) 258-263
 - Structure-mechanical property relationship of tough hydrogels

Shibayama M.
Soft Matter **8** (2012) 8030–8038

- Fabrication, Structure, Mechanical Properties, and Application of Tetra-PEG Hydrogels
Shibayama M., Sakai T.
Polymeric and Self Assembled Hydrogels: Fundamentals to Applications, Ed(s). Scherman O. and Loh X. J. (RSC Publishing, Cambridge, UK, 2012) pp. 2–38
- Aggregation of 1-Dodecyl-3-methylimidazolium Nitrate in Water and Benzene Studied by SANS and ¹H NMR
Takamuku T., Shimomura T., Sadakane K., Koga M., Seto H.
Phys. Chem. Chem. Phys. **14** (2012) 11070–11080
- Amide-induced Phase Separation of Hexafluoroisopropanol–Water Mixtures Depending on the Hydrophobicity of Amide
Takamuku T., Wada H., Kawatoko C., Shimomura T., Kanzaki R., Takeuchi M.
Phys. Chem. Chem. Phys. **14** (2012) 8335–8347
- Quantum spin fluctuations in the spin-liquid state of Tb₂Ti₂O₇
Takatsu H., Kadowaki H., Sato T. J., Lynn J. W., Tabata Y., Yamazaki T., Matsuhira K.
Journal of Physics Condensed Matter **24** (2012) 52201–1–4
- Simultaneous softening of acoustic and optical modes in cubic PbTiO₃
Tomeno I., Fernandez-Baca J. A., Marty K. J., Oka K., Tsunoda Y.
Phys. Rev. B **86** (2012) 134306–1–15
- Hydrogen release from Li alanates originates in molecular lattice instability emerging at ~100 K
Tomiyasu K., Sato T., Horigane K., Orimo S., Yamada K.
Appl. Phys. Lett. **100** (2012) 193901–1–3
- Observation of partial disorder-type spin fluctuations in frustrated Mn₃Pt
Tomiyasu K., Yasui H., Yamaguchi Y.
J. Phys. Soc. Jpn. **81** (2012) 114724–1–4
- Superconductivity in BaTi₂Sb₂O with a d1 Square Lattice
Yajima T., Nakano K., Takaeiri F., Ono T., Hosokoshi Y., Matsushita Y., Hester J., Kobayashi Y., Kageyama H.
J. Phys. Soc. Jpn. **81** (2012) 13706–1–4
- Kinetic process of formation and reconstruction of small unilamellar vesicles consisting of long- and short-chain lipids
Yamada N. L.
Langmuir **28** (2012) 17381–17388
- Relationship between mesoscale dynamics and shear relaxation of ionic liquids with long alkyl chain
Yamaguchi T., Mikawa K., Koda S., Fujii F., Endo H., Shibayama M., Hamano H., Umabayashi Y.
J. Chem. Phys. **137** (2012) 104511–1–7
- (Sr_{1-x}Ba_x)FeO₂ (0.4 ≤ x ≤ 1): a New Oxygen-Deficient Perovskite Structure
Yamamoto T., Kobayashi Y., Hayashi N., Tassel C., Saito T., Yamanaka S., Takano M., Ohoyama K., Kageyama H., Shimakawa Y., Yoshimura K.
J. Am. Chem. Soc. **134** (2012) 11444–11454
- 7.3 中性子散乱と回折
Yamamuro O.
「大学院講義物理化学 (第2版)」小谷正博, 幸田清一郎, 染田清彦, 阿波賀邦夫 編, 「Ⅲ. 固体の化学と物性」 (東京化学同人, 東京, 2012) pp. 181–190

- 1.4.3 ガラス状態
Yamamuro O.
「イオン液体の科学—新世代液体への挑戦—」イオン液体研究会監修, Ed(s). 西川恵子・大内幸雄・伊藤俊幸・大野弘幸・渡邊正義 編 (丸善, 東京, 2012) pp. 82-89
- Magnetic excitations in MnP
Yano S., Akimitsu J., Itoh S., Yokoo T., Satoh S., Kawana D., Yasuo E.
J. Phys.: Conf. Ser., Vol. 391 (IOP Publishing, U. K., 2012) pp. 12113-12113
- 中性子回折による無機材料の結晶構造とイオン拡散経路の研究
Yashima M.
表面科学 **33** (2012) 5-284-289
- 強誘電セラミックスの結晶構造解析
Yashima M.
熱測定 **39** (2012) 3-112-115
- Role of Ga³⁺ and Cu²⁺ in the High Interstitial Oxide-Ion Diffusivity of Pr₂NiO₄-Based Oxides: Design Concept of Interstitial Ion Conductors through the Higher-Valence d10 Dopant and Jahn-Teller Effect
Yashima M., Yamada H., Nuansaeng S., Ishihara T.
Chem. Mater. **24** (2012) 21-4100-4113
- Magnetic excitations in possible spin-Peierls system TiOBr
Yokoo T., Itoh S., Trouw F., Llobet-Megias A., Akimitsu J.
J. Phys.: Conf. Ser., Vol. 400 (IOP Publishing, U. K., 2012) pp. 32123-32123
- Star-Shaped Trimeric Quaternary Ammonium Bromide Surfactants: Adsorption and Aggregation Properties
Yoshimura T., Kusano T., Iwase H., Shibayama M., Ogawa T., Kurata H.
Langmuir **28** (2012) 9322-9331

2011

- Spin-Driven Ferroelectricity and Magneto-Electric Effects in Frustrated Magnetic Systems
Arima T.
J. Phys. Soc. Jpn. **80** (2011) 52001-1-14
- Spin Density Wave Ordering in CeIrSi₃
Aso N., Takahashi M., Yoshizawa H., Iida H., Kimura N., Aoki H.
J. Phys. Soc. Jpn. **80** (2011) 95004-1-2
- Density Distributions of Poly(methyl methacrylate)Thin Films in Non-Solvents
Atarashi H., Fujii Y., Yamazaki D., Hino M., Morita H., Tanaka K.
Koubunshi Ronbunshu **68** (2011) 608-615
- Static Structure of Polyrotaxane in Solution Investigated by Contrast Variation Small-Angle Neutron Scattering
Endo H., Mayumi K., Osaka N., Ito K., Shibayama M.
Polymer J. **43** (2011) 155-163
- Experimental evidences for molecular origin of low-Q peak in neutron/x-ray scattering of 1-alkyl-3-methylimidazolium bis(trifluoromethanesulfonyl)amide ionic liquids
Fujii K., Kanzaki R., Takamuku T., Kameda Y., Kohara S., Kanakubo M., Shibayama M., Ishiuro S., Umebayashi Y.
J. Chem. Phys. **135** (2011) 244502-1-11

- Structural Aspects of the LCST Phase Behavior of Poly(benzylmethacrylate) in Room-temperature Ionic Liquid
Fujii K., Ueki T., Niitsuma K., Matsunaga T., Watanabe M., Shibayama M.
Polymer **52** (2011) 1589-1595
- Hidden Itinerant-Spin Phase in Heavily Overdoped $\text{La}_{2-x}\text{Sr}_x\text{CuO}_4$ Superconductors Revealed by Dilute Fe Doping: A Combined Neutron Scattering and Angle-Resolved Photoemission Study
He R. H., Fujita M., Enoki M., Hashimoto M., Iikubo S., Mo S. -K., Yao H., Adachi T., Koike Y., Hussain Z., Shen Z. -X., Yamada K.
Phys. Rev. Lett. **107** (2011) 127002-1-4
- Plastically deformed Si-crystal wafers for neutron-monochromator elements
Hiraka H., Fujiwara K., Yamada K., Morishita K., Nakajima K.
Nucl. Instrum. Methods Phys. Res. A **635** (2011) 137-140
- 中性子科学における学生教育
Hiraka H., Iwasa K., Ohoyama K.
波紋 **21** (2011) 37-41
- Application of Hot-Pressed Ge-Crystal Monochromators for Reactor-Based Neutron Beam Experiments.
Hiraka H., Miyake Y., Che S.-C., Murakami N., Ohkawara M., Nemoto K., Horigane K., Ohoyama K., Yamaguchi Y., Yamada K.
J. Phys. Soc. Jpn. suppl. **80** (2011) 12-1-4
- Magnetic and Superconducting Properties of CeRhGe_2 and CePtSi_2
Hirose Y., Nishimura N., Honda F., Matsuura M., Hirota K., Hagiwara M., Kindo K., Settai R., Onuki Y., Sugiyama K., Takeuchi T., Yamamoto E., Haga Y., Yasui A., Yamagami H.
J. Phys. Soc. Jpn. **80** (2011) 24711-24722
- Magnetic properties of the Ag-In-rare-earth 1/1 approximants
Ibuka S., Iida K., Sato T. J.
J. Phys.: Condens. Matter **23** (2011) 56001-1-8
- Dependence of Thermodynamic Stability, Crystal and Electronic Structures and Battery Characteristic on Synthetic Condition and Li Content for $\text{Li}_x\text{Mn}_{0.5}\text{Ni}_{0.5}\text{O}_2$ as a Cathode Active Material of Li-Ion Battery
Idemoto Y., Hasegawa T., Kitamura N., Uchimot Y.
Electrochemistry **79** (2011) 1-15-23
- Nb多量置換 $\text{Pb}(\text{Zr}, \text{Ti}, \text{Nb})\text{O}_3$ の強誘電特性と結晶構造の関係
Idemoto Y., Mizoguchi T., Kitamura N.
粉体および粉末冶金 **58** (2011) 703-709
- Dzyaloshinsky-Moriya interaction and long life time of the spin state in the Cu_3 triangular spin cluster by inelastic neutron scattering measurements
Iida K., Qiu Y., Sato T. J.
Phys. Rev. B **84** (2011) 94449-1-6
- Distributions of glass transition temperature and thermal expansivity in multi-layered polystyrene thin film studied by neutron reflectivity
Inoue R., Kawashima K., Matsui K., Kanaya T., Nishida K., Matsuba G., Hino M.
Phys. Rev. E **83** (2011) 21801-1-7
- Irradiation properties of T0 chopper components
Itoh S., Ueno K., Ohkubo R., Sagehashi H., Funahashi Y., Yokoo T.
Nucl. Instrum. Methods Phys. Res. A **654** (2011) 527-531
- High Resolution Chopper Spectrometer (HRC) at J-PARC
Itoh S., Yokoo T., Satoh S., Yano S., Kawana D., Suzuki J., Sato T. J.

- New Aspects of Electronic Ordered States due to f2 Configuration of Pr-Based Systems
Iwasa K., Igarashi R., Saito K., Laulhe C., Orihara T., Kunii S., Kuwahara K., Nakao H., Murakami Y., Iga F., Sera M., Tsutsui S., Uchiyama H., Baron A. Q. R. *Phys. Rev. B* **84** (2011) 214308-1-6
- Softening of the Longitudinal Phonon Mode along the [100] Direction in GdB6
Iwasa K., Igarashi R., Saito K., Laulhe C., Orihara T., Kunii S., Kuwahara K., Nakao H., Murakami Y., Iga F., Sera M., Tsutsui S., Uchiyama H., Baron A. Q. R. *Chinese Journal of Physics*, Vol. 49 (The Physical Society of Republic of China, Taiwan, 2011) pp. 231-238
- Motion of the guest ion as precursor to the first-order phase transition in the cage system GdB6
Iwasa K., Igarashi R., Saito K., Laulhe C., Orihara T., Kunii S., Kuwahara K., Nakao H., Murakami Y., Iga F., Sera M., Tsutsui S., Uchiyama H., Baron A. Q. R. *Phys. Rev. B* **84** (2011) 214308-1-6
- Softening of phonon by filled rare-earth ion motion common to skutterudite with Sb cages
Iwasa K., Mori Y., Itobe S., Igarashi R., Murakami Y., Sugawara H., Kohgi M., Sato H. *J. Phys. Soc. Jpn. Supplement A (Proc. Int. Conf. Heavy Electrons (ICHE2010))*, Vol. 80 (The Physical Society of Republic of Japan, Japan, 2011) pp. 32-32
- Modernization of the small-angle neutron scattering spectrometer SANS-U by upgrade to a focusing SANS spectrometer
Iwase H., Endo H., Katagiri M., Shibayama M. *J. Appl. Crystallogr.* **44** (2011) 558-568
- Synthesis and Properties of a Deuterated Phenolic Resin
Izumi A., Nakao T., Shibayama M. *J. Polym. Sci., Part A: Polym. Chem.* **49** (2011) 4941-4947
- Dynamic light scattering and small-angle neutron scattering studies on phenolic resin solutions
Izumi A., Takeuchi T., Nakao T., Shibayama M. *Polymer* **52** (2011) 4355-4361
- Hydration Structure of Pyridine Molecule Studied by Neutron Diffraction with Isotopic Substitution Method
Kameda Y., Amo Y., Usuki T. *J. Mol. Liquids* **164** (2011) 29-33
- Large Topological Hall Effect in a Short-Period Helimagnet MnGe
Kanazawa N., Onose Y., Arima T., Okuyama D., Ohoyama K., Wakimoto S., Kakurai K., Ishiwata S., Tokura Y. *Phys. Rev. Lett.* **106** (2011) 156603-1-4
- Ion-Exchange Synthesis, Crystal Structure, and Electrochemical Properties of Li₂Ti₆O₁₃
Kataoka K., Awaka J., Kijima N., Hayakawa H., Ohshima K., Akimoto J. *Chem. Mater.* **23** (2011) 2344-2352
- Phase Behavior of Hexa-peri-hexabenzocoronene Derivative in Organic Solvent
Kim H. S., Lee J. H., Kim T. H., Okabe S., Shibayama M., Choi S. M. *J. Phys. Chem. B* **115** (2011) 7314-7320
- Holmium Oxide Single Crystals and Their Properties
Kimura H., Numazawa T., Sato T. J. *Advances in Chemistry Research*, Vol. 6, Ed(s). J. C. Taylor (Nova Science Publishers, New York, 2011) pp. 185-199

- Dependence of property, cathode characteristics, thermodynamic stability, average and local structures on heat-treatment condition for $\text{LiNi}_{0.5}\text{Mn}_{0.5}\text{O}_2$ as a cathode active material for Li-ion battery
Kitamura N., Hasegawa T., Uchimoto Y., Amezawa K., Idemoto Y.
Electrochimica Acta **56** (2011) 9453-9458
- Applications of Polymer Brushes to Structural Nano-Coatings
Kobayashi M., Mitamura K., Terada M., Kikuchi M., Murakami D., Yamaguchi H., Arita H., Ishikawa T., Terayama Y., Takahara A.
Proceeding of IEEE NMDC 2011 (IEEE, New York, 2011) pp. 69-74
- Characterization of Swollen States of Polyelectrolyte Brushes in Salt Solution by Neutron Reflectivity,
Kobayashi M., Mitamura K., Terada M., Yamada N. L., Takahara A.
J. Phys. Conf. Ser. **272** (2011) 12019-12019
- Stability of hexamer-type spin excitations in the frustrated spinel $\text{Mg}_{1-x}\text{Cr}_2\text{O}_4$ -x
Kousaka Y., Tomiyasu K., Yokobori T., Horigane K., Hiraka H., Yamada K., Akimitsu J.
J. Phys.: Conf. Ser., Vol. 320 (IOP science, United Kingdom, 2011) pp. 12040-12040
- Incommensurate spin fluctuations in hole-overdoped superconductor KFe_2As_2
Lee C. H., Kihou K., Kawano-Furukawa H., Saito T., Iyo A., Eisaki H., Fukazawa H., Kohori Y., Suzuki K., Usui H., Kuroki K., Yamada K.
Phys. Rev. Lett. **106** (2011) 67003-1-4
- Ordering Process in Sodium Nitrite Observed by Using Neutron Diffractometry
Mashiyama H., Miyoshi T., Asahi T., Kasano H., Noda Y., Kimura H.
J. Korean Phys. Soc. **59** (2011) 2515-2518
- Crystal structure of Eu-doped magnetoplumbite-type lanthanum aluminum oxynitride with emission site splitting
Masubuchi Y., Hata T., Motohashi T., Kikkawa S.
J. Solid State Chem. **184** (2011) 2533-2537
- Spin Density Wave in Insulating Ferromagnetic Frustrated Chain LiCuVO_4
Masuda T., Hagihala M., Kondoh Y., Kaneko K., Metoki N.
J. Phys. Soc. Jpn. **80** (2011) 1137051-1137054
- Dzyaloshinskii-Moriya interaction and spin reorientation transition in the frustrated kagome lattice antiferromagnet
Matan K., Bartlett B. M., Helton J. S., Sikolenko V., Matas S., Prokes K., Chen Y., Lynn J. W., Grohol D., Sato T. J., Tokunaga M., Nocera D. G., Lee Y. S.
Phys. Rev. B **83** (2011) 214406-1-12
- Structure analysis of polymer materials with small angle neutron scattering measurements
Matsuba G.
Material Raifu Gakkaishi **23** (2011) 98-103
- Fiber Structure Formation Studied with Quantum Beams
Matsuba G., Nishida K., Kanaya T.
The 11th Asian Textile Conference (FAPTA, Deagu, 2011) pp. 102-105
- Successive magnetic phase transitions of component orderings in DyB_4
Matsumura T., Okuyama D., Mouri T., Murakami Y.
J. Phys. Soc. Jpn. **80** (2011) 74701-1-9
- SANS Studies on Tetra-PEG Gel under Uniaxial Deformation
Matsunaga T., Asai H., Akagi Y., Sakai T., Chung U., Shibayama M.
Macromolecules **44** (2011) 1203-1210
- 中性子スピンエコー法によるリラクサー誘電体の格子ダイナミクスの研究
Matsuura M.

- 中性子スピンエコー法を用いたリラクサー誘電体の研究
Matsuura M.
波紋 (日本中性子学会誌) **21** (2011) 3-164-168
- A New Growth Mechanism of Polar Nanoregions by Phonon-Relaxation Mode-Coupling in a Relaxor Ferroelectric
Matsuura M., Hiraka H., Yamada K., Hirota K.
J. Phys. Soc. Jpn. **80** (2011) 10-104601-104605
- Hydrogen Atom of KH_2AsO_4 Determined by Neutron Diffraction Study
Miyoshi T., Akimoto T., Mashiyama H.
J. Phys. Soc. Jpn. **80** (2011) 74607-1-3
- Single-Crystal Neutron Structural Analyses of Potassium Dihydrogen Phosphate and Potassium Dideuterium Phosphate
Miyoshi T., Mashiyama H., Asahi T., Kimura H., Noda Y.
J. Phys. Soc. Jpn. **80** (2011) 44709-44709-44709
- Long-time variation of magnetic structure in rare-earth intermetallic compounds
Motoya K., Moyoshi T., Shigeoka T.
J. Phys.: Conf. Ser. **273** (2011) 12124-1-4
- Incommensurate Magnetic Structure and Its Long-Time Variation in a Geometrically Frustrated Magnet $\text{Ca}_3\text{Co}_2\text{O}_6$
Moyoshi T., Motoya K.
J. Phys. Soc. Jpn. **80** (2011) 34701-1-9
- Incommensurate Magnetic Structure and Its Long-Time Variation in a Geometrically Frustrated Magnet $\text{Ca}_3\text{Co}_2\text{O}_6$
Moyoshi T., Takahashi R., Motoya K.
J. Phys.: Conf. Ser. **273** (2011) 12125-1-4
- Unified Effect of Hydrophobic Hydration on the Dynamics and the Structure of Water Molecules in Lower Alcohol Aqueous Solutions
Nakada M., Maruyama K., Yamamuro O., Kikuchi T., Misawa M.
J. Phys. Soc. Jpn. **80** (2011) 44604-1-6
- Spin Wave Spectrum in 'Single-Domain' Magnetic Ground State of Triangular Lattice Antiferromagnet CuFeO_2
Nakajima T., Mitsuda S., Haku T., Shibata K., Yoshitomi K., Noda Y., Aso N., Uwatoko Y., Terada N.
J. Phys. Soc. Jpn. **80** (2011) 14714-1-4
- Control of ferroelectric polarization via uniaxial pressure in the spin-lattice-coupled multiferroic $\text{CuFe}_{1-x}\text{Ga}_x\text{O}_2$
Nakajima T., Mitsuda S., Nakamura T., Ishii H., Haku T., Honma Y., Kosaka M., Aso N., Uwatoko Y.
Phys. Rev. B **83** (2011) 220101-1-4
- 鉄系化合物における磁気構造— CaFe_4As_3 の複雑な磁性から
Nambu Y.
波紋 **21** (2011) 160-163
- Mixed Conductivity, Nonstoichiometric Oxygen, and Oxygen Permeation Properties in Co-Doped $\text{Sr}_3\text{Ti}_2\text{O}_7-\delta$
Nuansaeng S., Yashima M., Matsuka M., Ishihara T.
Chem. Eur. J. **17** (2011) 40-11324-11331
- Preparation, crystal structure, and superconductive characteristics of new oxynitrides $(\text{Nb}_{1-x}\text{M}_x)(\text{N}_{1-y}\text{O}_y)$ where $\text{M} = \text{Mg}, \text{Si}$, and $x \sim y$
Ohashi Y., Motohashi T., Masubuchi Y., Moriga T., Murai K., Kikkawa S.

- Magnetism and magnetoelectricity of a U-type hexaferrite Sr₄Co₂Fe₃₆O₆₀
Okumura K., Ishikura T., Soda M., Asaka T., Nakamura H., Wakabayashi Y., Kimura T.
Appl. Phys. Lett. **98** (2011) 212504–1–3
- 2D-Ising-like critical behavior in mixtures of water and 3-methylpyridine including antagonistic salt or ionic surfactant
Sadakane K., Iguchi N., Nagao M., Endo H., Melnichenko Y. B., Seto H.
Soft Matter **7** (2011) 1334–1340
- Effects of supersonic treatment on the electrochemical properties and crystal structure of LiMn_{1.5}Ni_{0.5}O₄ as a cathode material for Li ion batteries
Saruwatari H., Ishikawa T., Korechika Y., Kitamura N., Takami N., Idemoto Y.
J. Power Sources **196** (2011) 10126–10132
- On the Magnetic Excitation Spectra of Ba(Fe_{0.9}Co_{0.1})₂As₂ in the Superconducting State
Sato M., Tatematsu S., Yasui Y., Kobayashi Y., Moyoshi T., Motoya K., Kakurai K.
J. Phys. Soc. Jpn., Vol. 80 (JPSJ, Japan, 2011) pp. SB002–SB002
- Errata: Doping dependence of spin dynamics in electron-doped Ba(Fe_{1-x}Co_x)₂As₂ (vol 82, 054515, 2010)
Sato T. J., Matan K., Ibuka S., Morinaga R., Chi S. X., Lynn L. W., Christianson A. D., Lumsden M.
Phys. Rev. B **83** (2011) 59901–1–2
- Fe-Site Substitution Effect on the Structural and Magnetic Properties in SrFeO₂
Seinberg L., Yamamoto T., Tassel C., Kobayashi Y., Hayashi N., Kitada A., Sumida Y., Watanabe T., Masakazu N., Ohoyama K., Yoshimura K., Takano M., Paulus W., Kageyama H.
Inorg. Chem. **50** (2011) 3988–3995
- Crystal and electronic structure change determined by various method for delithiation process of Li_x(Ni,Mn)O₂-based cathode material
Sekizawa O., Hasegawa T., Kitamura N., Idemoto Y.
J. Power Sources **196** (2011) 6651–6656
- Small-angle Neutron Scattering on Polymer Gels: Phase behavior, Inhomogeneities, and Deformation Mechanisms
Shibayama M.
Polym. J. **43** (2011) 18–34
- Inhomogeneous Structure and Dynamics of Condensed Soft Matter
Shibayama M.
Neutrons in Soft Matter, Ed(s). Imae T., Kanaya T., Furusaka M., Torikai N. (John Wiley & Sons, Singapore, 2011) pp. 493–516
- Structures and Phase Transitions in Rb₂MoO₄ and Rb₂WO₄
Shigematsu H., Nomura K., Nishiyama K., Tojo T., Kawaji H., Atake T., Kawamura Y., Miyoshi T., Matsushita Y., Tanaka M., Mashiyama H.
Ferroelectrics **414** (2011) 195–200
- Dynamical Properties on the Protonic Conductor K₃H(SeO₄)₂
Shikanai F., Tomiyasu K., Aso N., Itoh S., Ikeda S., Kamiyama T., Tsukada S., Kano J., Kojima S.
Ferroelectrics **416** (2011) 101–107
- Clusters of Imidazolium-based Ionic Liquid in Benzene Solutions
Shimomura T., Takamuku T., Yamaguchi T.
J. Phys. Chem. B **115** (2011) 8518–8527
- Magnetic Ordering in Relation to the Room-Temperature Magnetoelectric Effect of Sr₃Co₂Fe₂₄O₄₁
Soda M., Ishikura T., Nakamura H., Wakabayashi Y., Kimura T.

- Superparamagnetism induced by polar nanoregions in relaxor ferroelectric (1-x)BiFeO₃-xBaTiO₃
Soda M., Matsuura M., Wakabayashi Y., Hirota K.
J. Phys. Soc. Jpn. **80** (2011) 43705–43705
- Kinetic Asymmetry of Subunit Exchange of Homo-Oligomeric Protein as Revealed by Deuteration-assisted Small-Angle Neutron Scattering
Sugiyama M., Kurimoto E., Yagi H., Mori K., Fukunaga T., Hirai M., Zaccai G., Kato K.
Biophysical J. **101** (2011) 2037–2042
- Quasi-elastic neutron scattering of cyanobiphenyl compounds with different terminal chains
Suzuki H., Inaba A., Krawczyk J., Massalska-Arodz M., Kikuchi T., Yamamuro O.
J. Non-Cryst. Solids **357** (2011) 734–739
- Studies on structure and physical properties of soft matter utilizing SANS under steady shear flow
Takahashi Y.
放射線化学 **91** (2011) 45–50
- N,N-Dimethylformamide-induced Phase Separation of Hexafluoroisopropanol-Water Mixtures
Takamuku T., Shimomura T., Tachikawa M., Kanzaki R.
Phys. Chem. Chem. Phys. **13** (2011) 11222–11232
- Rheo-SANS Studies on Shear-thickening/thinning in Aqueous Rod-like Micellar Solutions
Takeda M., Kusano T., Matsunaga T., Endo H., Shibayama M., Shikata T.
Langmuir **27** (2011) 1731–1738
- Growth of gold nanorods in gelled surfactant solutions
Takenaka Y., Kitahata H., Yamada N. L., Seto H., Hara M.
J. Coll. Int. Sci. **356** (2011) 111–117
- Recovery of reduced fringe visibility due to finite crossing angle between two paths of a neutron interferometer
Taketani K., Hino M., Shimizu H. M.
Physica B **406** (2011) 2377–2380
- Kinetics of Miniemulsion Polymerization Investigated by Small-Angle Neutron Scattering Technique
Taniguchi T., Kohri M., Nakahira T., Motokawa R.
Polymer Preprints Japan, Vol. 60 (2011, Tokyo, 2011) pp. 4412–4413
- Neutron Scattering Study of Magnetic Excitation Spectra of Ba(Fe_{0.9}Co_{0.1})₂As₂
Tatematsu S., Yasui Y., Moyoshi T., Motoya K., Kakurai K., Sato M.
J. Phys. Soc. Jpn. **80** (2011) 7–73703–73703
- Chain dimensions in free and immobilized brush states of polysulfobetaine in aqueous solution at various salt concentrations
Terayama Y., Arita H., Ishikawa T., Kikuchi M., Mitamura K., Kobayashi M., Yamada N. L., Takahara A.
J. Phys. Conf. Ser. **272** (2011) 12010–12010
- Salt Concentration Dependence of Swelling States for Poly(sulfobetaine) Brush at Aqueous Solution Interface
Terayama Y., Kikuchi M., Mitamura K., Yamada N. L., Kobayashi M., Takahara A.
Amphiphiles: Molecular Assembly and Applications, Vol. 1070 (ACS Symposium Series, New York, 2011) pp. 135–143
- Neutron scattering study of acoustic phonon softening in BiVO₄

Tomeno I., Sato N., Sato Y., Oka K., Tsunoda Y.
Phys. Rev. B **84** (2011) 14302-1-8

- Molecular Spin-Orbit Excitations in the Jeff = 1/2 Frustrated Spinel GeCo₂O₄
Tomiyasu K., Crawford M. K., Adroja D. T., Manuel P., Tominaga A., Hara S., Sato H., Watanabe T., Ikeda S. I., Lynn J. W., Iwasa K., Yamada K.
Phys. Rev. B **84** (2011) 54405-1-7
- Spin-orbit coupling inactivity of Co²⁺ ion in geometrically frustrated magnet GeCo₂O₄
Tomiyasu K., Tominaga A., Hara S., Sato H., Watanabe T., Ikeda S. I., Hiraka H., Iwasa K., Yamada K.
International Conference on Frustration in Condensed Matter (ICFCM), Vol. 320 (J. Phys.: Conf. Ser., UK, 2011) pp. 12038-5
- Molecular spin-liquid state in spin-3/2 frustrated spinel HgCr₂O₄
Tomiyasu K., Ueda H., Matsuda M., Yokoyama M., Iwasa K., Yamada K.
Phys. Rev. B **84** (2011) 3115-1-5
- Interplay between quantum criticality and geometric frustration in Fe₃Mo₃N with stella quadrangula lattice
Waki T., Terazawa S., Yamazaki T., Tabata Y., Sato K., Kondo A., Kindo K., Yokoyama M., Takahashi Y., Nakamura H.
Europhys. Lett. **94** (2011) 37004-1-6
- Crystalline electric field study in the pyrochlore Nd₂Ir₂O₇ with metal-insulator transition
Watahiki M., Tomiyasu K., Matsuhira K., Iwasa K., Yokoyama M., Takagi S., Wakeshima M., Hinatsu Y.
International Conference on Frustration in Condensed Matter (ICFCM), Vol. 320 (J. Phys.: Conf. Ser., UK, 2011) pp. 12080-5
- Neutron Quasi-elastic Scattering Studies on Dynamics of Water Confined in Nanoporous Copper Rubinate Hydrates
Yamada T., Yonamine R., Yamada T., Kitagawa H., Tyagi M., Nagao M., Yamamuro O.
J. Phys. Chem. B **115** (2011) 13563-13569
- Hierarchical Structure and Dynamics of an Ionic Liquid 1-Octyl-3-methylimidazolium Chloride
Yamamuro O., Yamada T., Kofu M., Nakakoshi M., Nagao M.
J. Chem. Phys. **135** (2011) 54508-54508
- Data acquisition system for high resolution chopper spectrometer (HRC) at J-PARC
Yano S., Itoh S., Satoh S., Yokoo T., Kawana D., Sato T. J.
Nucl. Instrum. Methods Phys. Res. A **654** (2011) 421-426
- Structure of photocatalysts which yield hydrogen from water
Yashima M.
Materials Stage **11** (2011) 5-15-17
- 中性子粉末回折法による触媒の結晶構造解析
Yashima M.
中性子回折の基礎と応用 (日本アイソトープ協会, tokyo, 2011) pp. 79-87
- 中性子粉末回折法による触媒の結晶構造解析
Yashima M.
中性子回折の基礎と応用 (日本アイソトープ協会, 東京, 2011) pp. 59-68
- 水から水素を作る光触媒の構造 ~窒素と共有結合が可視光に応答させる~
Yashima M.
Materials Stage **11** (2011) 15-17
- Experimental Visualization of Chemical Bonding and Structural Disorder in

- Relationship between ferroelectricity and magnetic structure of $\text{PbCuSO}_4(\text{OH})_2$ with CuO_2 ribbon chains
Yasui Y., Yanagisawa Y., Sato M., Terasaki I.
J. Phys.: Conf. Ser., Vol. 320 (Kawamura H., Osaka University, Japan, 2011) pp. 12087-12087
- Neutron scattering study of spiral-type spin correlations in the frustrated spinel $\text{Mn}_{0.07}\text{Mg}_{0.93}\text{Cr}_2\text{O}_4$
Yokobori T., Tomiyasu K., Kousaka Y., Matsui H., Hiraka H., Iwasa K., Yamada K., Akimitsu J.
J. Phys.: Conf. Ser., Vol. 320 (IOP Publishing, United Kingdom, 2011) pp. 12040-12040
- Examination of gas desorption by B4C resin for use in neutron scattering experiment
Yokoo T., Kaneko N., Itoh S., Otomo T., Suzuya K., Suetsugu Y., Shirai M.
Rev. Sci. Instrum. **82** (2011) 95109-1-7
- Magnetic properties and magnetic structures of $\text{Sr}_{3-x}\text{Ca}_x\text{Ru}_2\text{O}_7$
Yoshida Y., Iwata K., Katano S., Aso N.
J. Phys. Chem. Solids **72** (2011) 559-561
- Magnetic Correlation in the Square-Lattice Spin System (CuBr) $\text{Sr}_2\text{Nb}_3\text{O}_{10}$: a Neutron Diffraction Study
Yusuf S. M., Bera A. K., Ritter C., Tsujimoto Y., Ajiro Y., Kageyama H., Attfield J. P.
Phys. Rev. B **84** (2011) 64407-1-6
- Local anionic ordering and anisotropic displacement in dielectric perovskite SrTa_2O_7
Zhang Y. R., Matohashi T., Masubuchi Y., Kikkawa S.
J. Ceram. Soc. Jpn. **119** (2011) 581-586

2010

- Short-range spin correlations in $\beta''\text{-LiFeO}_2$ from bulk magnetization, neutron diffraction and μSR experiments
Akiyama R., Ikedo Y., Mansson M., Goko T., Sugiyama J., Andreica D., Amato A., Matan K., Sato T. J.
Phys. Rev. B **81** (2010) 24404-1-9
- 中性子回折用ピストンシリンダー型圧力セルとその応用
Aso N., Fujiwara T., Uwatoko Y.
波紋 **20** (2010) 151-157
- Swelling Structure of Thin Poly(methyl methacrylate) Films in Various Alkyl Length Alcohols
Atarashi H., Morita H., Yamazaki D., Hino M., Nagamura T., Tanaka K.
J. Phys. Chem. Lett. **1** (2010) 881-885
- Neutron powder diffraction study of tetragonal $\text{Li}_7\text{La}_3\text{Hf}_2\text{O}_{12}$ with the garnet-related type structure
Awaka J., Kijima N., Kataoka K., Hayakawa H., Ohshima K., Akimoto J.
J. Solid State Chem. **183** (2010) 180-185
- Inelastic and Quasielastic Neutron Scattering in $\text{PbMg}_{1/3}\text{Nb}_{2/3}\text{O}_3$ Above the Burns

Temperature

Burkovsky R., Vakhrushev S. B., Shapiro S. M., Ivanov A., Hirota K., Matsuura M.
Ferroelectrics **400** (2010) 372-386

- Antiferromagnetic magnetic transition and spin fluctuations in the deformed pyrochlore compound $\beta\text{-Fe}_2(\text{OH})_3\text{Cl}$
Fujihala M., Hagihala M., Zheng X. G., Kawae T.
Phys. Rev. B **82** (2010) 24425-24425
- Orthogonal Spin Arrangement in Quasi-Two-Dimensional $\text{La}_2\text{Co}_2\text{O}_3\text{Se}_2$
Fuwa Y., Endo T., Wakeshima M., Hinatsu Y., Ohoyama K.
J. Am. Chem. Soc. **132** (2010) 18020-18022
- Successive phase transitions with multi-k and non-coplanar spin order, spin fluctuations and field-induced phases in deformed pyrochlore antiferromagnet $\text{Co}_2(\text{OH})_3\text{Br}$
Hagihala M., Zheng X. G., Kawae T., Sato T. J.
Phys. Rev. B **82** (2010) 214424-1-12
- Incommensurate spin correlations induced by magnetic Fe ions substituted into overdoped $\text{Bi}_{1.75}\text{Pb}_{0.35}\text{Sr}_{1.90}\text{CuO}_6+z$
Hiraka H., Hayashi Y., Wakimoto S., Takeda M., Kakurai K., Adachi T., Koike Y., Yamada I., Miyazaki M., Hiraishi M., Takeshita S., Kohda A., Kadono R., Tranquada J. M., Yamada K.
Phys. Rev. B **81** (2010) 144501-1-6
- Fe-doping effects on magnetism in hole-type superconductors of $(\text{Bi,Pb})_2\text{Sr}_2\text{CuO}_6$
Hiraka H., Wakimoto S., Takeda M., Kakurai K., Matsumura D., Nishihata Y., Mizuki J., Yamada K.
J. Phys.: Conf. Ser. **200** (2010) 12059-1-4
- Composition dependences of T_c , J_c , physical property and crystal structure of $\text{Bi}_{1.8}\text{Pb}_{0.3}\text{Sr}_{2.0}\text{Ca}_{0.9}\text{Y}_{0.1}\text{Cu}_{2.0-x}\text{M}_x\text{O}_y$ ($\text{M}=\text{Zr}, \text{Zn}$) superconducting oxide
Idemoto Y., Sekizawa O., Kitamura N.
Physica C **471** (2010) 205-212
- Sinusoidally Modulated Magnetic Structure of a Kondo Lattice Compound CePd_5Al_2
Inoue Y. F., Onimaru T., Ishida A., Takabatake T., Oohara Y., Sato T. J., Adroja D. T., Hillier A. D., Coremychkin E. A.
J. Phys.: Conf. Ser. **200** (2010) 32023-1-4
- Strong carrier-scattering in iron-pnictide superconductors LnFeAsO_{1-y} ($\text{Ln}=\text{La}$ and Nd) obtained from charge transport experiments
Ishida S., Nakajima M., Tomioka Y., Ito T., Miyazawa K., Kito H., Lee C. H., Ishikado M., Shamoto S., Iyo A., Eisaki H., Kojima K. M., Uchida S.
Phys. Rev. B **81** (2010) 94515-1-6
- Development of T0 chopper at KEK
Itoh S., Ueno K., Ohkubo R., Funahashi Y., Sagehashi H., Yokoo T., Sato T. J., Otomo T., Satoh S.
Proceedings of the 19th Meeting of the International Collaboration on Advanced Neutron (ICANS-XIX) (Paul Scherrer Institut, Switzerland, 2010) pp. IP121-IP121
- T0チョッパーの開発(2)
Itoh S., Ueno K., Ohkubo R., Sagehashi H., Funahashi Y.
波紋, Vol. 20 (日本中性子科学会, 東京都, 2010) pp. 146-150
- Development of Fermi chopper at KEK
Itoh S., Ueno K., Yokoo T., Funahashi Y., Kamiyama T., Sato H., Miyamoto N., Kiyonagi Y., Sato T. J., Otomo T., Satoh S.
Proceedings of the 19th Meeting of the International Collaboration on Advanced Neutron Sources (ICANS XIX) (Paul Scherrer Institut, Switzerland, 2010) pp. IP120-IP120

- Construction Status of High Resolution Chopper Spectrometer (HRC) at J - PARC
Itoh S., Yokoo T., Sato T. J., Satoh S., Yano S., Suzuki J., Ueno K., Kuwahara K., Kamiyama T., Iwasa K., Ohoyama K., Otomo T., Endoh Y., Akimitsu J., Kuroda S., Sato K., Nasu K., Iwano K., Yoshizawa H., Yamamuro O., Ohara Y., Kawamura Y., Asami T., Sugiura R.
Proceedings of the 19th Meeting of the International Collaboration on Advanced Neutron Sources (ICANS XIX) (Paul Scherrer Institut, Switzerland, 2010) pp. IO079-IO079
- Temperature evolution of crystal field splitting in Pr-filled skutterudite
Iwasa K., Saito K., Murakami Y., Sugawara H.
ICM2009, Vol. 200 (IOP science, England, 2010) pp. 12071-12071
- Partial pair correlation functions of highly concentrated aqueous urea solutions determined by neutron diffraction with $^{14}\text{N}/^{15}\text{N}$ and H/D isotopic substitution methods
Kameda Y., Maki A., Amo Y., Usuki T.
Bull. Chem. Soc. Jpn. **83** (2010) 131-144
- Investigation of the Spin-Glass Regime between the Antiferromagnetic and Superconducting Phases in $\text{Fe}_{1+y}\text{SexTe}_{1-x}$
Katayama N., Sungdae J., Louca D., Lee S. H., Fujita M., Sato T. J., Wen J., Xu Z., Gu G., Xu G., Lin Z., Enoki M., Chang S., Yamada K., Tranquada J. M.
J. Phys. Soc. Jpn. **79** (2010) 113702-1-4
- Structure and Rheology of a Self-Standing Nanoemulsion
Kawada H., Kume T., Matsunaga T., Iwai H., Sano T., Shibayama M.
Langmuir **26** (2010) 2430-2437
- High Temperature Multiferroic State in RBaCuFeO_5 (R=Y, Lu and Tm)
Kawamura Y., Kai T., Satomi E., Yasui Y., Kobayashi Y., Sato M., Kakurai K.
J. Phys. Soc. Jpn. **79** (2010) 73705-1-4
- Coexistence of Ferromagnetic and Antiferromagnetic States in $\text{CaRu}_{1-x}\text{Mn}_x\text{O}_3$
Kawanaka H., Noguchi A., Yokoyama M., Bando H., Nishihara Y.
J. Phys.: Conf. Ser. **200** (2010) 32033-1-4
- Development of a pixel detector for ultra-cold neutrons
Kawasaki S., Ichikawa G., Hino M., Kamiya Y., Kitaguchi M., Komamiya S., Sanuki T., Sonoda S.
Nucl. Instrum. Methods A **615** (2010) 42-47
- Thermoelectric properties of LaFeAsO_{1-y} at low temperature
Kihou K., Lee C. H., Miyazawa K., Shirage P. M., Iyo A., Eisaki H.
J. Appl. Phys. **108** (2010) 33703-1-3
- Boson Peaks of Lithium Borate Glasses Studied by Inelastic Neutron and Light Scattering
Kojima S., Matsuda Y., Fukawa Y., Kawashima M., Moriya Y., Yamada T., Yamamuro O., Kodama M.
J. Non-Cryst. Solids **356** (2010) 2524-2527
- Effect of K Doping on Phonons in $\text{Ba}_{1-x}\text{K}_x\text{Fe}_2\text{As}_2$
Lee C. H., Kihou K., Horigane K., Tsutsui S., Fukuda T., Eisaki H., Iyo A., Yamaguchi H., Baron A. Q. R., Braden M., Yamada K.
J. Phys. Soc. Jpn. **79** (2010) 14714-1-4
- Novel Frustrated Behavior in Quantum Heisenberg Antiferromagnets on the Pyrochlore Lattice: NMR Studies of $\text{R}_2(\text{OH})_3\text{Cl}$ (R=Cu and Ni)
Maegawa S., Oyamada A., Sato S.
J. Phys. Soc. Jpn. **79** (2010) 11002-1-12
- The Role of Dopants in SnO_2 -based Semiconductor Gas Sensing Materials (1) Effects

of Dopants on Sensing Performances and Reliability of Sensors

Maekawa T., Minagoshi C., Kanda K., Nomura K., Kageyama H.

Cemical Sensors, Supplement B, Vol. 26 (Japan Association of Chemical Sensors, The Electrochemical Society of Japan, Japan, 2010) pp. 106-108

- Instability of magnons in two-dimensional antiferromagnets at high magnetic fields
Masuda T., Kitaoka S., Takamizawa S., Metoki N., Kaneko K., Rule K.C., Kiefer K., Manaka H., Nojiri H.
Phys. Rev. B **81** (2010) 1004021-1004024
- Doping dependence of spin dynamics in electron-doped Ba(Fel-xCox)2As2
Matan K., Ibuka S., Morinaga R., Chi S., Lynn J. W., Christianson A. D., Lumsden M. D., Sato T. J.
Phys. Rev. B **82** (2010) 54515-1-5
- Pinwheel valence-bond solid and triplet excitations in the two-dimensional deformed kagome lattice
Matan K., Ono T., Fukumoto Y., Sato T. J., Yamaura J., Yano M., Morita K., Tanaka H.
Nature Phys. **6** (2010) 865-869
- Composition dependence of the boson peak and universality on lithium borate binary glasses: Inelastic neutron and Raman scattering study
Matsuda Y., Fukawa Y., Kawashima M., Moriya M., Yamada T., Yamamuro O., Kojima S.
J. Phys. Soc. Jpn. **79** (2010) 33801-33801
- Microscopic structure analysis of clay-poly(ethylene oxide) mixed solution in a flow field by contrast-variation small-angle neutron scattering
Matsunaga T., Endo H., Takeda M., Shibayama M.
Macromolecules **43** (2010) 5075-5082
- ダイヤモンド格子状構造をもつ高分子ゲルの構造とダイナミクス
Matsunaga T., Shibayama M.
機能材料 **30** (2010) 6-13
- Antiferromagnetic Alignment of Magnetic Dipolar Moments Observed by Neutron Powder Diffraction in Rare-Earth Palladium Bronze PrPd3S4
Matsuoka E., Usui D., Sasaki Y., Watahiki M., Iwasa K., Shida H., Ohoyama K., Onodera H.
J. Phys. Soc. Jpn. **79** (2010) 64708-1-4
- Study of Slow Lattice Dynamics in Relaxor Ferroelectric PMN-30%PT by Neutron Spin Echo Technique
Matsuura M., Endo H., Matsushita M., Tachi Y., Iwasaki Y., Hirota K.
J. Phys. Soc. Jpn. **79** (2010) 33601-33604
- Structure and dynamics of polyrotaxane and slide-ring materials
Mayumi K., Ito K.
Polymer **51** (2010) 959-967
- Hot pressing of Ge crystals toward a reflection-plane-selective neutron monochromator
Miyake Y., Hiraka H., Ohoyama K., Yamaguchi Y., Yamada K.
J. Phys.: Conf. Ser. **200** (2010) 112006-1-4
- Long-time variation of magnetic structure in in CeIr3Si2
Motoya K., Muro Y., Takabatake T.
J. Phys.: Conf. Ser. **200** (2010) 32048-1-4
- Real-time observation of magnetic structural change in the multistep metamagnet in CeIr3Si2
Motoya K., Muro Y., Takabatake T.
J. Phys.: Conf. Ser. **251** (2010) 12019-1-4

- Superconducting transition temperature and the thickness of CoO₂ planes of Na_xCoO₂·yH₂O
Moyoshi T., Kobayashi Y., Yasui Y., Sato M., Kakurai K.
Solid State Sciences **12** (2010) 656–659
- Magnetic Excitations of Superconducting LaFeAsO_{0.89}F_{0.11}
Moyoshi T., Lee S. C., Tatematsu S., Yasui Y., Kobayashi Y., Sato M., Kakurai K.
Physica C **470** (2010) S470–S471
- High Pressure Apparatus for Neutron Scattering at Low Temperatures
Munakata K., Aso N., Uwatoko Y.
RADIOISOTOPES, Vol. 59 (Japan Radioisotope Association, RADIOISOTOPES, 2010) pp. 751–762
- Electric field dependence of magnetic correlation in magneto-electric multiferroic CuFe_{1-x}Al_xO₂
Nakajima T., Mitsuda S., Takahashi K., Kaneko Y., Ito T., Fukunaga M., Kimura H., Noda Y.
ICM2009 proceedings, Vol. 200 (Institute of Physics, UK, 2010) pp. 12139–12139
- Spin-helicity-dependent magnetic domain growth in a spin-driven multiferroic under applied electric field
Nakajima T., Mitsuda S., Takahashi K., Yamazaki H., Yoshitomi K., Soda M., Matsuura M., Hirota K.
Phys. Rev. B **82** (2010) 64418–1–5
- The Role of Dopants in SnO₂-based Semiconductor Gas Sensing Materials (3) Crystal Structure Analyses Using X-ray and Neutron Diffraction Methods
Nomura K., Kageyama H., Minagoshi C., Maekawa T., Kanda K.
Chemical Sensors, Supplement B, Vol. 26 (Japan Association of Chemical Sensors, The Electrochemical Society of Japan, Japan, 2010) pp. 112–114
- Crystal structure and superconductive characteristics of Nb_{0.89}Al_{0.11} oxynitrides
Ohashi Y., Motohashi T., Masubuchi Y., Kikkawa S.
J. Solid State Chem. **183** (2010) 1710–1714
- Pressure-Induced Antiferromagnetic Order in Filled Skutterudite PrFe₄P₁₂ Studied by Single-Crystal High-Pressure Neutron Diffraction
Osakabe T., Kuwahara K., Kawana D., Iwasa K., Kikuchi D., Aoki Y., Kohigi M., Sato H.
J. Phys. Soc. Jpn. **79** (2010) 34711–1–7
- Rh-substitution effect on 4f-electron states in multipole ordered phase of PrRu₄P₁₂
Saito K., Laulhe C., Iwasa K., Murakami Y.
Rh-substitution effect on 4f-electron states in multipole ordered phase of PrRu₄P₁₂, Vol. 200 (IOP science, England, 2010) pp. 12170–12170
- A Novel Isomorphic Phase Transition in β -Pyrochlore Oxide KOs₂O₆: A Study Using High-resolution Neutron Powder Diffraction
Sasai K., Kofu M., Ibberson R. M., Hirota K., Yamaura J., Hiroi Z., Yamamuro O.
J. Phys.: Cond. Matter **22** (2010) 15403–15403
- Studies on the Superconducting State of Na_xCoO₂·yH₂O -Overview-
Sato M., Kobayashi Y., Moyoshi T.
Physica C **470** (2010) S673–S677
- On the Non-superconducting State of Na_xCoO₂·yH₂O
Sato M., Kobayashi Y., Moyoshi T.
Physica C **470** (2010) S752–S754
- Relationship between Magnetic Structure and Ferroelectricity of Systems with CuO₂ ribbon chains
Sato M., Yasui Y., Kobayashi Y., Sato K., Naito Y., Tarui Y., Kawamura Y.
Solid State Science **12** (2010) 670–675. **12** (2010) 670–675

- Effect of Li content on electronic structure by first-principle calculation for $\text{Li}_{1+x}\text{Ni}_{0.5}\text{Mn}_{0.5}\text{O}_2$ cathode active material of lithium-ion battery
Sekizawa O., Kitamura N., Idemoto Y.
Electrochemistry **78** (2010) 367-369
- 第一原理計算を用いたLiイオン電池用正極活物質 $\text{LiNi}_{0.5}\text{Mn}_{0.5}\text{O}_2$ における過剰Li及びカチオンミキシングの電子構造への影響
Sekizawa O., Kitamura N., Idemoto Y.
Electrochemistry **79** (2010) 80-85
- 小角中性子散乱によるナノ構造解析
Shibayama M.
RADIOISOTOPES **59** (2010) 395-403
- 中性子散乱で観た高強カゲルの構造
Shibayama M.
高分子 **59** (2010) 701-704
- Pressure- and Temperature-Induced Phase Separation Transition in Homopolymer, Block Copolymer, and Protein in Water
Shibayama M., Osaka N.
Macromol. Symp. **291-292** (2010) 115-121
- Effects of Alkyl-chain Length on Mixing State of Imidazolium-based Ionic Liquid-Methanol Solutions
Shimomura T., Fujii K., Takamuku T.
Phys. Chem. Chem. Phys. **12** (2010) 12316-12324
- Superconductivity at 28.3 and 17.1 K in $(\text{Ca}_4\text{Al}_2\text{O}_6-y)(\text{Fe}_2\text{Pn}_2)$ (Pn = As and P)
Shirage P. M., Kihou K., Lee C. H., Kito H., Eisaki H., Iyo A.
Appl. Phys. Lett. **97** (2010) 172506-1-3
- Structure and electrical properties of the new pyrochlore-type protonic solid electrolyte $\text{K}_{0.88}\text{Nb}_{207.58}\text{H}_{4.28}$
Smirnova O. A., Kumada N., Yonesaki Y., Yashima M., Takei T., Kinomura N.
Acta Crystallogr. Sect. B **66** (2010) 594-602
- Domain rearrangement and spin-spiral-plane flop as sources of magnetoelectric effects in delafossite CuCrO_2
Soda M., Kimura K., Kimura T., Hirota K.
Phys. Rev. B **81** (2010) 100406-1-4
- Non-uniformity in Cross-linked Natural Rubber as Revealed by Contrast-variation Small-angle Neutron Scattering
Suzuki T., Osaka N., Endo H., Shibayama M., Ikeda Y., Asai H., Higashitani N., Kokubo Y., Kohjiya S.
Macromolecules **43** (2010) 1556-1563
- Anomalous Water Molecules and Mechanistic Effects of Water Nanotube Clusters Confined to Molecular Porous Crystals
Tadokoro M., Ohhara T., Ohhata Y., Suda T., Miyasato Y., Yamada T., Kikuchi T., Tanaka I., Kurihara K., Oguni M., Nakasuji K., Yamamuro O., Ryota K.
J. Phys. Chem. B **114** (2010) 2091-2099
- Solvation of the Amphiphilic Diol Molecule in Aliphatic Alcohol-Water and Fluorinated Alcohol-Water Solutions
Takamuku T., Tanaka M., Sako T., Shimomura T., Fujii K., Kanzaki R., Takeuchi M.
J. Phys. Chem. B **114** (2010) 4252-4260
- Rheo-SANS Studies on Structure Evolution in Clay-Poly(ethylene oxide) Mixed Solutions
Takeda M., Endo H., Matsunaga T., Nishida T., Takahashi A., Shibayama M.

- Synthesis, Structural and Magnetic Properties of the Solid Solution (CuCl_{1-x}Br_x)LaNb₂O₇ (0 ≤ x ≤ 1)
Tsujiimoto Y., Kitada A., Kageyama H., Nishi M., Narumi Y., Kindo K., Kiuchi Y., Ueda Y., Uemura Y. J., Ajiro Y., Yoshimura K.
J. Phys. Soc. Jpn. **79** (2010) 14709-1-4
- Synthesis, Structural and Magnetic Properties of the Solid Solution (CuCl_{1-x}Br_x)LaNb₂O₇ (0 ≤ x ≤ 1)
Tsujiimoto Y., Kitada A., Kageyama H., Nishi M., Narumi Y., Kindo K., Kiuchi Y., Ueda Y., Uemura Y. J., Ajiro Y., Yoshimura K.
J. Phys. Soc. Jpn. **79** (2010) 14709-1-4
- Non-Fermi-Liquid Behavior on an Iron-Based Itinerant Electron Magnet Fe₃Mo₃N
Waki T., Terasawa S., Tabata Y., Oba F., Michioka C., Yoshimura K., Ikeda S., Kobayashi H., Ohoyama K., Nakamura H.
J. Phys. Soc. Jpn. **79** (2010) 43701-1-4
- Magnetic field effect on Fe-induced short-range magnetic correlation and electrical conductivity in Bi_{1.75}Pb_{0.35}Sr_{1.90}Cu_{0.91}Fe_{0.09}O_{6+y}
Wakimoto S., Hiraka H., Kudo K., Okamoto D., Nishizaki T., Kakurai K., Hong T., Zheludev A., Tranquada J. M., Kobayashi N., Yamada K.
Phys. Rev. B **82** (2010) 64507-1-7
- Calorimetric and Neutron Diffraction Studies on Novel Transitions of Water Confined in Nano-porous Copper Rubeanate
Yamada T., Yonamine R., Yamada T., Kitagawa H., Yamamuro O.
J. Phys. Chem. B **114** (2010) 8405-8409
- Synthesis and Thermal Stability of the Solid Solution AFeO₂ (A = Ba, Sr, Ca)
Yamamoto T., Li Z., Tassel C., Hayashi N., Takano M., Isobe M., Ueda Y., Ohoyama K., Yoshimura K., Kageyama H.
Inorg. Chem. **49** (2010) 221-229
- Synthesis and Thermal Stability of the Solid Solution AFeO₂ (A = Ba, Sr, Ca)
Yamamoto T., Li Z., Tassel C., Hayashi N., Takano M., Isobe M., Ueda Y., Ohoyama K., Yoshimura K., Kobayashi Y., Kageyama H.
Inorg. Chem. **49** (2010) 5957-5962
- 中性子回折によるイオン伝導性セラミック材料の結晶構造解析
Yashima M.
RADIOISOTOPES **59** (2010) 201-210
- 触媒の結晶構造解析
Yashima M.
RADIOISOTOPES **59** (2010) 221-229
- 化学掲示板： 2月2日毎日新聞，プラセオジムニッケル系酸化物の構造を解明
Yashima M.
化学 **65** (2010) 74-75
- イオン伝導性セラミック材料におけるイオン拡散経路の可視化
Yashima M.
燃料電池 **9** (2010) 83-89
- ニッケル酸プラセオジム系混合伝導体における酸素透過メカニズム
Yashima M.
未来材料 **10** (2010) 8-35-40
- Imma Perovskite-Type Oxynitride LaTiO₂N, Structure and Electron Density
Yashima M., Saito M., Nakano H., Takata T., Ogisu K., Domen K.

- Crystal Structure, Diffusion Path and Oxygen Permeability of a Pr₂NiO₄-Based Mixed Conductor (Pr_{0.9}La_{0.1})₂(Ni_{0.74}Cu_{0.21}Ga_{0.05})O_{4+d}
Yashima M., Sirikanda N., Ishihara T.
J. Am. Chem. Soc. **132** (2010) 10-2385-2392
- 高分解能チヨッパー分光器HRC
Yokoo T., Itoh S., Satoh S., Sato T. J., Yano S.
波紋, vol. 20 (日本中性子科学会, 東京都, 2010) pp. 45-48
- Gas Desorption Examination of B₄C Resin for Neutron Vacuum Chamber
Yokoo T., Kaneko N., Itoh S., Otomo T., Suetsugu Y., Shirai M., Suzuya K.
Proceedings of the 19th Meeting of the International Collaboration on Advanced Neutron (ICANS-XIX) (Paul Scherrer Institut, Switzerland, 2010) pp. IP144-IP144
- Magnetic-field dependence of antiferromagnetic structure in CeRh_{1-x}CoxIn₅
Yokoyama M., Ikeda Y., Kawasaki I., Nishikawa D., Tenya K., Kuwahara K., Amitsuka H.
J. Phys.: Conf. Ser. **200** (2010) 12239-1-4
- A Study of alcohol-induced gelation of beta-lactoglobulin with small-angle neutron scattering, neutron spin echo, and dynamic light scattering measurements
Yoshida K., Yamaguchi T., Osaka N., Endo H., Shibayama M.
Phys. Chem. Chem. Phys. **12** (2010) 3260-3269
- Spray-drying synthesized lithium-excess Li_{4+x}Ti_{5-x}O₁₂-□ and its electrochemical property as negative electrode material for Li-ion batteries
Yoshikawa D., Kadoma Y., Kim J. M., Ui K., Kumagai N., Kitamura N., Idemoto Y.
Electrochimica Acta **55** (2010) 1872-1879
- Ferroelectric Properties of Magnetoferroelectric YMnO₃ Epitaxial Films at around the Neel Temperature
Yoshimura T., Maeda K., Ashida A., Fujimura N.
Key Eng. Mater. **455** (2010) 144-147

Dissertations

2018

- Title: Novel magnetic excitations in spin systems investigated by neutron scattering
Author: Hayashida S.
Degree type: Doctor/Ph.D
Received from: ISSP, University of Tokyo (2018)
- Title: Molecular Studies of Solvation for Polymers in Ionic Liquids
Author: Hirosawa K.
Degree type: Doctor/Ph.D
Received from: The University of Tokyo (2018)
- Title: マルチフェロイック物質CeFe₃(BO₃)₄のバルク物性と磁気構造解析
Author: Kato D.
Degree type: Master

Received from: ISSP, University of Tokyo (2018)

- Title: Thermodynamic and neutron scattering study on super-high entropy liquids alkylated tetraphenylporphyrin
Author: Nirei M.
Degree type: Master
Received from: University of Tokyo (2018)
- Title: Fabrication of Physical Gels crosslinked with double-stranded DNA
Author: Yoshikawa Y.
Degree type: Master
Received from: The University of Tokyo (2018)

2017

- Title: Studies on cross-correlated phenomena in multiferroic CuFeO₂
Author: Tamatsukuri H.
Degree type: Doctor/Ph.D
Received from: Tokyo University of Science (2017)
- Title: 反転対称性の破れた希土類化合物R₅Ru₃Al₂ (R=La, Ce, Pr)の新奇磁気秩序
Author: Makino K.
Degree type: Master
Received from: IMRAM, Tohoku University (2017)
- Title: Quantum-Beam Scattering Study on Superlattice Phase Transition and Electronic State of R₃Rh₄Sn₁₃ (R = Ce, La)
Author: Suyama K.
Degree type: Master
Received from: Tohoku University (2017)

2016

- Title: ブリージングパイロクロア格子系Ba₃Yb₂Zn₅O₁₁の中性子散乱研究
Author: Haku T.
Degree type: Doctor/Ph.D
Received from: ISSP, University of Tokyo (2016)
- Title: 梯子形鉄系化合物における結晶及び磁気構造と輸送現象に関する研究
Author: Hawai T.
Degree type: Doctor/Ph.D
Received from: The University of Tokyo (2016)
- Title: Synthesis and structural analysis of metastable transition metal oxides with unique magnetic properties
Author: Kawamoto T.
Degree type: Doctor/Ph.D
Received from: Kyoto University (2016)
- Title: パラジウムナノ結晶における水素の吸蔵特性と運動状態の研究
Author: Hashimoto N.
Degree type: Master
Received from: University of Tokyo (2016)
- Title: Structural Study on Ovalbumin Gels in the Presence of N-terminal

Amphiphilic Region
Author: Okazumi Y.
Degree type: Master
Received from: The University of Tokyo (2016)

- Title: Electronic phase transition accompanied by chiral structural transformation of $R_3Co_4Sn_{13}$ ($R = Ce, La$)
Author: Otomo Y.
Degree type: Master
Received from: Tohoku University (2016)
- Title: 一次元フラストレート物質 $NaCuMoO_4(OH)$ の磁性
Author: Oyama T.
Degree type: Master
Received from: ISSP, University of Tokyo (2016)
- Title: トポロジカル近藤絶縁体 YbB_{12} のZr置換によるフェルミ準位チューニング
Author: Wada T.
Degree type: Master
Received from: Ibaraki University (2016)
- Title: Quantum spin liquid state of $Tb_{2+x}Ti_{2-x}O_{7+y}$
Author: Wakita M.
Degree type: Master
Received from: Department of Physics, Tokyo Metropolitan University, Hachioji-shi, Tokyo 192-0397 (2016)
- Title: $Sr_2MSi_2O_7$ ($M=Cu, Co, Mn$)の磁気構造
Author: Yoshida T.
Degree type: Master
Received from: ISSP, University of Tokyo (2016)

2015

- Title: Structural Study of Self-Assembled Aggregates Formed by Ionic Oligomeric Surfactants
Author: Kusano T.
Degree type: Doctor/Ph.D
Received from: The University of Tokyo (2015)
- Title: マルチフェロイクス物質 $NdFe_3(BO_3)_4$ の中性子散乱研究
Author: Hayashida S.
Degree type: Master
Received from: ISSP, University of Tokyo (2015)
- Title: 低温蒸着法による単純分子ガラスの構造研究
Author: Mizuno Y.
Degree type: Master
Received from: ISSP, University of Tokyo (2015)
- Title: Electronic phase transition accompanied by chiral structural transformation of $R_3Co_4Sn_{13}$ ($R = Ce, La$)
Author: Otomo Y.
Degree type: Master
Received from: Tohoku University (2015)
- Title: Structural Analysis of Lipophilic Polyelectrolytes and Gels in Low Polar Solvents by using Scattering Methods
Author: Tochioka S.

Degree type: Master
Received from: The University of Tokyo (2015)

- Title: PrRu₄P₁₂のf電子多極子秩序への磁性イオン置換効果
Author: Yonemoto A.
Degree type: Master
Received from: Tohoku University (2015)

2014

- Title: Hydration Structure of Biomolecules Studied by Neutron and X-ray Diffraction Techniques
Author: Miyazaki T.
Degree type: Doctor/Ph.D
Received from: Yamagata university (2014)
- Title: Studies on gelation kinetics of model polymer networks
Author: Nishi K.
Degree type: Doctor/Ph.D
Received from: Science (2014)
- Title: Small Angle Neutron Scattering Studies of Vortex States in Type-II Superconductors
Author: Kure M.
Degree type: Master
Received from: Ochanomizu University (2014)
- Title: 中性子散乱と熱容量測定によるプロトン伝導性多孔性配位高分子の研究
Author: Miyatsu S.
Degree type: Master
Received from: ISSP, University of Tokyo (2014)
- Title: サマリウム系充填スクッテルダイトSmFe₄P₁₂の多重項励起に関する研究
Author: Suzuki A.
Degree type: Master
Received from: Ibaraki University (2014)
- Title: 輸送および熱力学特性の測定と中性子非弾性散乱実験による層状ニッケル酸化物R₂-xSr_xNiO₄ (R=La, Nd) の市松模様相の研究
Author: Suzuki M.
Degree type: Master
Received from: ISSP, University of Tokyo (2014)

2013

- Title: Synthesis and Structural Analysis of High Performance Gel Containing Ionic Liquid
Author: Asai H.
Degree type: Doctor/Ph.D
Received from: The University of Tokyo (2013)
- Title: Cross-link Inhomogeneity of Phenolic Resins
Author: Izumi A.
Degree type: Doctor/Ph.D
Received from: Ph D. (2013)

- Title: リチウムイオン電池用チタン酸化物電極材料の合成と電池特性に関する研究
Author: Sakao M.
Degree type: Doctor/Ph.D
Received from: Yokohama National University (2013)
- Title: 第一原理計算、中性子・放射光x線によるリチウムイオン電池正極材料 $\text{Li}_2\text{MnO}_3\text{-Li}(\text{Ni}_{1/3}\text{Co}_{1/3}\text{Mn}_{1/3})\text{O}_2$ 固溶体の充電過程の平均・局所構造及び電子構造
Author: Akatsuka K.
Degree type: Master
Received from: Faculty of Science and Technology, Tokyo University of Science (2013)
- Title: スピンギャップ物質の中性子散乱研究
Author: Haku T.
Degree type: Master
Received from: ISSP, University of Tokyo (2013)
- Title: 酸素分子磁性の研究
Author: Honma Y.
Degree type: Master
Received from: University of Tokyo (2013)
- Title: 2次元層状Ni酸化物の絶縁体金属転移近傍におけるスピンドYNAMIXス
Author: Nakabayashi T.
Degree type: Master
Received from: ISSP, University of Tokyo (2013)
- Title: 遍歴電子反強磁性体 $\text{Mn}(3-x)\text{Fe}(x)\text{Si}$ のスピンドYNAMIXスの研究
Author: Nara S.
Degree type: Master
Received from: Graduate School of Science, Tohoku University (2013)
- Title: リエントラント金属-非金属転移を示す $\text{Pr}_{1-x}\text{Ce}_x\text{Ru}_4\text{P}_{12}$ の超格子構造の研究
Author: Sato T.
Degree type: Master
Received from: Tohoku University (2013)
- Title: フラストレート磁性体 $\text{Tb}_{2+x}\text{Ti}_{2-x}\text{O}_{7+y}$ の多極子秩序と新奇量子相
Author: Taniguchi T.
Degree type: Master
Received from: Department of Physics, Tokyo Metropolitan University, Hachioji-shi, Tokyo 192-0397 (2013)

2012

- Title: 鉄ニクタイド化合物 BaFe_2As_2 における反強磁性相関の中性子散乱による研究
Author: Ikuka S.
Degree type: Doctor/Ph.D
Received from: University of Tokyo (2012)
- Title: 軌道縮退したスピネル型酸化物におけるスピン-軌道-格子結合と交差相関物性
Author: Nii Y.
Degree type: Doctor/Ph.D
Received from: Tohoku University (2012)
- Title: Structural Analysis and Mechanical Properties of High Performance

Nanocomposite Gels
Author: Nishida T.
Degree type: Doctor/Ph.D
Received from: The University of Tokyo (2012)

- Title: Study on ordering and fluctuation of totally symmetric multipoles inducing metal-nonmetal transition
Author: Saito K.
Degree type: Doctor/Ph.D
Received from: Tohoku University (2012)
- Title: A study of valence ordering in YbPd and $\text{EuPtP}_{1-x}\text{As}_x$
Author: Sugishima M.
Degree type: Doctor/Ph.D
Received from: Kyushu University (2012)
- Title: 長周期スピン構造における 磁気構造解析と磁気励起の研究 –中性子散乱の実験技術開発を通して–
Author: Yano S.
Degree type: Doctor/Ph.D
Received from: Aoyama Gakuin University (2012)
- Title: LaCoO_3 のスピン状態制御によって誘起される弱強磁性
Author: Asai S.
Degree type: Master
Received from: Nagoya University (2012)
- Title: Dynamics and structure of water confined in organic-inorganic hybrid mesoporous materials
Author: Aso M.
Degree type: Master
Received from: Fukuoka University (2012)
- Title: 有機-無機ハイブリッドメソ多孔性物質中に閉じ込められた水のダイナミクスと構造
Author: Aso M.
Degree type: Master
Received from: Fukuoka University (2012)
- Title: $(\text{Bi}, \text{Na}) (\text{Ti}, \text{Nb}, \text{Ta})\text{O}_3$ 系強誘電体の物性、結晶・電子構造と強誘電特性
Author: Fujishiro N.
Degree type: Master
Received from: Faculty of Science and Technology, Tokyo University of Science (2012)
- Title: ハロゲン化アルカリ塩誘起によるアセトニトリル-水混合溶液の相分離
Author: Haramaki H.
Degree type: Master
Received from: Saga University (2012)
- Title: 中性子散乱による層状ニッケル酸化物 $\text{R}_2-x\text{SrxNiO}_4$ ($\text{R}=\text{La}, \text{Pr}$) のスピン・電荷相関の研究
Author: Imasato T.
Degree type: Master
Received from: Tohoku University (2012)
- Title: 超音波処理による5V級リチウムイオン電池正極材料 $\text{LiMn}_{1.5}\text{Ni}_{0.5}\text{O}_4$ の物性、結晶・電子構造と電池特性
Author: Ishikawa T.
Degree type: Master
Received from: Faculty of Science and Technology, Tokyo University of Science (2012)
- Title: 還元熱処理によるリチウムイオン電池正極材料 $\text{Li}_2\text{MnO}_3\text{-Li}(\text{Mn}, \text{Co}, \text{Ni})\text{O}_2$ 系固溶体の物性、平

均・局所構造、電子構造と電池特性

Author: Kashima T.

Degree type: Master

Received from: Faculty of Science and Technology, Tokyo University of Science (2012)

- Title: Neutron scattering study on localization and itinerancy involving f_2 electron state in PrCu_4T (T=Au, Ag)
Author: Kobayashi H.
Degree type: Master
Received from: Tohoku University (2012)
- Title: サマリウム系充填スクッテルダイト及びセリウムヘキサボライドの純良単結晶育成
Author: Konno T.
Degree type: Master
Received from: Ibaraki University (2012)
- Title: 銅酸化物 $\text{R}_{2-x}(\text{Ce}, \text{Ca})_x\text{CuO}_4$ (R=rare earth)における磁気相関の電子-ホール対称性の研究
Author: Miura T.
Degree type: Master
Received from: Tohoku University (2012)
- Title: $\text{Ce}_x\text{La}_{1-x}\text{B}_6$ のIV相への希土類イオン添加および圧力効果の研究
Author: Soejima K.
Degree type: Master
Received from: Graduate School of Advanced Sciences of Matter, Hiroshima University (2012)
- Title: Rare earth ion doping and high pressure effect on the phase IV of $\text{Ce}_x\text{La}_{1-x}\text{B}_6$
Author: Soejima K.
Degree type: Master
Received from: AdSM, Hiroshima University (2012)
- Title: High temperature structure of KDP and DKDP
Author: Kaki Y.
Degree type: Bachelor
Received from: Yamaguchi University (2012)
- Title: High temperature structure of DKDP and KDP
Author: Yamamoto Y.
Degree type: Bachelor
Received from: Yamaguchi University (2012)

2011

- Title: 非溶媒界面における高分子の凝集状態に関する研究
Author: Atarashi H.
Degree type: Doctor/Ph.D
Received from: Kyushu University (2011)
- Title: 単層 CuO_2 面を持つ銅酸化物超伝導体のアンダードープ領域における磁気励起研究
Author: Enoki M.
Degree type: Doctor/Ph.D
Received from: Tohoku University (2011)
- Title: Precise Analyses of High Performance Polymer Gels
Author: Matsunaga T.
Degree type: Doctor/Ph.D

- Received from: The University of Tokyo (2011)
- Title: ポリロタキサンの分子ダイナミクスと環動ゲルの力学物性
Author: Mayumi K.
Degree type: Doctor/Ph.D
Received from: University of Tokyo (2011)
 - Title: Study on Potassium Dihydrogen Phosphate and Potassium Dideuterium Phosphate by Single-Crystal Neutron Structural Analyses
Author: Miyoshi T.
Degree type: Doctor/Ph.D
Received from: Yamaguchi University (2011)
 - Title: Investigation of Structural Modeling and Diffusion Dynamics by Quasi-elastic Neutron Scattering Technique on Hydrophobic Hydration in Lower Alcohol Aqueous Solutions
Author: Nakada M.
Degree type: Doctor/Ph.D
Received from: Niigata University (2011)
 - Title: 鉄酸化物系熱電半導体の物性と応用
Author: Nozaki T.
Degree type: Doctor/Ph.D
Received from: Department of Applied Physics, Graduate School of Engineering, Tohoku University (2011)
 - Title: Studies on Mixing States of Ionic Liquids - Molecular Liquids at the Molecular Level
Author: Shimomura T.
Degree type: Doctor/Ph.D
Received from: Saga University (2011)
 - Title: Studies on adsorption property and its effects on proton conductivity in functionalized porous coordination polymers
Author: Shitematsu A.
Degree type: Doctor/Ph.D
Received from: Kyushu University (2011)
 - Title: Phase Structure Control of Multi-Component Polymer Systems by Tuning the Interaction Strength via Molecular Design
Author: Siti Sarah A. R.
Degree type: Doctor/Ph.D
Received from: Nagoya University (2011)
 - Title: Characterization of interface at water/ sulfobetaine-type polymer brushes prepared by controlled radical polymerization
Author: Terayama Y.
Degree type: Doctor/Ph.D
Received from: Kyushu University (2011)
 - Title: パルス中性子散乱実験に向けた微少YBCO単結晶の育成とアSEMBルした試料を用いた磁気シグナルの観測
Author: Ai Y.
Degree type: Master
Received from: Tohoku University (2011)
 - Title: Surface Active Properties of Tadpole-type Amphiphilic Dendrimers and Nano-Structural Analysis of Aggregates Formed in Aqueous
Author: Ebihara A.
Degree type: Master
Received from: Graduated School of Humanities and Sciences, Nara Women's University (2011)

- Title: リチウムイオン電池正極材料Li (Mn,M)0.5(Ni, M')0.5O2の結晶・電子構造と電池特性の組成依存
Author: Endo H.
Degree type: Master
Received from: Faculty of Science and Technology, Tokyo University of Science (2011)
- Title: The effects of surfactant and initiator on miniemulsion polymerization kinetics
Author: Enomoto Y.
Degree type: Master
Received from: Graduate School on Engineering, Chiba University (2011)
- Title: フラストレーション反強磁性体CuFe_{1-x}MnxO₂の磁性と強誘電性
Author: Fukatsu R.
Degree type: Master
Received from: Department of Applied Physics, Graduate School of Engineering, Tohoku University (2011)
- Title: 擬二次元オキシカルコゲナイドLn₂M₂O₃Se₂ (Ln=希土類元素, M=遷移金属元素)の結晶構造と磁性
Author: Fuwa Y.
Degree type: Master
Received from: Division of Chemistry, Graduate School of Science, Hokkaido University (2011)
- Title: LaMg₄O₄ (M=Sr, Ba)系イオン伝導体における欠陥構造の回折・散乱測定による評価と第一原理計算による理論解析
Author: Hamao N.
Degree type: Master
Received from: Faculty of Science and Technology, Tokyo University of Science (2011)
- Title: 水界面における高分子ブレンド表面の構造制御とバイオ関連機能
Author: Hirata T.
Degree type: Master
Received from: Dept. of Appl. Chem., Kyushu University (2011)
- Title: 塩化アルカリ塩誘起によるHFIP-水混合溶液の相分離
Author: Kouda Y.
Degree type: Master
Received from: Saga University (2011)
- Title: Sr-Bi-(M, M', Si)-O (M=Ta, Nb, M'=W, Mo)強誘電体の結晶・電子構造と強誘電特性の組成依存
Author: Muroi R.
Degree type: Master
Received from: Faculty of Science and Technology, Tokyo University of Science (2011)
- Title: 中性子散乱分光による電子ドーパ型銅酸化物Pr_{1.4-x}La_{0.6}CexCuO₄の反強磁性磁気秩序相における磁気励起の研究
Author: Shigiya K.
Degree type: Master
Received from: Tohoku University (2011)
- Title: Impurity effect on the magnetism in two kinds of triangular lattice magnets
Author: Takahashi R.
Degree type: Master
Received from: Tokyo University of Science (2011)
- Title: リチウムイオン電池正極材料 Li(Ni, Co, M)O₂ (M=Cu, Zn)の熱力学的安定性、結晶・電子構造と

電池特性

Author: Tsukada Y.

Degree type: Master

Received from: Faculty of Science and Technology, Tokyo University of Science (2011)

- Title: クラスレート化合物Eu₈Ga₁₆Ge₃₀の特異な強磁性に対するキャリア制御と圧力の効果
Author: Yamane H.
Degree type: Master
Received from: Hiroshima University (2011)
- Title: フラストレーション系クロムスピネルのスピンの励起
Author: Yokobori T.
Degree type: Master
Received from: Aoyama-Gakuin University (2011)
- Title: 延伸ポリエチレンの各分子量成分の役割
Author: Tomita N.
Degree type: Bachelor
Received from: Yamagata University (2011)
- Title: Low temperature structure of KDA
Author: Tsukamoto H.
Degree type: Bachelor
Received from: Yamaguchi University (2011)

2010

- Title: らせん磁性強誘電体における電気分極の磁場による制御
Author: Abe N.
Degree type: Doctor/Ph.D
Received from: Tohoku University (2010)
- Title: 少数スピン系分子磁性体の中性子動的散乱関数の解明
Author: Iida K.
Degree type: Doctor/Ph.D
Received from: University of Tokyo (2010)
- Title: 規則構造をもつ三角格子コバルト酸化物の研究
Author: Igarashi D.
Degree type: Doctor/Ph.D
Received from: Graduate School of Engineering, Tohoku University (2010)
- Title: 機能性酸化物と低分子糖類の結晶構造と電子密度分布に関する研究
Author: Kataoka K.
Degree type: Doctor/Ph.D
Received from: University of Tsukuba (2010)
- Title: Neutron Scattering Study on Formation Mechanism of Gas Hydrates and Dynamic Structures of Related Materials
Author: Kikuchi T.
Degree type: Doctor/Ph.D
Received from: University of Tokyo (2010)
- Title: 幾何学的にフラストレートした三角格子反強磁性体CuCrO₂の電気磁気特性
Author: Kimura K.
Degree type: Doctor/Ph.D
Received from: Graduate school of engineering science, Osaka University (2010)

- Title: 擬力ゴメ格子系反強磁性体YbAgGeにおける磁気フラストレーションの圧力と元素置換による緩和
Author: Kubo H.
Degree type: Doctor/Ph.D
Received from: Hiroshima University (2010)
- Title: ハニカム格子系の物性研究 -spin gapを持つNa₃Cu₂SbO₆の磁気励起およびLi₂RuO₃の新型相転移機構-
Author: Miura Y.
Degree type: Doctor/Ph.D
Received from: Department of Physics, Nagoya University (2010)
- Title: Comprehensive study on ferroelectricity induced by a proper-screw-type magnetic order in a delafossite multiferroic CuFeO₂
Author: Nakajima T.
Degree type: Doctor/Ph.D
Received from: Tokyo University of Science (2010)
- Title: Modeling of biomembranes using simple lipid mixture systems
Author: Sakuma Y.
Degree type: Doctor/Ph.D
Received from: Ochanomizu University (2010)
- Title: Thermoelectric and Phononic Properties of Type-I Clathrates Sr₈Ga₁₆Si_{30-x}Gex and Ba₈Ga₁₆Sn₃₀
Author: Suekuni K.
Degree type: Doctor/Ph.D
Received from: Hiroshima University (2010)
- Title: Influence of the 2nd Component Distribution on Macroscopic Properties and Microscopic Structures of Polymer Gels
Author: Takuya S.
Degree type: Doctor/Ph.D
Received from: University of Tokyo (2010)
- Title: Low Temperature Synthesis and Properties of Novel Iron Oxides with Square Planar Coordination
Author: Tassel C.
Degree type: Doctor/Ph.D
Received from: Graduate School of Engineering, Kyoto University (2010)
- Title: Magnetoelectricity in Multiferroic Oxides
Author: Yamasaki Y.
Degree type: Doctor/Ph.D
Received from: University of Tokyo (2010)
- Title: Neutron diffraction and AFMR studies of alkali-metal clusters in sodalite
Author: Hanazawa A.
Degree type: Master
Received from: Osaka University (2010)
- Title: 低次元量子スピン物質BaCo₂V₂O₈, Pb₂V₃O₉, およびO₂吸着CPL-1の磁気励起
Author: Hondo S.
Degree type: Master
Received from: International graduate schools of arts and sciences, Yokohama City University (2010)
- Title: GdB₆ の電子-格子相互作用に関わるフォノン異常の研究
Author: Igarashi R.
Degree type: Master
Received from: Tohoku University (2010)
- Title: Bi₄Si₃O₁₂, F添加(Bi, M)₄(Ti, M')₃O₁₂ (M=La, Nd; M'=Mo) 強誘電体の物性、結晶構造と強誘電

特性

- Author: Iiyama T.
Degree type: Master
Received from: Faculty of Science and Technology, Tokyo University of Science (2010)
- Title: 層状化合物CePd₅Al₂とカゴ状化合物RT₂Zn₂₀ (R=La,Ce,Pr,Nd, T=Ru,Ir)の磁性と伝導
Author: Inoue F. Y.
Degree type: Master
Received from: Hiroshima University (2010)
 - Title: 鉄系超伝導体 SrFe₂As₂ 単結晶の高圧下中性子回折実験
Author: Ishida H.
Degree type: Master
Received from: University of Tokyo (2010)
 - Title: 中性子散乱による電子ドープ型Pr_{1.4-x}La_{0.6}Ce_xCuO₄の反強磁性相における磁気相関の研究
Author: Kaminaga J.
Degree type: Master
Received from: Faculty of Science Tohoku Univ. (2010)
 - Title: イオン交換法による層状ペロブスカイトの合成, 構造, 二次元量子磁性
Author: Kitada A.
Degree type: Master
Received from: Graduate School of Science, Kyoto University (2010)
 - Title: 中性子単色化Ge単結晶素子の高反射率 化と二波長中性子回折への応用
Author: Miyaka Y.
Degree type: Master
Received from: Faculty of Science Tohoku Univ. (2010)
 - Title: Magnetic anisotropy and an anomalous metamagnetism in a rare-earth compound ErNi₂Ge₂
Author: Okue M.
Degree type: Master
Received from: Kyoto University (2010)
 - Title: Pr_xFe₄Sb₁₂ の弱い磁気秩序に関する中性子散乱実験による研究
Author: Orihara T.
Degree type: Master
Received from: Tohoku University (2010)
 - Title: 金属水素化物を低温還元剤として用いた新規無機物質の合成
Author: Sumida Y.
Degree type: Master
Received from: Graduate School of Science, Kyoto University (2010)
 - Title: 銅イオン交換MFI型ゼオライトにおけるH₂分子の吸着状態
Author: Takahara K.
Degree type: Master
Received from: Okayama University (2010)
 - Title: Component and temperature dependence of crystal and magnetic structure of MnRh alloy
Author: Takasaki A.
Degree type: Master
Received from: Nara Women's University (2010)
 - Title: 中性子反射率法を用いたトライボロジー界面のナノ構造解析—添加剤吸着分子膜が摩擦特性に及ぼす影響—
Author: Torii T.

Degree type: Master

Received from: Faculty of Engineering, Doshisha Univ. (2010)

- Title: 新規鉄酸化物BaFeO₂の合成と構造物性

Author: Yamamoto T.

Degree type: Master

Received from: Graduate School of Science, Kyoto University (2010)

- Title: 量子スピン系の実験と計算

Author: Shiramizu M.

Degree type: Bachelor

Received from: Yokohama City University (2010)